AN INVESTIGATION OF THE AERODYNAMIC CHARACTERISTICS OF A STREAMLINED ROAD VEHICLE

A Thesis
Submitted to the Faculty
of the
Georgia School of Technology
in
Partial Fulfillment of the Requirements
for the Degree of

MASTER OF SCIENCE IN AERONAUTICAL ENGINEERING

by

Thomas E. Moodie
B. S. in M. E., M.I.T., 1924

Atlanta, Georgia
Georgia School of Technology
1933 - 1934

35950

Approved by:

Committee on Advanced Degrees

Date

INDEX

INDEX (continued)

SUMMARY

This report describes a series of tests made at the Daniel Guggenheim School of Aeronautics, of the Georgia School of Technology, to determine the performance, control, maneuverability, and stability characteristics of a Roadplane. The report includes the results of wind tunnel tests on a one-sixteenth scale model, and road tests on a full-sized machine. The lift, drag, yawing moments and pitching moment coefficients were determined in the tunnel for various cabin and body forms and for three different tail surface designs. The drag coefficients, yawing moment coefficients, cross wind force coefficients, and the longitudinal and vertical side center of pressure locations, were determined for various angles of yaw, and for various rudder settings. The drag coefficients, pitching moment coefficients, rolling moment coefficients, and the center of pressure locations, were obtained for various elevator settings. The performance, stability, and controllability characteristics were evaluated from the data thus obtained, and the results compared with the behavior of the full scale machine, which was determined from road tests.

INTRODUCTION

Before beginning the detailed discussion of this research it may be well to consider the application of streamlining to road vehicles, and especially to automobiles, since this is a subject of keen engineering interest at the present time.

The motor car is just entering the stage in its development where increased performance cannot be obtained economically by the simple expedient of increasing the engine power, or even the power loading. In fact, the present day automobile cannot operate efficiently on the modern high speed highways which were constructed primarily for its use. Such a statement, radical as it may sound, becomes clearly apparent when we consider a modern, moderate sized coupe which requires approximately one hundred horsepower and twenty five hundred to three thousand pounds of dead weight to carry three people in comfort and safety at speeds up to, and including eighty-five miles per hour. The explanation for such poor performance is obvious when we recall that the coupe referred to above is so poorly shaped, from an aerodynamic standpoint; that approximately four-fifths of its power is used to overcome air resistance at sixty five miles per hour, and even at thirty miles per hour the air resistance consumes approximately one half of the power output. (Reference 1)

The facts just mentioned have been obvious to engineers for some time, and the logical solution of the problem is to streamline the car. Very able researches directed toward improving the streamline characteristics of the modern motor car are now in progress, not to mention the work that has already been done on this subject. (See references in appendix) In spite of the apparently obvious solution of the problem, the worker in this field is immediately impressed with several practical difficulties of very serious proportions.

For instance, it is practically impossible to streamline the lower surface of the present style of car without either raising its center of gravity to an extreme extent, or shortening its wheelbase to a material degree. Both of these alternatives are impractical however, for obvious reasons, and the result is that the bottom surface remains unstreamlined, and in most cases uncovered.

The situation for the rest of the car appears much better until it is discovered that the conventional style of car, when properly streamlined, becomes about twenty feet long. This renders parking and traffic operation very difficult.

In the opinion of the author, the modern automobile is essentially a low speed machine which has been subjected to a process of continuous refinement, until it has finally reached the stage where it can be used with reasonable comfort and safety for high speed travel. In contrast to this, the machine which forms the subject matter of this investigation is fundamentally suited for high speed road travel. Satisfactory slow speed operation is obtained by means of certain refinements, the details of which will be given later in this report.

Due to the fact that this machine bears a very close relationship to the airplane it will be referred to throughout this report as a Roadplane.

DESCRIPTION OF ROADPLANE

The experimental Roadplane, which has been built, consists essentially of a main body which has the shape of an inverted airfoil (Figures 1 and 2). This body is surmounted by a streamlined cabin structure which is large enough to seat two passengers side by side. The main driving wheels are located one on each side of the body, and enclosed therein. These wheels are driven through a standard differential and are located at a point 37.3 % of the main body length back from the radiators. The engine, which in the present full scale machine is a four cylinder 1928 Whippet, is located in front, in the usual manner, and is cooled by two special radiators located in the nose of the body. A small wheel mounted on a free swivel is located at the extreme front of the machine. (Figure 3) This wheel is supported by a hydraulic strut. The main driving wheels are unsprung in the present experimental machine. At the rear part of the machine are two vertical rudders which are controlled by a stick in the cabin and are used for steering at speeds beyond thirty miles per hour. A horizontal elevator surface (Figures 4 and 5) is located between these two rudder surfaces. The low speed steering, parking, etc., is accomplished by means of individual wheel brakes, which are operated by two pedals in the cabin.

In addition, there is a service and parking brake located on the drive shaft. The throttle is operated by a hand grip on the control stick. The clutch is operated in a similar manner. The gear shift lever and other details of the car are conventional in practically every respect. The present machine has no lights or front bumper. A rear bumper is built into the trailing edge. The machine, in spite of its high degree of streamlining, is about four inches narrower, and a few inches shorter than the average moderate-size coupe.

FIGURE 1
FULL SCALE MACHINE SIDE VIEW

FIGURE 2
FULL SCALE MACHINE THREE QUARTER FRONT VIEW

FIGURE 3
FULL SCALE MACHINE FRONT VIEW

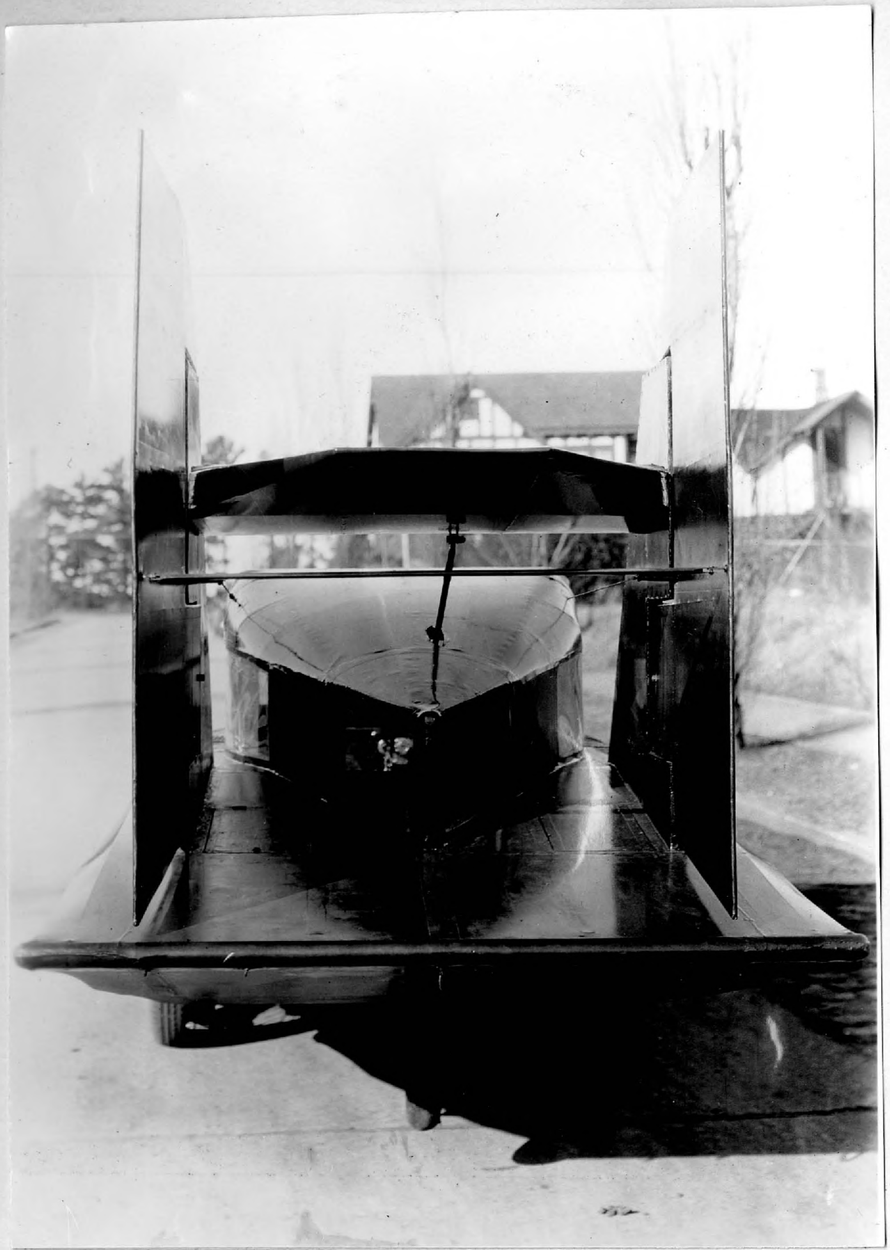

FIGURE 4
FULL SCALE MACHINE REAR VIEW

FIGURE 5
FULL SCALE MACHINE THREE QUARTER REAR VIEW

MODELS AND APPARATUS

The models used for the wind tunnel tests were made of mahogany and were accurate to plus or minus 0.01 inch. These models were one sixteenth scale and were complete in all major details except for the radiators. No effort was made to simulate the radiators as it was obviously impossible to reproduce such parts on models of this size.

In this report, the model which was used for most of the tests, will be referred to as the Prototype Model, and in most cases will be further designated as Body No.2, Cabin No.9, with Modified Rudders, (Figures 6 and 9) or with Original Rudders, which ever the case may be. By referring to figures 7, 8, and 9, it will be possible to compare this form of the model with the various other forms. The term, Original Rudders, refers to the unbalanced rudders, as shown in drawings 7 and 8. The Modified Rudders are those shown in figures 6 and 9. The Modified Rudders were tested only in conjunction with No. 2 Body, and No. 9 Cabin, while the Original Rudders were tested with all the body and cabin forms. Due to a peculiar flow condition which developed when the model was yawed, most of the yaw runs with the Original Rudders were discarded and the runs with the Modified Rudders were used.

It will be observed by reference to figures 7, 8, and 9, that the Prototype Model was tested with nine different cabin shapes and with two different tail surface shapes as just referred to.

In addition, it was tested with both large and small body fillets; Body No. 1 referring to the small fillets (Figure 7) and Body No. 2 (Figures 7, 8, and 9) referring to the large fillets. Both the elevator and rudders on this model are movable, and the model was tested for various control surface settings, and for various angles of pitch and yaw. The Prototype Model with Body No. 2 and Cabin No. 9, and with Modified Rudders differed only slightly from the full scale machine which is illustrated in Figures 1, 2, 3, 4, 5, and 10. It will be noticed that there is a slight difference in cabin shape and also some difference in front wheel mounting. In addition the full scale machine has a small rear wheel which was added after the model tests were completed. In the model, the driving wheels are shown in a further forward position than they are on the full sized machine, but this difference was corrected for in the calculations so that the coefficients are based on identical driving wheel locations. There are some other slight differences which will be obvious by referring to the figures.

In addition to the Prototype Model just referred to, an entirely different type of model referred to as the Tail-Boom Model (Figures 11 and 12) was tested. In the Tail-Boom Model the control surfaces were not movable, and there were no provisions made for altering the shape of the cabin, etc.. This model was tested primarily to show just what could be accomplished by streamlining if no restrictions were placed on the designer. It will be noticed that a full scale reproduction of this model would call for a liberal use of curved glass and other unusual mechanical and structual features. A car built on the lines of the Tail-Boom Model would be about the same size as the 1934 model cars. The Tail-Boom Model was tested for various angles of yaw and pitch. The control surfaces were fixed in all cases. The wind tunnel tests were all made in the small wind tunnel of the Daniel Guggenheim School of Aeronautics at the Georgia School of Technology. This tunnel is a single return tunnel of the open jet type. The jet has a square cross section which is 2.5 feet by 2.5 feet in size. (Figures 11, 13, and 14 show the Tail-Boom Model mounted in the tunnel.) The tests were run at an average Barometric pressure of 736.77 mm. of Hg., and an average room temperature of 31.36 degrees C. The average sea level velocity for the tests was 70.0 miles per hour. The Reynolds number was 594,000 for the tests on the Tail-Boom Model and 500,000 for the tests on the Prototype Model. For further details of this tunnel and the balance system used to support the models see Reference No. 3.

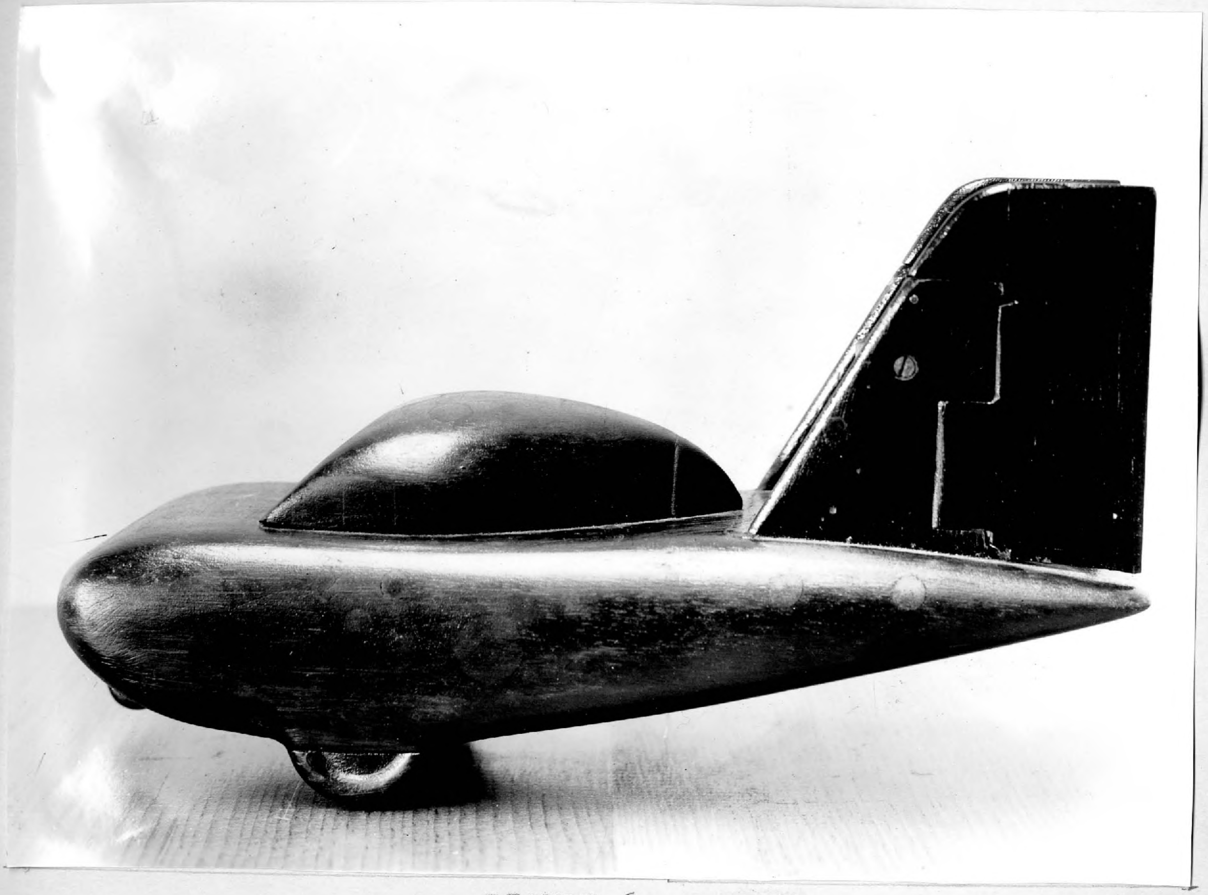

FIGURE 6
SIDE VIEW OF PROTOTYPE MODEL

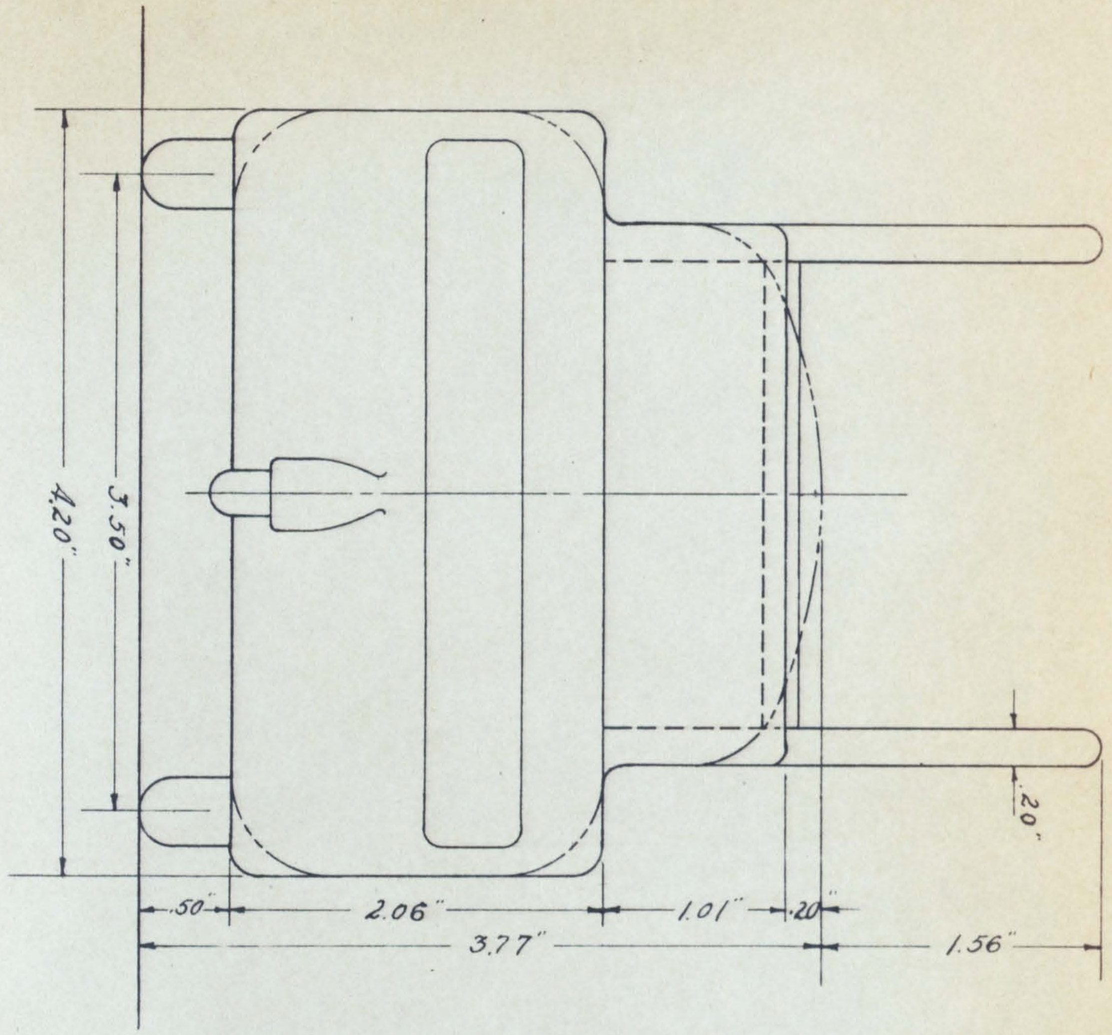

BODY TYPE NO. 1 5/32" FILLETS

CABIN TYPE NO. 1 FLAT ROOF; STRAIGHT BACK; 3/32" FILLETS.

CABIN TYPE NO. 2 FLAT ROOF; ARCHED BACK; 3/32" FILLETS.

BODY TYPE NO. 2 9/16" FILLETS

CABIN TYPE NO. 3 FLAT ROOF; ARCHED VEE BACK; 9/16" FILLETS.

CABIN TYPE NO. 4 ROUNDED ROOF; ARCHED VEE BACK; 9/16" FILLETS.

CABIN TYPE NO. 5 ROUNDED ROOF; ARCHED VEE BACK; 9/16" FILLETS.

AREA AT MAXIMUM CROSS SECTION CAR IN HORIZONTAL RUNNING POSITION

BODY NO. 1	AREA IN SQ. IN.
CABIN NO. 1	12.94
CABIN NO. 2	12.94
BODY NO. 2	
CABIN NO. 3	12.74
CABIN NO. 4	12.86
CABIN NO. 5	12.86

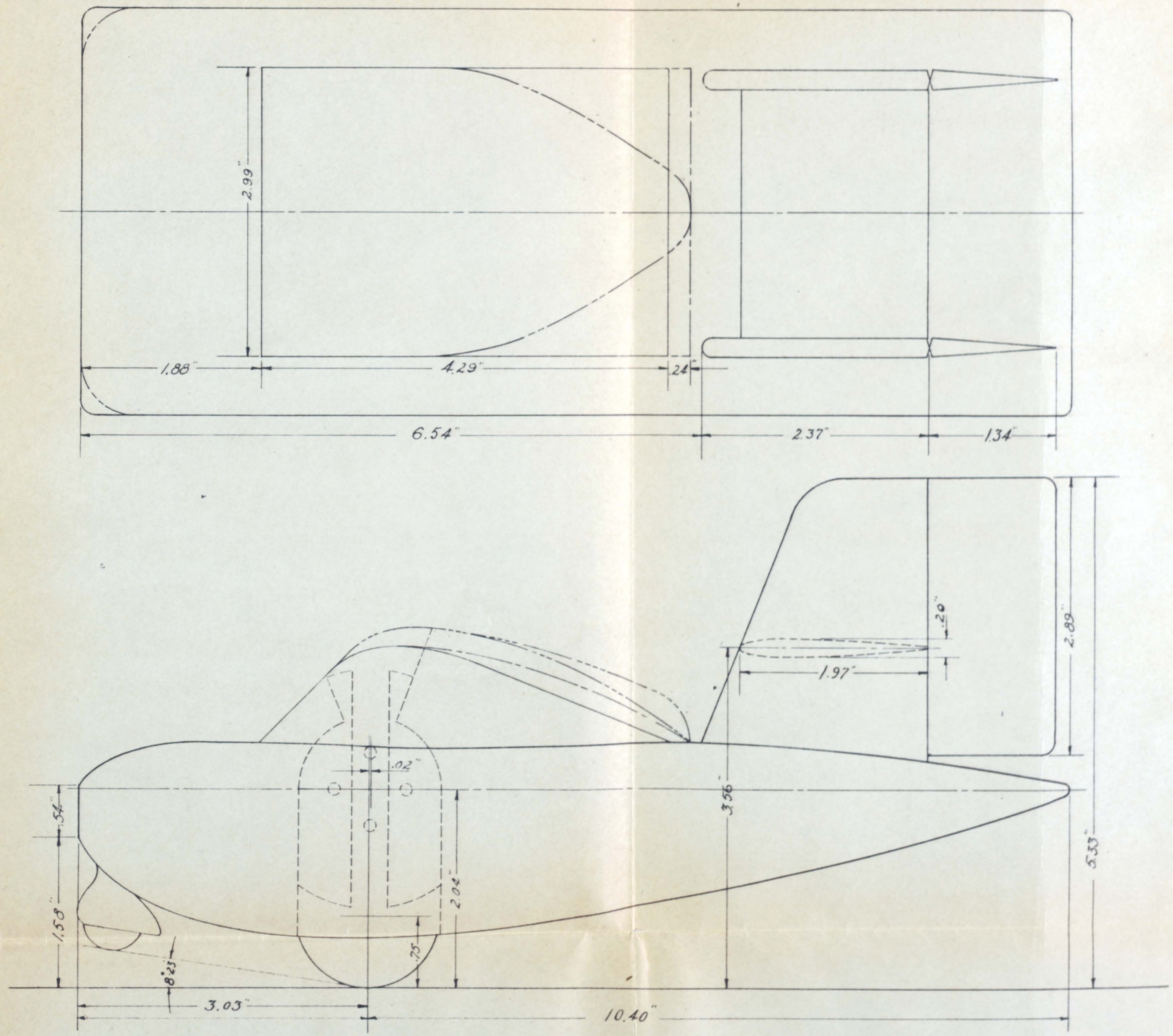

FIG. 7

WIND TUNNEL MODEL PROTOTYPE

FULL SIZE 1/16 SCALE

6-30-'33

RLS

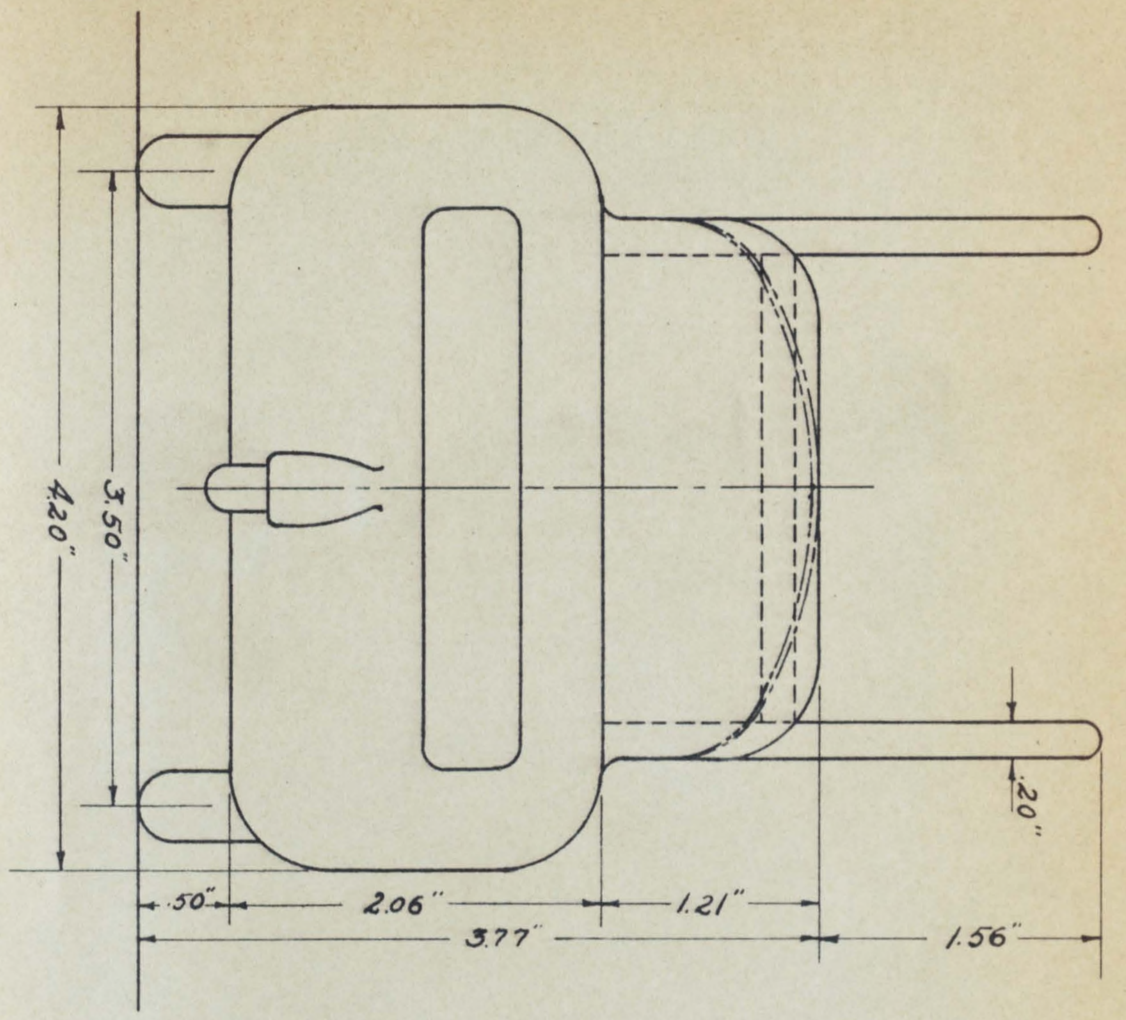

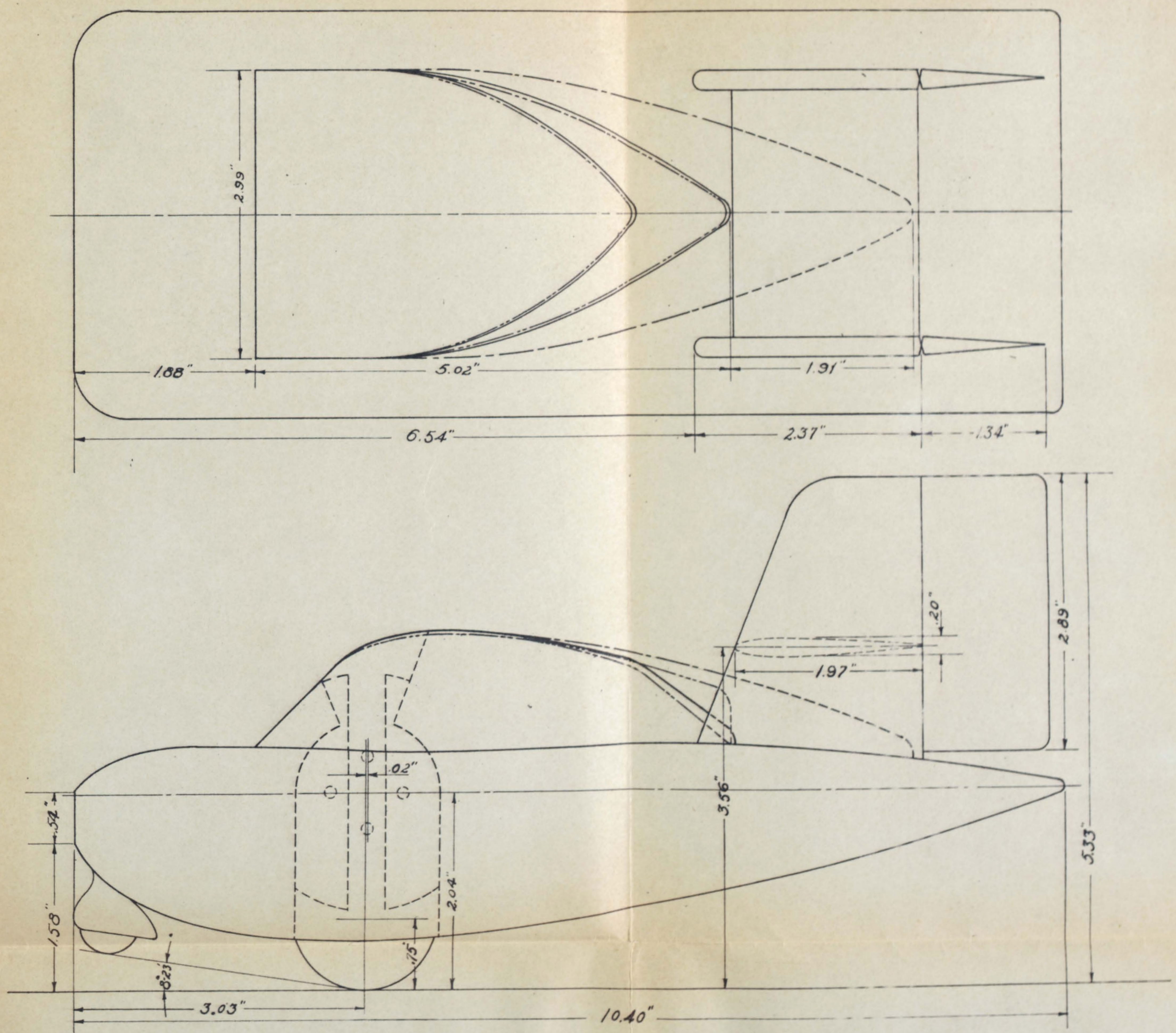

BODY TYPE NO. 2 9/16" FILLETS

CABIN TYPE NO. 6 FLAT ROOF ARCHED VEE BACK ENDING IN A SLOPING WEDGE 9/16" FILLETS.

CABIN TYPE NO. 7 ROUNDED ROOF LONG ARCHED VEE BACK 9/16" FILLETS.

CABIN TYPE NO. 8 ROUNDED ROOF ARCHED VEE BACK ENDING IN A VERTICAL WEDGE 9/16" FILLETS.

CABIN TYPE NO. 9 ROUNDED ROOF ARCHED VEE BACK ENDING IN A SLOPING WEDGE 9/16" FILLETS.

AREA AT MAXIMUM CROSS SECTION CAR IN HORIZONTAL RUNNING POSITION

BODY NO. 2	AREA IN SQ. IN.
CABIN NO. 6	12.99
CABIN NO. 7	12.88
CABIN NO. 8	12.68
CABIN NO. 9	12.68

FIG. 8

WIND TUNNEL MODEL
PROTOTYPE
FULL SIZE
1/16 SCALE

7-1-'33 RFS

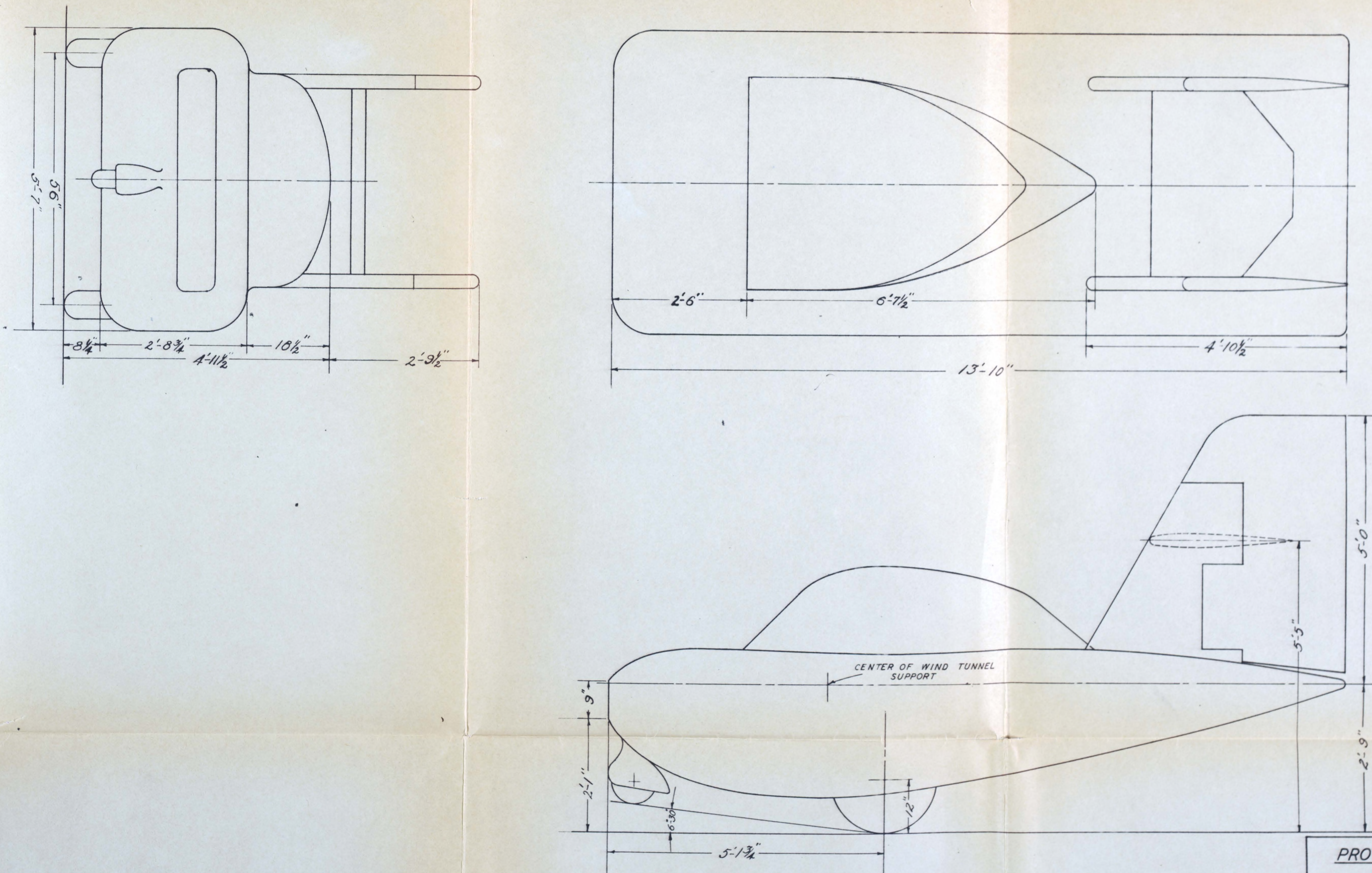

FIG. 9

PROTOTYPE MODEL
FINAL FORM
SCALE 3/4" = 12"

7-23-'33 RES

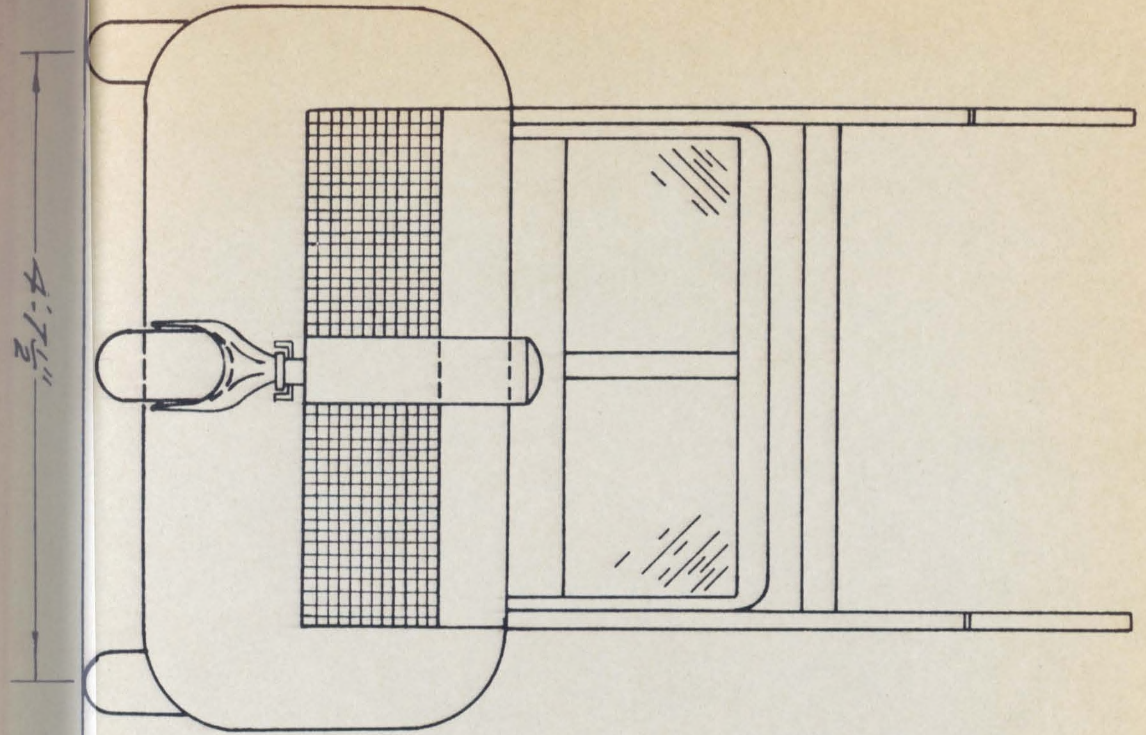

AREA AT MAXIMUM GROSS SECTION CAR IN HORIZONTAL
RUNNING POSITION 23.50 SQ. FT.
PLAN AREA 72.50 SQ. FT. STATIC MOMENT 126.75 $FT.^3$
SIDE AREA 59.73 SQ. FT. STATIC MOMENT 135.37 $FT.^3$ (WITH RUDDER)
SIDE AREA 47.00 SQ. FT. STATIC MOMENT 43.89 $FT.^3$ (WITHOUT RUDDER)

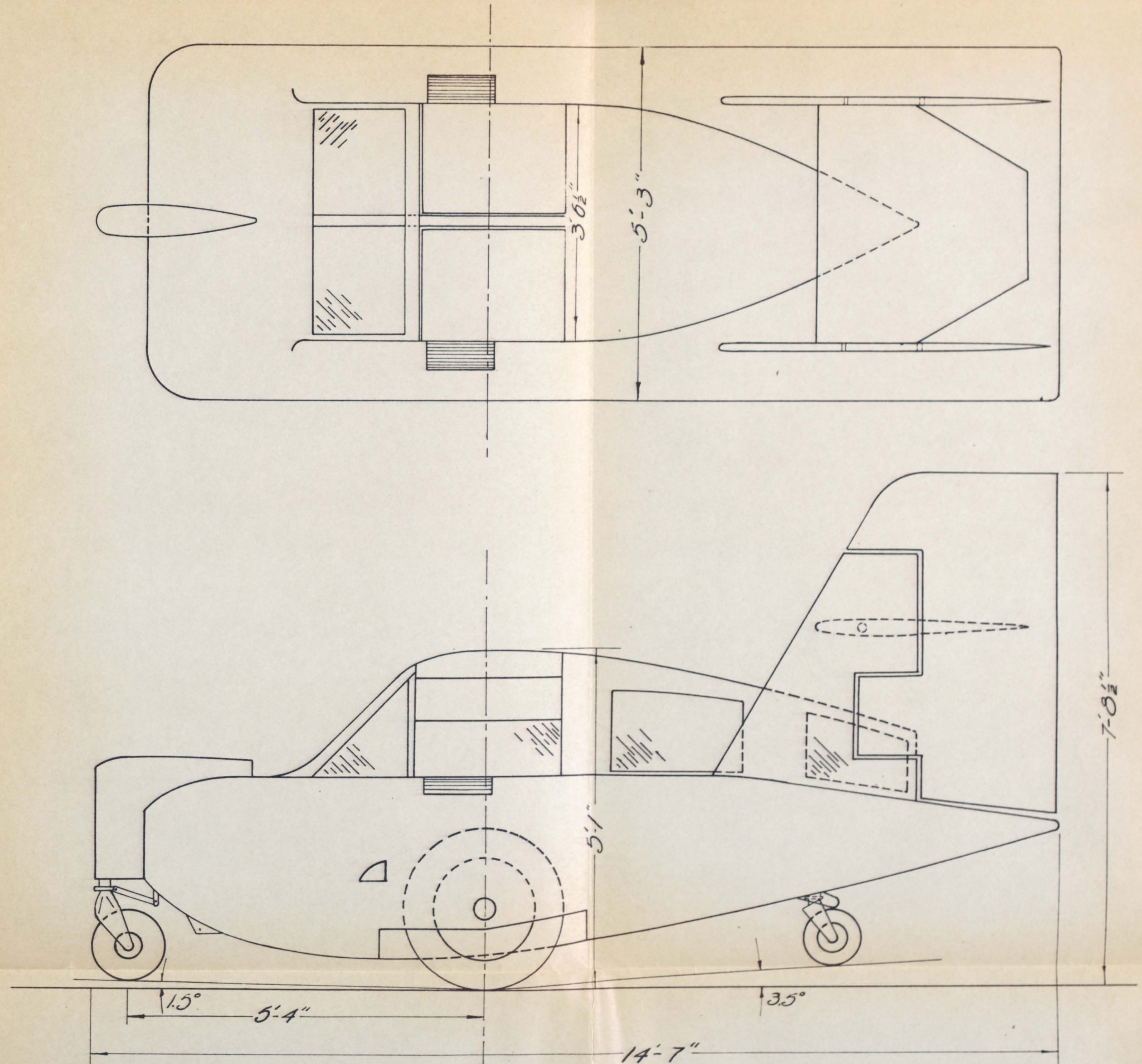

FIG. 10

ROAD PLANE
FULL SIZE
1/16 SCALE
3-2-34 M.W.P.

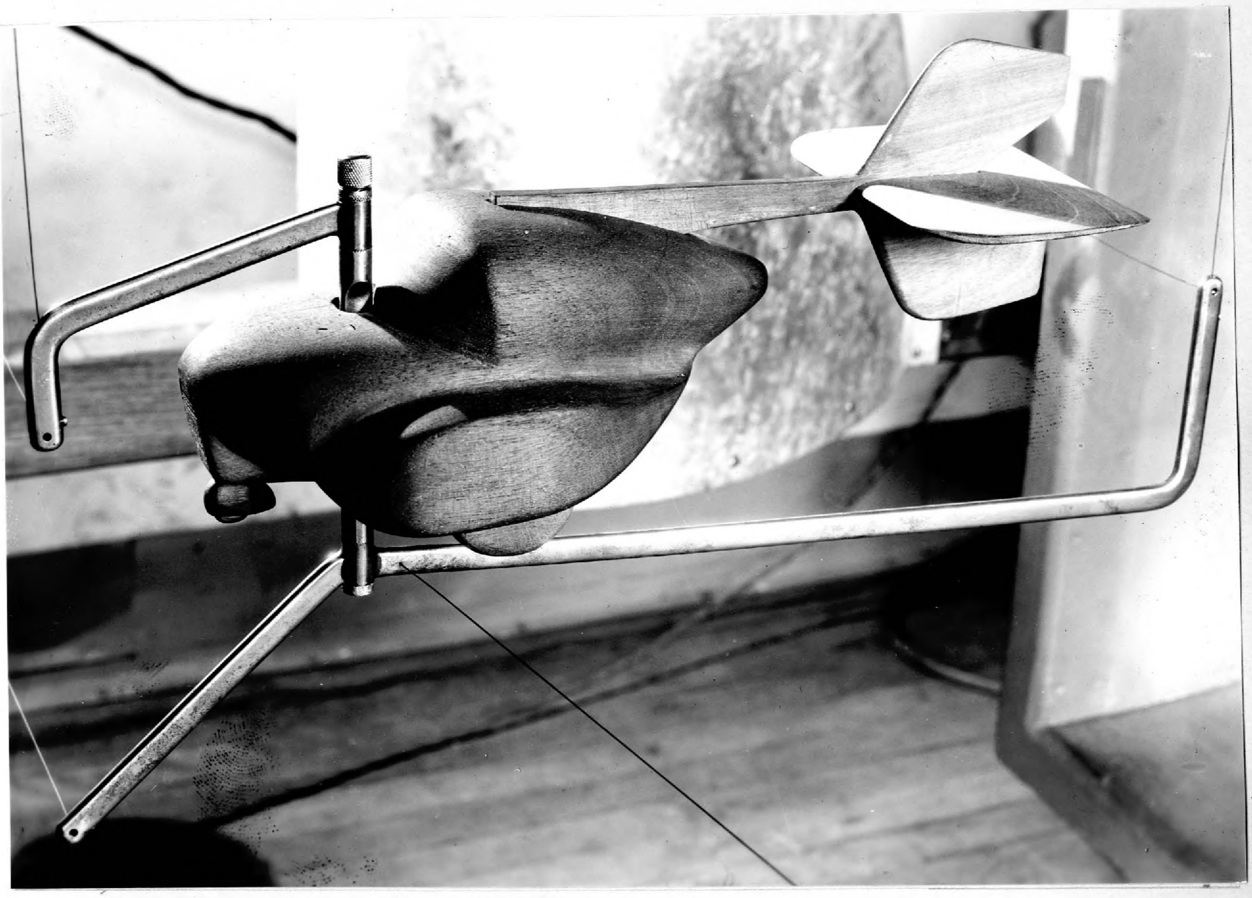

FIGURE 11
TAIL BOOM MODEL AND TUNNEL BALANCE

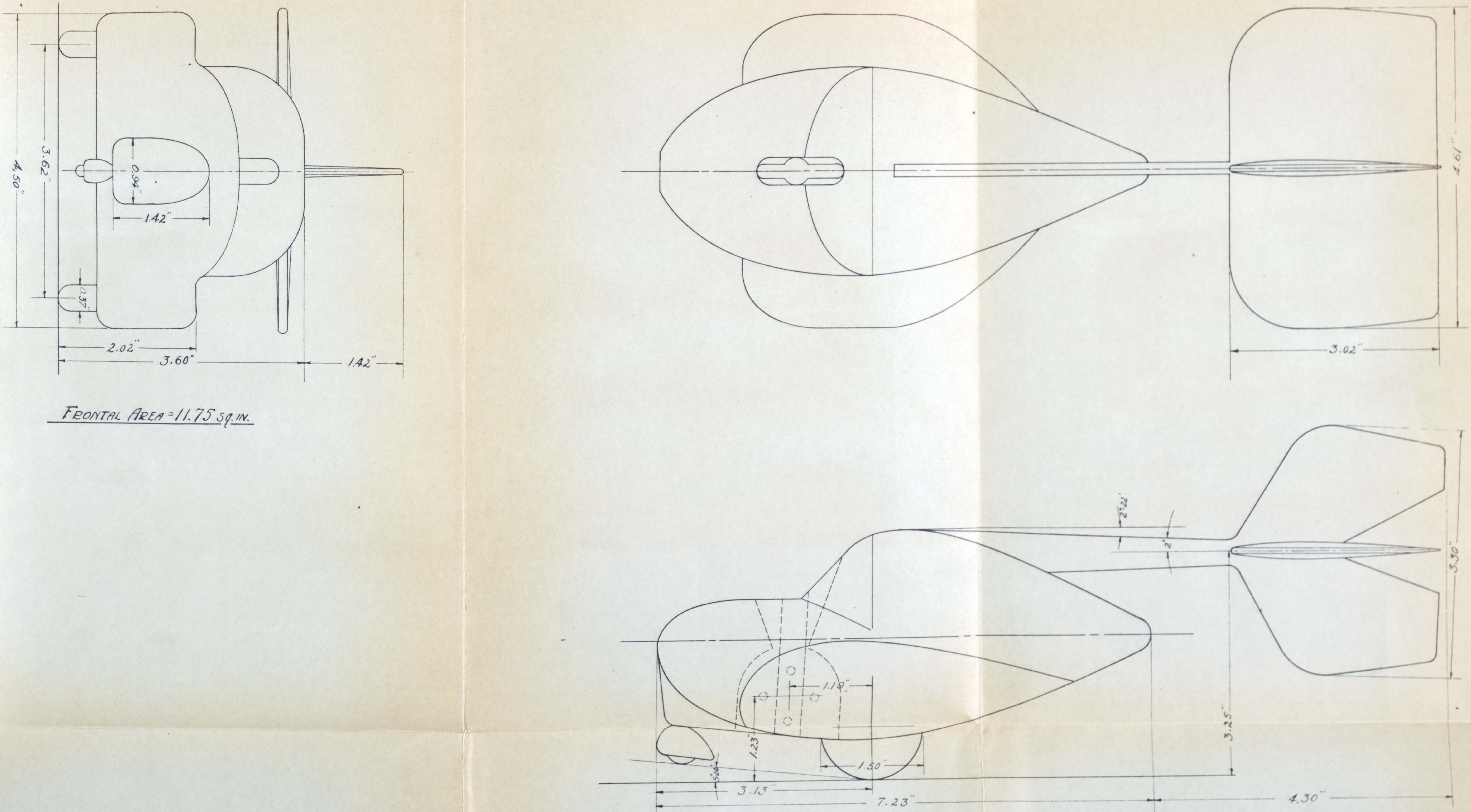

FIG. 12

WIND TUNNEL MODEL
TAIL BOOM TYPE
FULL SIZE
1/16 SCALE

FIGURE 13
TAIL BOOM MODEL IN TEST POSITION IN TUNNEL

FIGURE 14
TAIL BOOM MODEL AND TUNNEL BALANCE SYSTEM

WIND TUNNEL TESTS

The wind tunnel test program was as follows: Tests were run on the Tail Boom Model at zero yaw for various angles of pitch. Tests were also run at zero pitch for various angles of yaw. The tail surfaces were fixed in all cases. A test was also run on the model to determine the aerodynamic drag of the wind tunnel balance system in the presence of the model. For this test the model was externally supported in the test position and the aerodynamic forces on the tunnel balance system were measured.

The Prototype Model, with Original rudders, was tested at zero yaw, and various pitch angles to determine the effect of large and small body fillets, and also the effect of different cabin forms. These tests were made with all the control surfaces fixed in their neutral position. Tests were also made on the model,with modified rudders:

1. With the cabin and tail and surfaces removed.
2. With tail surfaces, but without cabin.
3. Complete
4. Complete less elevator.

After the best form of cabin was obtained, the Prototype Model was mounted in the position for zero yaw and zero pitch, and tests were made to determine the effect of various elevator settings.

Tests were also made at various pitch angles and various elevator settings with the model in the unyawed position. The rudders were displaced through various angles when the model was at zero pitch and data was obtained for the conditions of 0, 10, 20, 30, 40, and 50 degree yaw. The elevator was set at zero in most of the yawed runs, and the pitch angle was also zero. But in one run the model was placed at zero yaw and data was obtained for various elevator angles and for zero and 30 degree rudder settings, so as to note the effect of rudder displacement on elevator control.

After all the tests were completed, the model was externally supported in the test position, both with and without its cabin, and the aerodynamic tare of the balance system was determined.

FULL SCALE TESTS

The tests on the full scale machine were as follows: Due to the novel principles involved in the Roadplane, the formal tests were preceded by a great many road trips so that the operator might become familiar with the machine. After these trips had been completed, a series of economy runs were made to determine the fuel consumption.

Data (Figure 15) on these runs is included merely as a matter of general interest since the author does not feel that they are in any way indicative of the improvements in economy which are possible with proper streamlining. This statement is made in view of the fact that the economy runs were made with a motor, transmission, and differential system, which had been driven over 47,000 miles and in addition was entirely unsuited for the installation in which it was used. In any study of the fuel economies possible with the Roadplane due consideration should be given to the fact that a considerably better showing would have been made with a new power plant correctly designed for the duty which it had to perform and properly mounted in a vehicle complete with springs and shock absorbers. The economy runs were made in the following manner: An 8280 foot stretch of road was laid off with a surveyer's tape, and clearly marked at each end. This length was chosen since it was the longest length which could be obtained in this locality, (Atlanta, Ga.) free from steep grades. In spite of the extremely short length of this course,

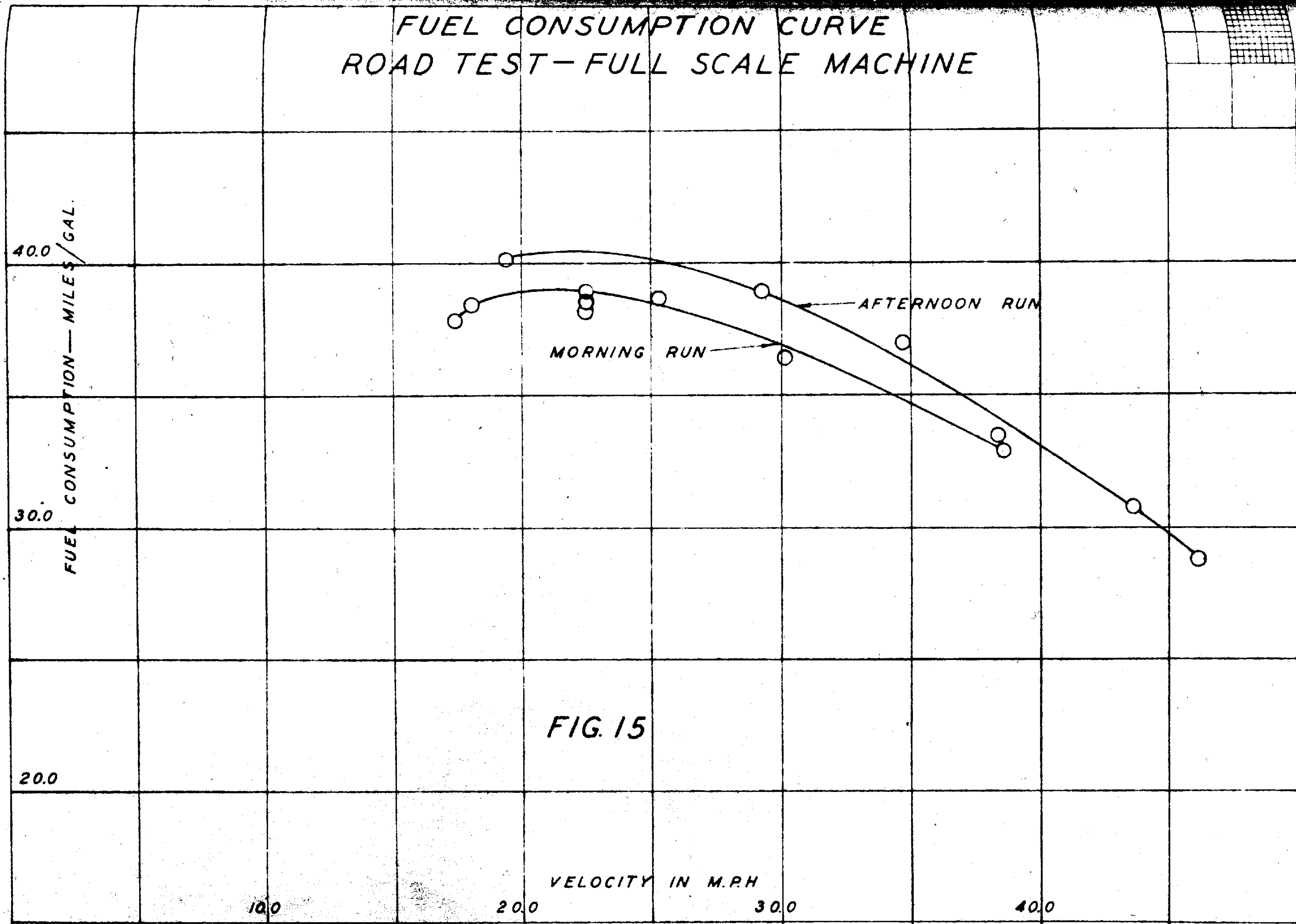

FUEL CONSUMPTION CURVE
ROAD TEST—FULL SCALE MACHINE
FUEL CONSUMPTION—MILES/GAL.
40.0
30.0
20.0
AFTERNOON RUN
MORNING RUN
VELOCITY IN M.P.H
10.0
20.0
30.0
40.0

FIG. 15

it included two curves and almost continuous grades, the steepest was a 2.406 grade, and the gentlest was a 0.535 grade.

The car was equipped with two special tanks. Each tank was connected to the carbureter and each tank was supplied with a shutoff valve. The run was made with the driver and one passenger in the car. The car was brought up to the proper speed before it crossed the starting line at which time the driver started a stop watch. As the car entered on the course, the passenger cut off the fuel supply from one of the tanks and the carbureter was switched onto the other tank which had been carefully weighed together with its contents before it was placed in the car. At the end of the run the driver stopped the watch and the passenger switched the carbureter back to the unweighed tank. The car was immediately turned around and the run repeated in the opposite direction, after which the auxiliary tank was again weighed and the mileage per gallon was computed. The speed was obtained by reference to the stop watch readings. In all the runs the speed was held as nearly constant as possible by means of the speedometer. The economy runs were made at speeds of 20, 22, 25, 30, 33, 35, and 44 miles per hour.

In order to make a comparison between the performance of the full sized machine and the wind tunnel model, and also compare the machine with the conventional car, it was necessary to determine the equivalent flat plate parasite area and the rolling resistance of the full sized machine. The most common method of obtaining these factors has been as follows. First, the Brake Horsepower R.P.M. curve of the motor is determined by dynamometer tests. The machine is then taken out on a straight level stretch of road and driven in two directions at full throttle over a measured course.

The time for these runs is obtained by any suitable means and the top speed of the machine determined.

In order to evaluate the rolling resistance, the car is pulled at a low speed (3 to 5 mi/hr) with a calibrated spring balance or other suitable measuring device, the assumption being justifiably made that at such low speeds the air resistance is negligable.

The author finds several criticisms with this testing procedure which are listed below.

1. No proper determination is made of the efficiency of the driving mechanism. It is of course estimated, but improper adjustment may make this estimate vary considerably. In any case the car's aerodynamic characters are tied up with this estimate.

2. It does not always follow that in the machine on the road, the motor is developing the same BHP. which was indicated on the dynamometer.

3. Determination of the rolling resistance, unless very carefully done, may be very inaccurate.

4. It is assumed that the rolling resistance does not vary with speed. Although this assumption is probably correct, it is still an assumption.

The method just referred to is sometimes improved upon in the following manner. (Ref.4) A special calibrated fifth wheel speedometer is used. The car is brought up to a speed of 60 or 70 miles per hour, shifted into neutral, and allowed to coast to a stop. The time for each five mile per hour drop in speed is accurately determined and recorded. This testing procedure is an improvement over the one first mentioned as it eliminates the difficulties referred to under 1. and 2. above. However, it involves the experimental determination and use of the rolling radius of the wheels and the moments of inertia of the rotating masses. It also presents certain fundamental mathematical difficulties since the forces acting during the deceleration period do not vary in accordance with any simple function of the velocity.

In addition to the general disadvantages of the ordinary testing procedures outlined above, the author was faced with certain special difficulties which may be enumerated as follows:

1. There was not available a smooth, level straight stretch of road of sufficient length for a top speed nor even for a uniform deceleration run.
2. In an experimental machine without springs, it was felt that speeds greater than 65 miles per hour might be dangerous.
3. The author desired to avoid the use of experimentally determined values for the rolling resistance except where such values were obtained for high speed conditions.

4. The author did not want to base his calculations on data obtained from an underpowered worn out motor and a defective differential system. For these and other reasons he decided on the following testing procedure.

Two hills of uniform slope were selected and measured courses were laid out on them. The car was brought up to speed and shifted into neutral after it was well on the hill, but a considerable distance ahead of the beginning of the course. The speed of the car was so adjusted that it entered the course each time at a speed as close as possible to its estimated constant coasting speed. From the time required to cover the first and second half of the course, it was possible to tell whether or not the car lost or gained speed during the coasting period, and by repeated trials it was possible to determine quite accurately the constant coasting speed for the hill in question. Knowing the car weight, and the slope angle of the hill, the constant propulsive force, $W \sin\alpha$, can be calculated.

In regard to rolling friction the opinion of most experimenters is that it does not vary appreciably with speed. The author has questioned this viewpoint when interpreted to mean that the rolling friction at 2 or 3 miles per hour is the same as it is at 50 or 60 miles per hour. He does not, however, question this viewpoint if comparisons are being made between two or more high speeds. Assuming then that the rolling friction is constant, the following equations may be written:

$$W\sin\alpha_1 = F + 0.001185\times1.28\times\overline{1.47}^2\times0.975\times A\times V_1^2 \quad (1)$$

$$W\sin\alpha_2 = F + 0.001185\times1.28\times\overline{1.47}^2\times0.975\times A\times V_2^2 \quad (2)$$

In these equations: A = the equivalent flat plate parasite area. F = the rolling friction. W = weight of loaded machine. α = the slope angle of the hill. 0.975 = the relative density of the air for Atlanta, Georgia, where the tests were made.

From Tables XIII and XIV it will be seen that the constant coasting speed on hill one was 45.0 miles per hour and on hill two was 53.1 miles per hour. Writing equations (1) and (2) and solving simultaneously:

$$2337\times0.0303 = F + 0.00319\times A\times\overline{45.0}^2 \quad (1)$$

$$2343\times0.0373 = F + 0.00319\times A\times\overline{53.1}^2 \quad (2)$$

A = 6.6 sq.ft. $\quad$ F = 28.2 lbs.

In view of the fact that most investigators use 0.0125W lbs. for the rolling resistance (Ref.1 - 7), the results seem quite logical since for a car weighing 2337 lbs, the rolling resistance would be 29.2 lbs. when calculated by the above formula.

It will be noted that this method determines directly the aerodynamic drag characteristics and the rolling resistance characteristics of the machine under investigation. The BHP and the differential drive gear efficiencies are not involved in any way. Once the resistance and rolling friction factors are known, it is possible to determine the performance of the car for any hypothetical engine and for any specified drive gear efficiency.

Before, during, and after the various tests and trial runs referred to above, the car was driven a total of about 1100 miles and a great deal of special information was obtained on its behavior. Many informal runs were made both in traffic and on the open road, weather conditions varying from warm, clear, calm weather to raw, gusty weather. Many runs were made in a strong cross wind. The runs were made at speeds all the way from five miles per hour up to 65 miles per hour. Due to the absence of springs on the experimental machine, only three trips were made on unpaved roads. These trips were particularly valuable since they were used to show the effects of streamlining. It is a well known fact that the more dust a car raises, the less perfect the streamline characteristics. In Figure A, a 1932 Essex coupe is shown on a dusty road running at 45 miles per hour. Figure B shows the Roadplane operating at the same speed on the same road. Notice the house back of the cars, the dust cloud back of the Essex is very dense and it is shoulder high, practically obliterating the house. Back of the Roadplane, the dust cloud is only about waist high and is quite light, leaving the house plainly visible. The difference in power wasted is quite obvious.

FIGURE A
1932 ESSEX COUPE ON DUSTY ROAD. SPEED 45 MILES PER HOUR

FIGURE B

ROADPLANE ON DUSTY ROAD. SPEED 45 MILES PER HOUR

RESULTS

The results of the wind tunnel tests as well as the full scale road tests are presented in this report in graphical form. Tables giving the reduced data are included at the end of the report. In practically all cases the results are shown in the forms of absolute coefficients. The Roadplane, unlike the airplane, operates under yawed conditions most of the time. For this reason there is some question as to whether the coefficients should be referred to wind axes or body axes. For the sake of uniformity the author has referred all coefficients to the wind axes, except in one instance, although in some cases the body axes would have been preferable. The notations used throughout this report are as follows; Lift forces are plus if acting down, minus if acting up. Drag forces are considered as plus if acting to the rear. A stalling moment is plus and a diving moment minus. Angles of attack are minus if the axis of reference is inclined downward toward the front and plus if upwardly inclined. Facing the car a force acting from left to right is plus, and from right to left, minus. Viewed from the same location, a clockwise rolling moment is plus, and a counterclockwise, minus. As seen from above, the yaw is positive if the front of the car is inclined to the right with respect to the relative wind. Viewed from the driver's seat a clockwise yawing moment is positive, and a counterclockwise is negative. The drag coefficients, C_D, are based on the projected frontal area(A), the lift coefficients(C_L), and cross wind coefficients(C_c), are based on the plan area and the car length. The C.P. locations are all calculated as a percent of the car length except the vertical side center of pressure location which is calculated as a percent of the total car height. Center of pressure locations below the road surface or ahead of the nose of the car are given a negative sign.

Several of the curves are plotted for a condition referred to as floating rudders. Such notation indicates that the rudders are set so as to line up into the wind. In other words the rudder angle and the angle of yaw are the same in magnitude, but opposite in signs. Certain curves are plotted for $C_n = 0$, meaning that the rudder deflection is such that the yawing moment is zero. In this report all pitching moments are calculated with reference to an axis passing through the point of contact of the wheels with the ground. This axis is considered to be perpendicular to the plane of symmetry of the car, and is located 37.3 % of the car length back from the radiator. (Except in the case of the Tail Boom Model where it is located at 27.1 % back). In Figures 7 and 8 the wheels are located further forward than 37.3 % of the body length, but all calculations are corrected so that the moments are determined about the 37.3 % point. The yawing moments are calculated about an axis passing through the differential perpendicular to the road surface. The rolling moments are calculated with reference to an axis lying in the road surface and perpendicular to the other two axes.

DISCUSSION

Comparison of Models

In any effort to design a streamlined car, a complete investigation should be made of various body shapes so as to determine that shape which offers the best aerodynamic characteristics, and is otherwise best suited for the purpose. In vehicles whose speed approaches or exceeds one hundred miles per hour, the aerodynamic forces become so large and consume so great a percent of the total power output that well formed shapes must be used unless the designer is willing to accept the penalty of inferior performance. Due allowance should also be given to the stabilizing effects of aerodynamic forces and moments of large magnitude, if safety and comfort are to be retained at the higher speeds. In the design and investigation of the Roadplane, three body shapes, nine cabin shapes, and three tail surface shapes were tested. Figure 16 shows the drag characteristics of these various forms, the outlines of which are shown in Figures 7, 8, 9, and 12. Figure 16 gives the absolute coefficient of drag (C_D) based on projected frontal area, the equivalent flat plate parasite area in square feet, and the drag coefficient expressed as a percent of the flat plate coefficient (1.28). The diagram shows that the Tail Boom Model (Figure 16) has the lowest drag with an equivalent flat plate parasite area of 2.20 square feet. The models with small body fillets (body No.1, cabin No.1, and body No.1, cabin No.2) have the largest drag coefficients. This bears out the results found by other investigations. (Reference 1).

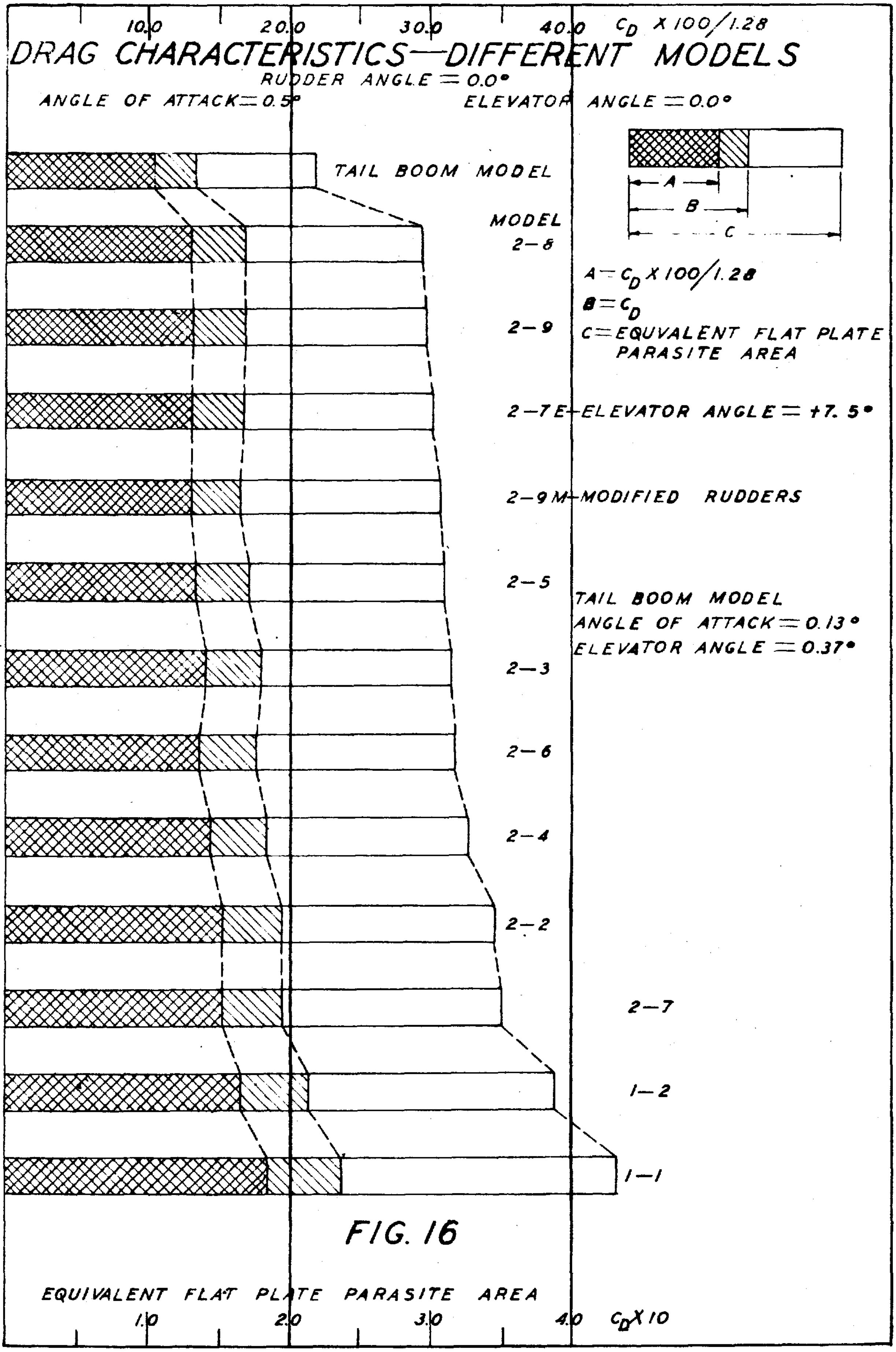
10.0
20.0
30.0
40.0
C_D X 100/1.28
DRAG CHARACTERISTICS—DIFFERENT MODELS
RUDDER ANGLE = 0.0°
ANGLE OF ATTACK = 0.5°
ELEVATOR ANGLE = 0.0°
A
B
C
TAIL BOOM MODEL
MODEL
2-8
A = C_D X 100/1.28
B = C_D
C = EQUIVALENT FLAT PLATE PARASITE AREA
2-9
2-7E ELEVATOR ANGLE = +7.5°
2-9M MODIFIED RUDDERS
2-5
TAIL BOOM MODEL
ANGLE OF ATTACK = 0.13°
ELEVATOR ANGLE = 0.37°
2-3
2-6
2-4
2-2
2-7
1-2
1-1
EQUIVALENT FLAT PLATE PARASITE AREA
1.0
2.0
3.0
4.0
C_D X 10
FIG. 16

One or two other factors of importance can be determined from these charts. It appears that the cabin forms which end in a wedge lying in a vertical plane (2-6, 2-8, 2-9) are superior to those ending in a horizontal edge. (2-2, 2-4). This would seem to indicate that streamlining in plan is superior to streamlining in elevation. The evidence is not conclusive however since interference effects between the main body and the tail surfaces cannot be accurately evaluated for the different cabin shapes. That such interference effects are large is illustrated by reference to 2-7, and 2-7E. In 2-7E the displaced elevator materially improves the flow in the crowded region between the rudders. It will be seen that with the exception of the Tail Boom Model, the model referred to as 2-9M (Body No. 2, Cabin No. 9 with modified rudders) has the lowest drag coefficient (C_D). This model was used in most of the tests. It is illustrated in Figures 6 and 9. Model No. 2-9 was also used in a great many of the tests. By reference to Figures 8 and 9 it will be seen that these models are the same except for their rudders. Both of these models are referred to throughout the report as the Prototype Models. The style of rudders illustrated in Figure 8 is referred to as original rudders, and the style illustrated in Figure 9 is referred to as modified rudders. In Figure 17 the various models are classified according to their C_L and L/D characteristics. In this figure the down forces are noted as plus and the up forces as minus. Several factors

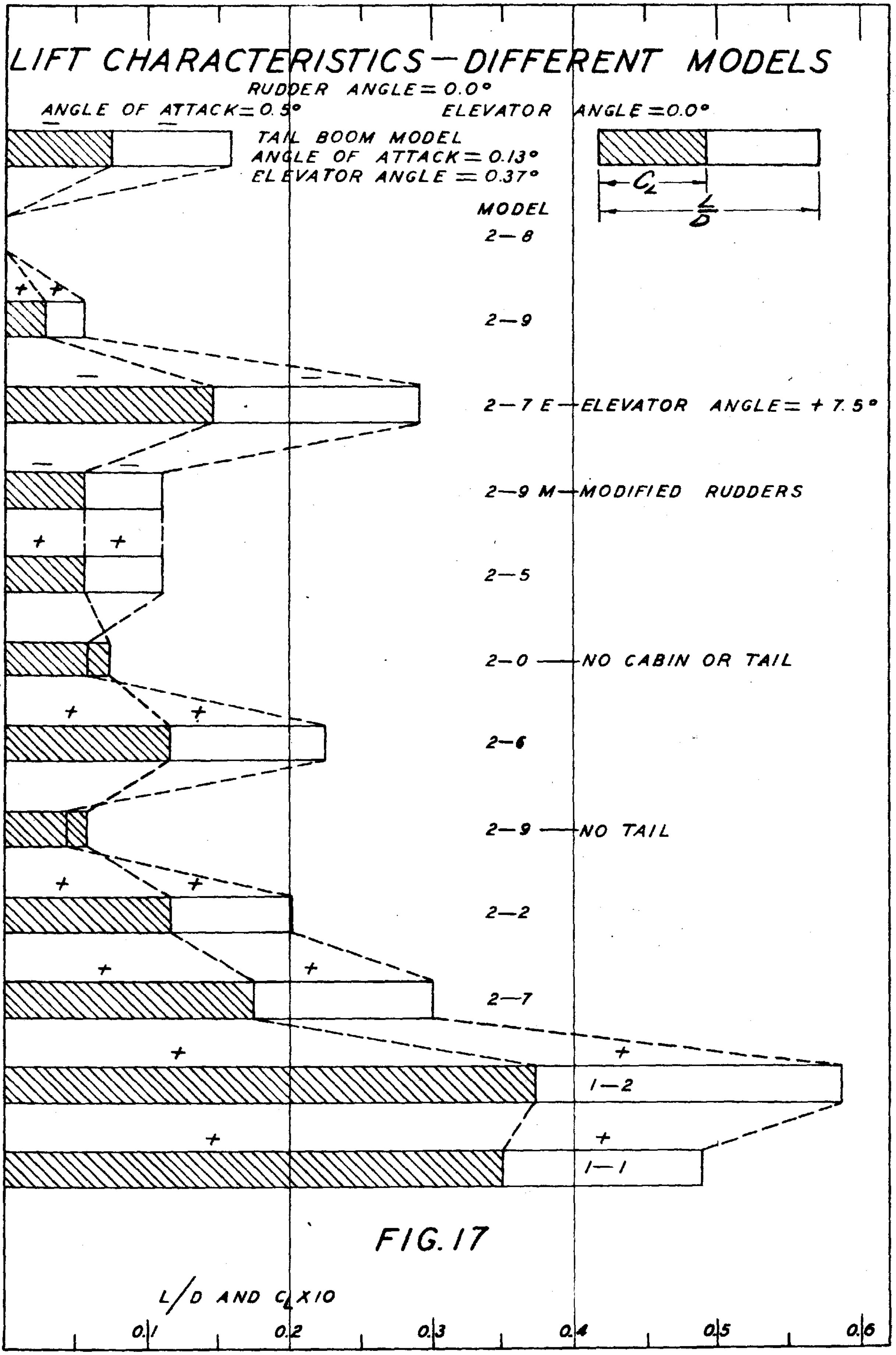
LIFT CHARACTERISTICS—DIFFERENT MODELS
RUDDER ANGLE = 0.0°
ANGLE OF ATTACK = 0.5°
ELEVATOR ANGLE = 0.0°
TAIL BOOM MODEL
ANGLE OF ATTACK = 0.13°
ELEVATOR ANGLE = 0.37°
C_L
L/D
MODEL
2—8
2—9
2—7 E—ELEVATOR ANGLE = + 7.5°
2—9 M—MODIFIED RUDDERS
2—5
2—0 —NO CABIN OR TAIL
2—6
2—9 —NO TAIL
2—2
2—7
1—2
1—1
L/D AND C_L X10
0.1
0.2
0.3
0.4
0.5
0.6

FIG. 17

seem to be important. The lift forces on the Tail Boom Model are up and are not very large at the attitude at which these tests were made. Referring to 1-1 and 1-2 it will be noted that small fillets give a large lift and a large L/D. The lift in this case is down. This factor is of importance since it is desirable to obtain a large lift coefficient in the Roadplane in order that balance may be effected. Since models 1-2 and 1-1 have poor drag characteristics, a compromise design is suggested. In such a design six inch fillets might be used instead of the two and one half inch fillets which are used on Body No. 1, or the nine inch fillets which are used on Body No. 2. By referring to models 2-7 and 2-7E it is seen that the lifting effect of the tail surface is large in proportion to the rest of the body since the small deflection of 7.5 degrees changes the lift coefficient from a minus value to a plus value of about the same magnitude.

Contribution of Parts

Eliminating now from further discussion all the models except 2-9M, 2-9, and the Tail Boom Model it is of interest to investigate the effect that different parts such as the cabin, tail surface, elevator, etc. have upon the aerodynamic characteristics of the model. Since the Tail Boom Model was built in one piece it could not be tested except as a unit, and it will be eliminated from this part of the discussion. By reference to Figure 18 which pertains to the Prototype Model, it will be seen that C_D and flat plate are a minimum at

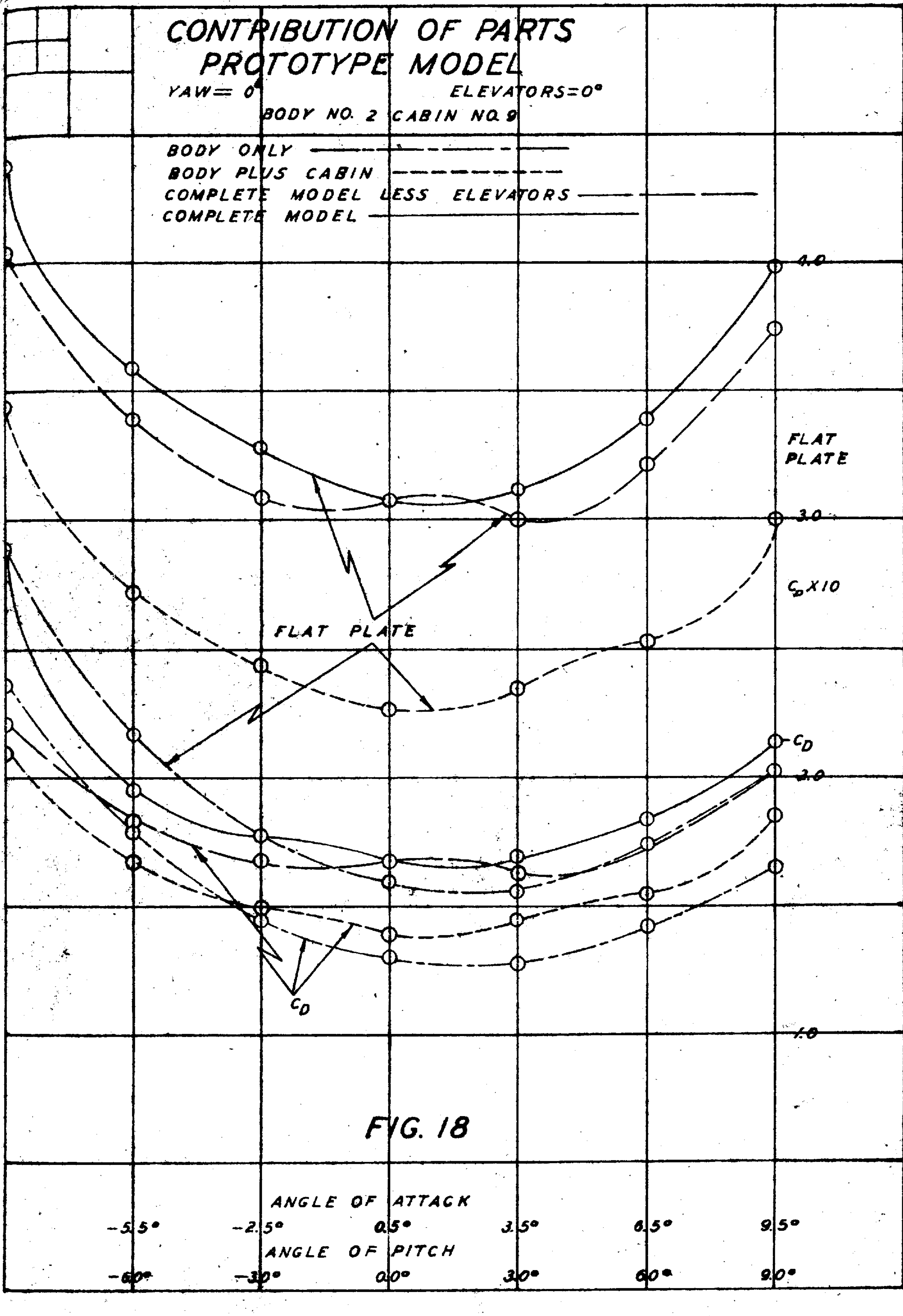
CONTRIBUTION OF PARTS
PROTOTYPE MODEL
YAW= 0°
ELEVATORS=0°
BODY NO. 2 CABIN NO. 9
BODY ONLY
BODY PLUS CABIN
COMPLETE MODEL LESS ELEVATORS
COMPLETE MODEL
4.0
FLAT PLATE
3.0
C_D X10
FLAT PLATE
C_D
2.0
C_D
1.0
ANGLE OF ATTACK
-5.5°
-2.5°
0.5°
3.5°
6.5°
9.5°
ANGLE OF PITCH
-6.0°
-3.0°
0.0°
3.0°
6.0°
9.0°

FIG. 18

0.5 degree angle of attack and increase on both sides of this point except when the model is tested without its elevator in which case the minimum value of the flat plate and C_D are reduced slightly and this reduction occurs at about a 2.0 degree angle of attack. It will be noted that addition of the cabin increases the Equivalent Flat Plate parasite area materially, but increases the C_D only slightly. This effect would be expected. It will be noted that generally speaking the drag effects of the cabin and the tail surfaces are of about the same order of magnitude.

In Figure 19, C_L and C_m for various parts are plotted against the angle of attack. The slope of the lift curves are positive and are steepest for the complete model and the model less elevator.

The effect of the tail surface and the cabin seems to increase the slope of the lift curve slightly. The angle of zero lift is smaller for the complete model than it is for the stripped or partially stripped machine. The curve of pitching moment (C_m) shows an unfortunate condition since it has a positive slope with increasing angle of attack which indicates an unstable condition. It will be seen that the pitching moment is materially effected by the removal or addition of parts as the complete model is much less unstable than the bare body. A small stable range will be noted for the complete model in the region of -5.5 degrees angle of attack. Before the Roadplane can be commercially utilized, the unstable pitching characteristics illustrated by these curves will have to be corrected. Such correction should however present no great difficulty.

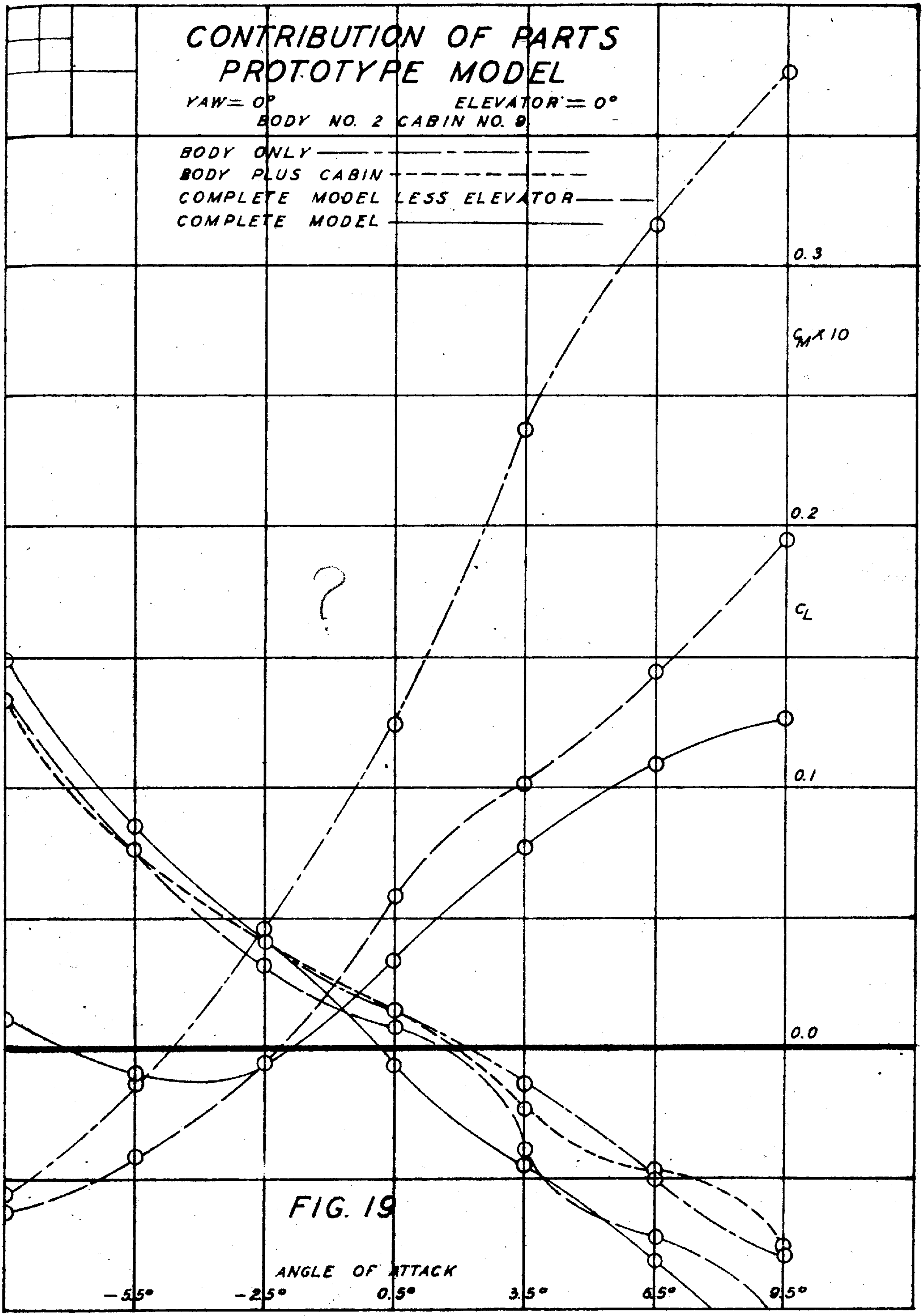
CONTRIBUTION OF PARTS
PROTOTYPE MODEL
YAW = 0°
ELEVATOR = 0°
BODY NO. 2 CABIN NO. 9
BODY ONLY
BODY PLUS CABIN
COMPLETE MODEL LESS ELEVATOR
COMPLETE MODEL
0.3
$C_M \times 10$
0.2
C_L
?
0.1
0.0
ANGLE OF ATTACK
-5.5°
-2.5°
0.5°
3.5°
6.5°
9.5°
FIG. 19

Pitching

In order to get a further insight into the longitudinal stability characteristics of the Prototype and Tail Boom Models, a consideration should be given to Figures 20 through 26. Figure 20 shows the C_D, C_m, and C_L characteristics of the Prototype and Tail Boom Models for various angles of attack. It will be noted from this figure that in both models, the C_L curve has a very steep negative slope and that the C_D curves are in general similar, although the C_D on the Prototype Model is much larger. One prohounced difference is noted. The Tail Boom Model has excellent stability characteristics, since its C_m curve has a pronounced negative slope, but the Prototype Model is definitely unstable. This instability can be explained in the following manner. The C_m curve for the main body of the Prototype Model has a positive slope (Figure 19) and although the addition of the cabin and tail surfaces decrease this slope materially, the tail surfaces are too small and too near the main body to completely correct the undesirable condition. In the Tail Boom Model the tail surfaces are larger and located further back of the wheels where their stabilizing effect is more pronounced. In addition, the body of this model has a more nearly streamlined shape so that the unstable effect of the body,if it exists, is not so pronounced. Referring again to Figures 21, 22, 23, 24, 25, and 26, the effect of the elevator settings on the C_D, C_L, C_m, and C. P. characteristics of the Prototype Model may be observed. Figure 21 shows that, in general, the C_D curve is

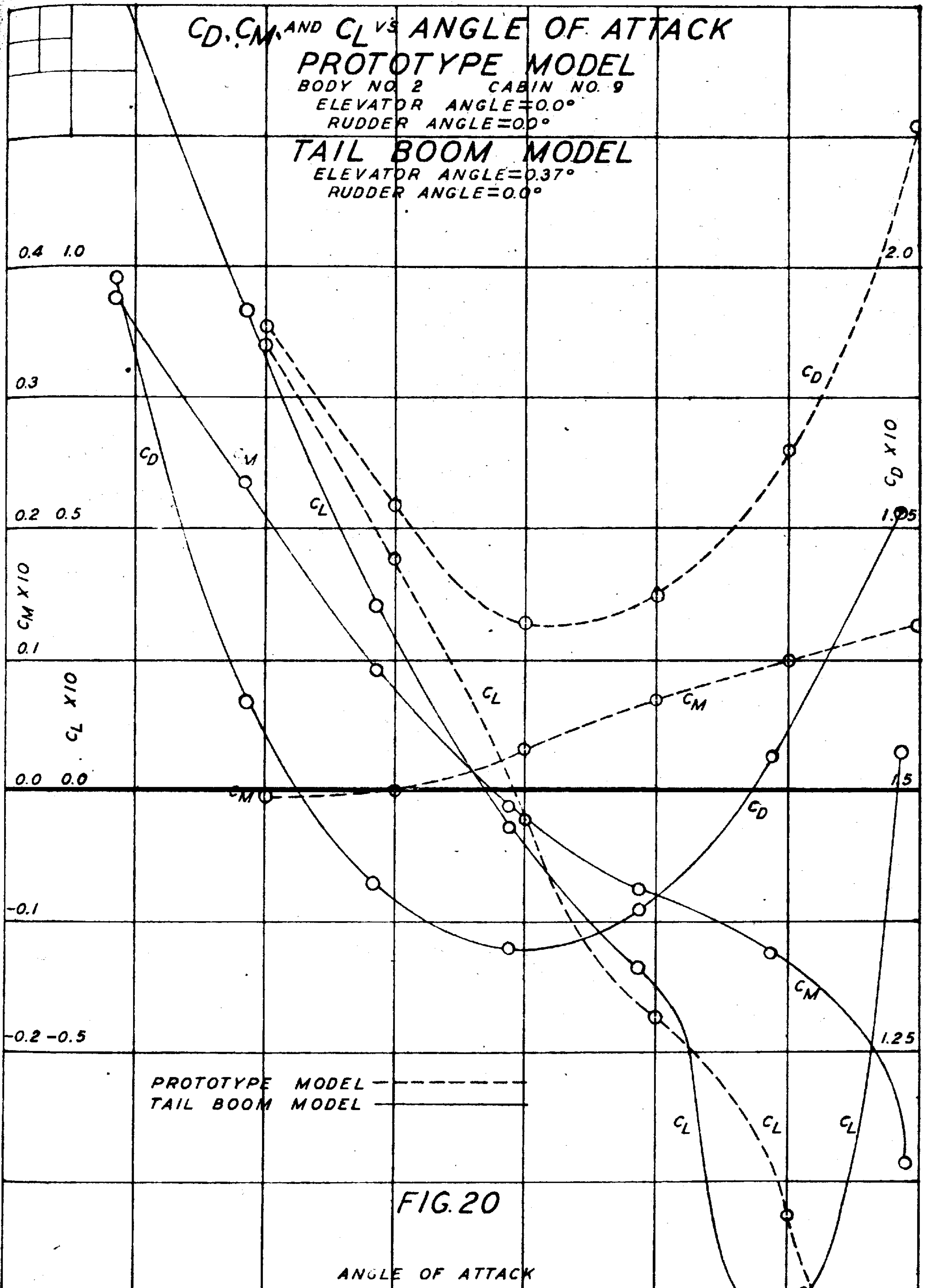

C_D, C_M AND C_L VS ANGLE OF ATTACK
PROTOTYPE MODEL
BODY NO. 2 CABIN NO. 9
ELEVATOR ANGLE=0.0°
RUDDER ANGLE=0.0°
TAIL BOOM MODEL
ELEVATOR ANGLE=0.37°
RUDDER ANGLE=0.0°
0.4 1.0
2.0
0.3
0.2 0.5
1.05
0.1
0.0 0.0
1.5
-0.1
-0.2 -0.5
1.25
C_M X10
C_L X10
C_D X10
C_D
C_M
C_L
PROTOTYPE MODEL
TAIL BOOM MODEL
ANGLE OF ATTACK
-8.5°
-5.5°
-2.5°
0.5°
3.5°
6.5°

FIG. 20

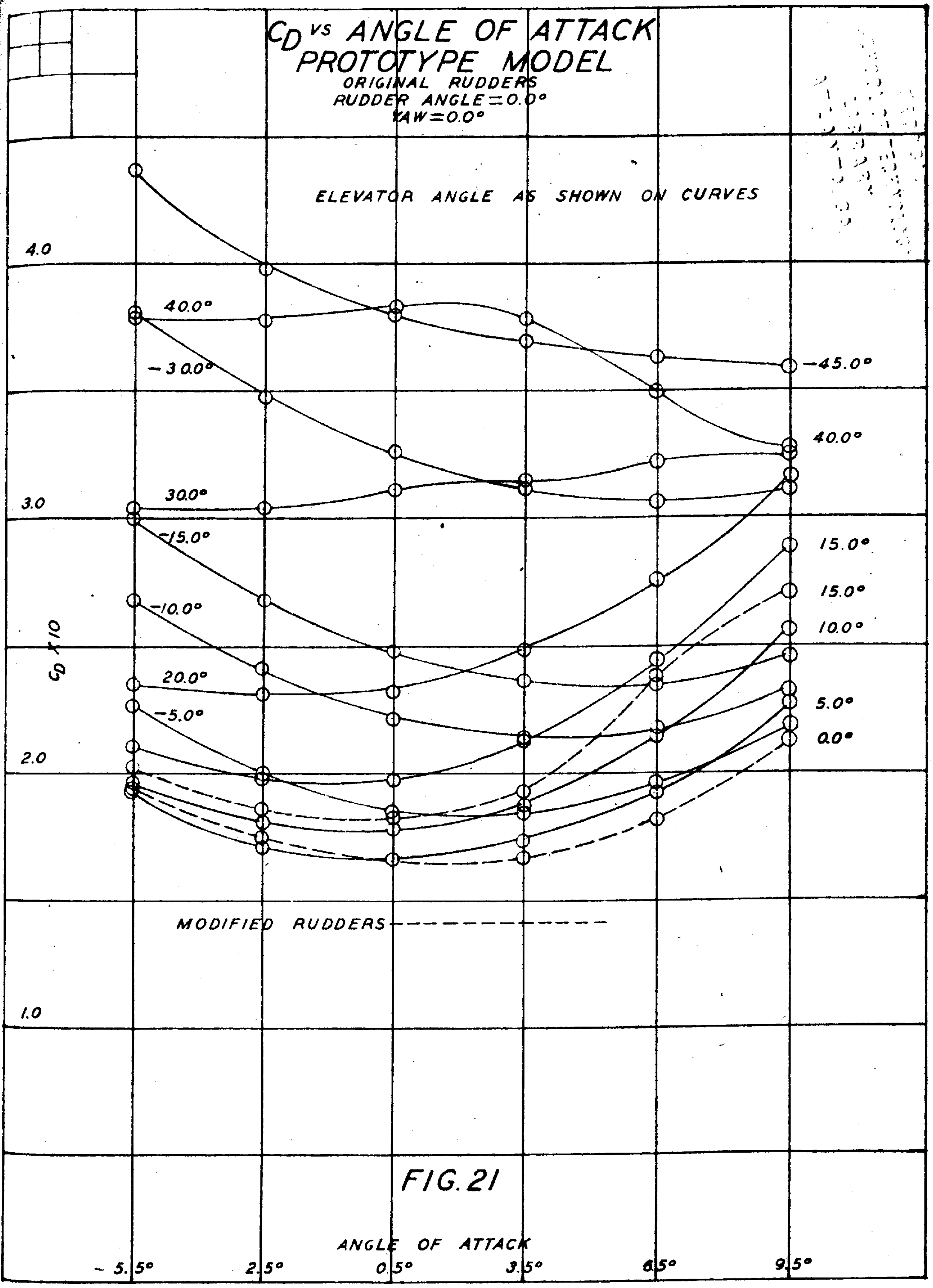

C_D vs ANGLE OF ATTACK
PROTOTYPE MODEL
ORIGINAL RUDDERS
RUDDER ANGLE = 0.0°
YAW = 0.0°
ELEVATOR ANGLE AS SHOWN ON CURVES
4.0
40.0°
−30.0°
−45.0°
40.0°
3.0
30.0°
−15.0°
15.0°
15.0°
−10.0°
10.0°
C_D X 10
20.0°
−5.0°
5.0°
0.0°
2.0
MODIFIED RUDDERS
1.0
ANGLE OF ATTACK
− 5.5°
2.5°
0.5°
3.5°
6.5°
9.5°

FIG. 21

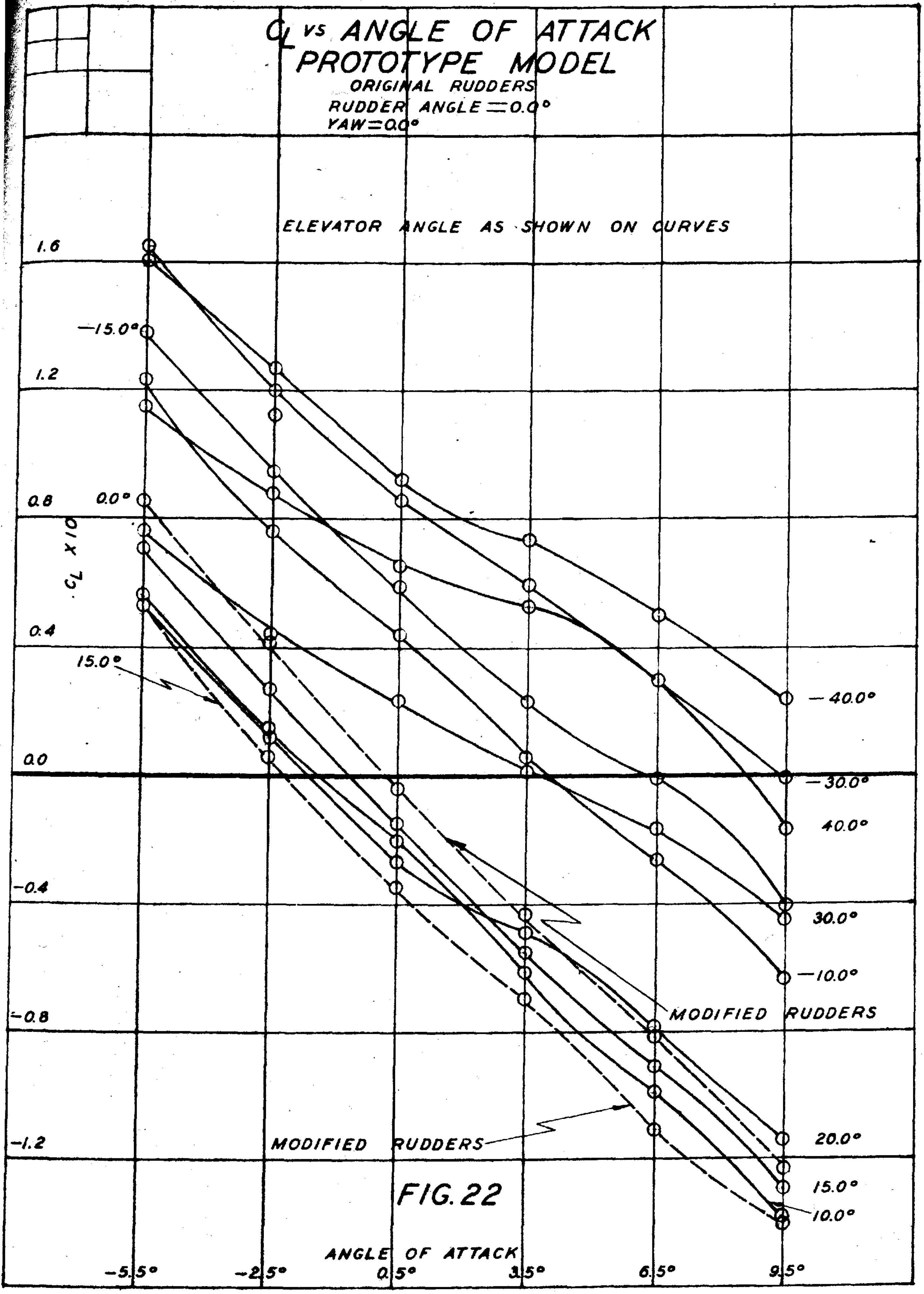

C_L vs ANGLE OF ATTACK
PROTOTYPE MODEL
ORIGINAL RUDDERS
RUDDER ANGLE = 0.0°
YAW = 0.0°
ELEVATOR ANGLE AS SHOWN ON CURVES
1.6
1.2
0.8
0.4
0.0
-0.4
-0.8
-1.2
$C_L \times 10$
-15.0°
0.0°
15.0°
-40.0°
-30.0°
40.0°
30.0°
-10.0°
MODIFIED RUDDERS
20.0°
15.0°
10.0°
MODIFIED RUDDERS
ANGLE OF ATTACK
-5.5°
-2.5°
0.5°
3.5°
6.5°
9.5°

FIG. 22

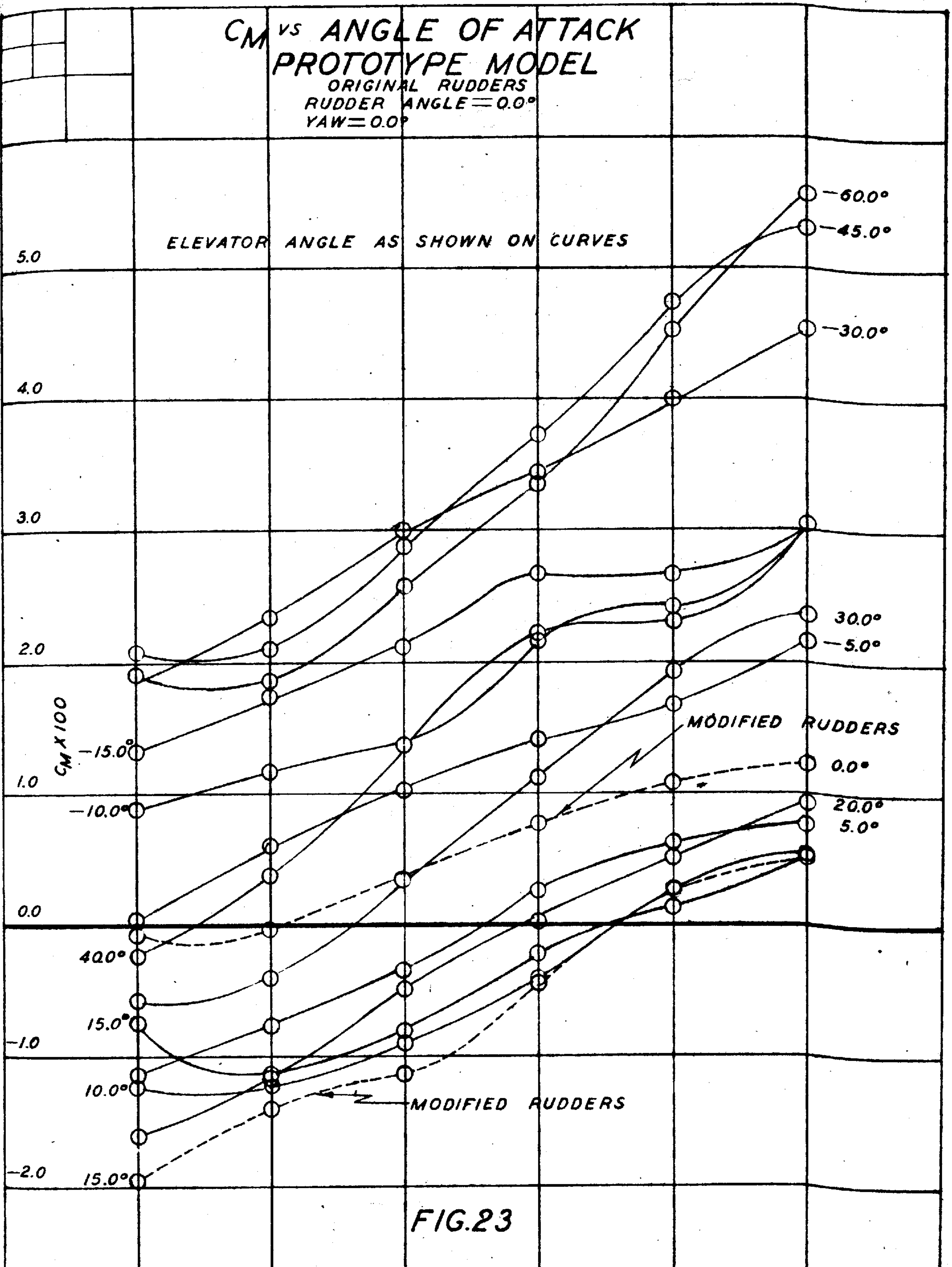

CM vs ANGLE OF ATTACK
PROTOTYPE MODEL
ORIGINAL RUDDERS
RUDDER ANGLE = 0.0°
YAW = 0.0°
ELEVATOR ANGLE AS SHOWN ON CURVES
CM X 100
5.0
4.0
3.0
2.0
1.0
0.0
-1.0
-2.0
-60.0°
-45.0°
-30.0°
30.0°
-5.0°
MODIFIED RUDDERS
0.0°
20.0°
5.0°
-15.0°
-10.0°
40.0°
15.0°
10.0°
15.0°
MODIFIED RUDDERS
ANGLE OF ATTACK
-5.5°
-2.5°
0.5°
3.5°
6.5°
9.5°

FIG. 23

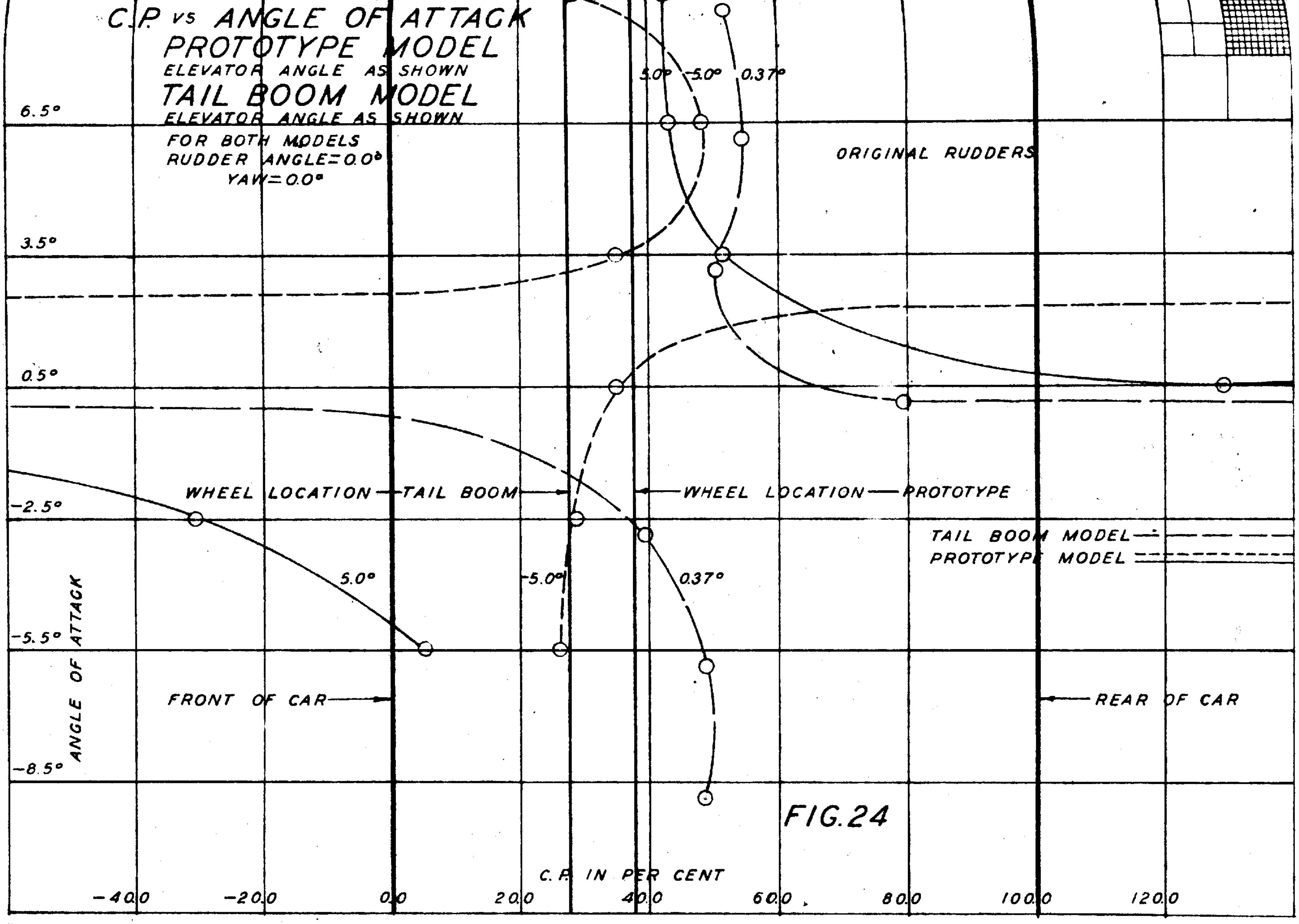

C.P. vs ANGLE OF ATTACK
PROTOTYPE MODEL
ELEVATOR ANGLE AS SHOWN
TAIL BOOM MODEL
ELEVATOR ANGLE AS SHOWN
FOR BOTH MODELS
RUDDER ANGLE=0.0°
YAW=0.0°
ORIGINAL RUDDERS
5.0°
-5.0°
0.37°
6.5°
3.5°
0.5°
-2.5°
-5.5°
-8.5°
WHEEL LOCATION—TAIL BOOM
WHEEL LOCATION—PROTOTYPE
TAIL BOOM MODEL
PROTOTYPE MODEL
5.0°
-5.0°
0.37°
ANGLE OF ATTACK
FRONT OF CAR
REAR OF CAR
C.P. IN PER CENT
-40.0
-20.0
0.0
20.0
40.0
60.0
80.0
100.0
120.0

FIG.24

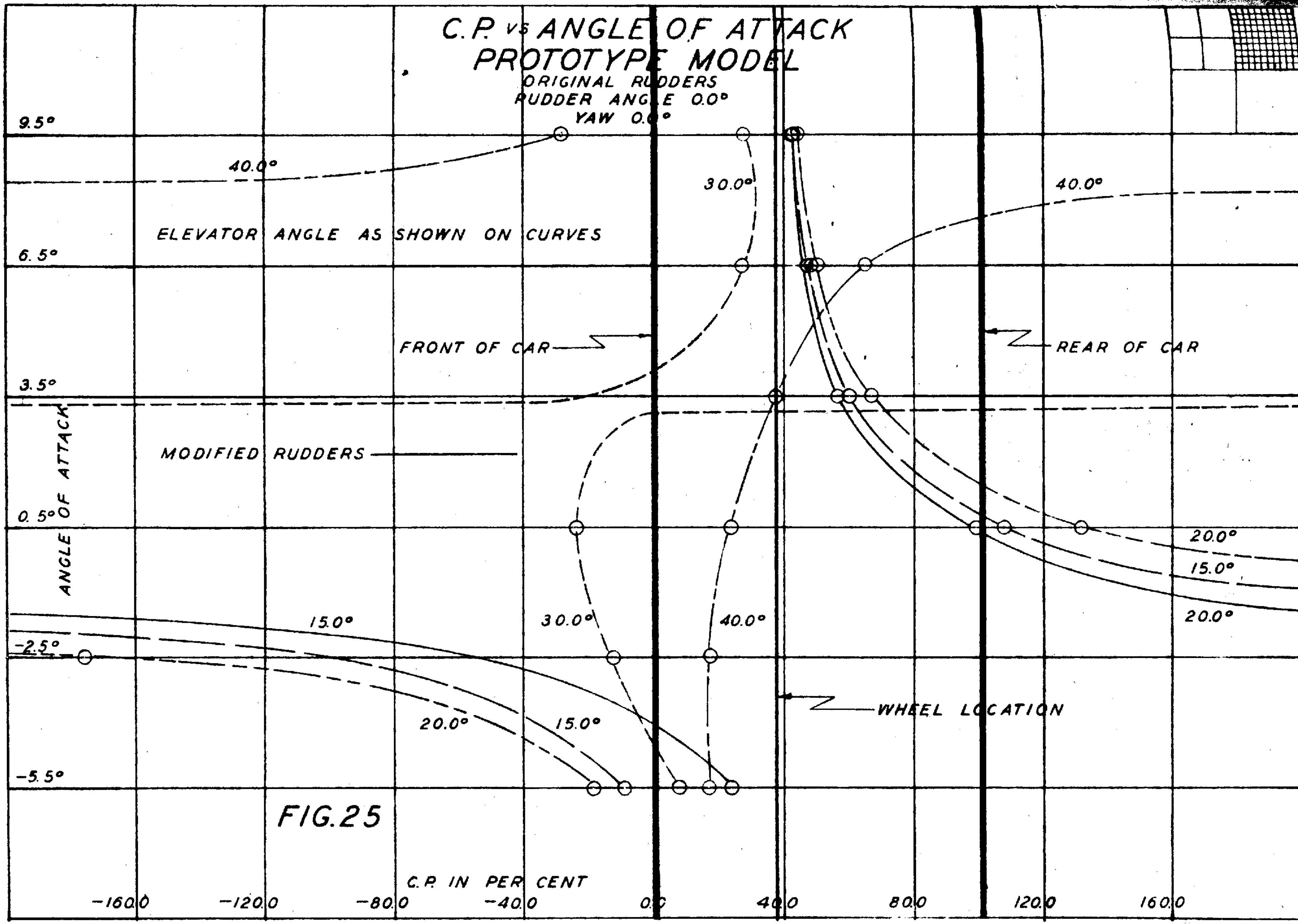

C.P. vs ANGLE OF ATTACK
PROTOTYPE MODEL
ORIGINAL RUDDERS
RUDDER ANGLE 0.0°
YAW 0.0°
ELEVATOR ANGLE AS SHOWN ON CURVES
FRONT OF CAR
REAR OF CAR
MODIFIED RUDDERS
WHEEL LOCATION
9.5°
6.5°
3.5°
0.5°
-2.5°
-5.5°
40.0°
30.0°
20.0°
15.0°
ANGLE OF ATTACK
C.P. IN PER CENT
-160.0
-120.0
-80.0
-40.0
0.0
40.0
80.0
120.0
160.0

FIG.25

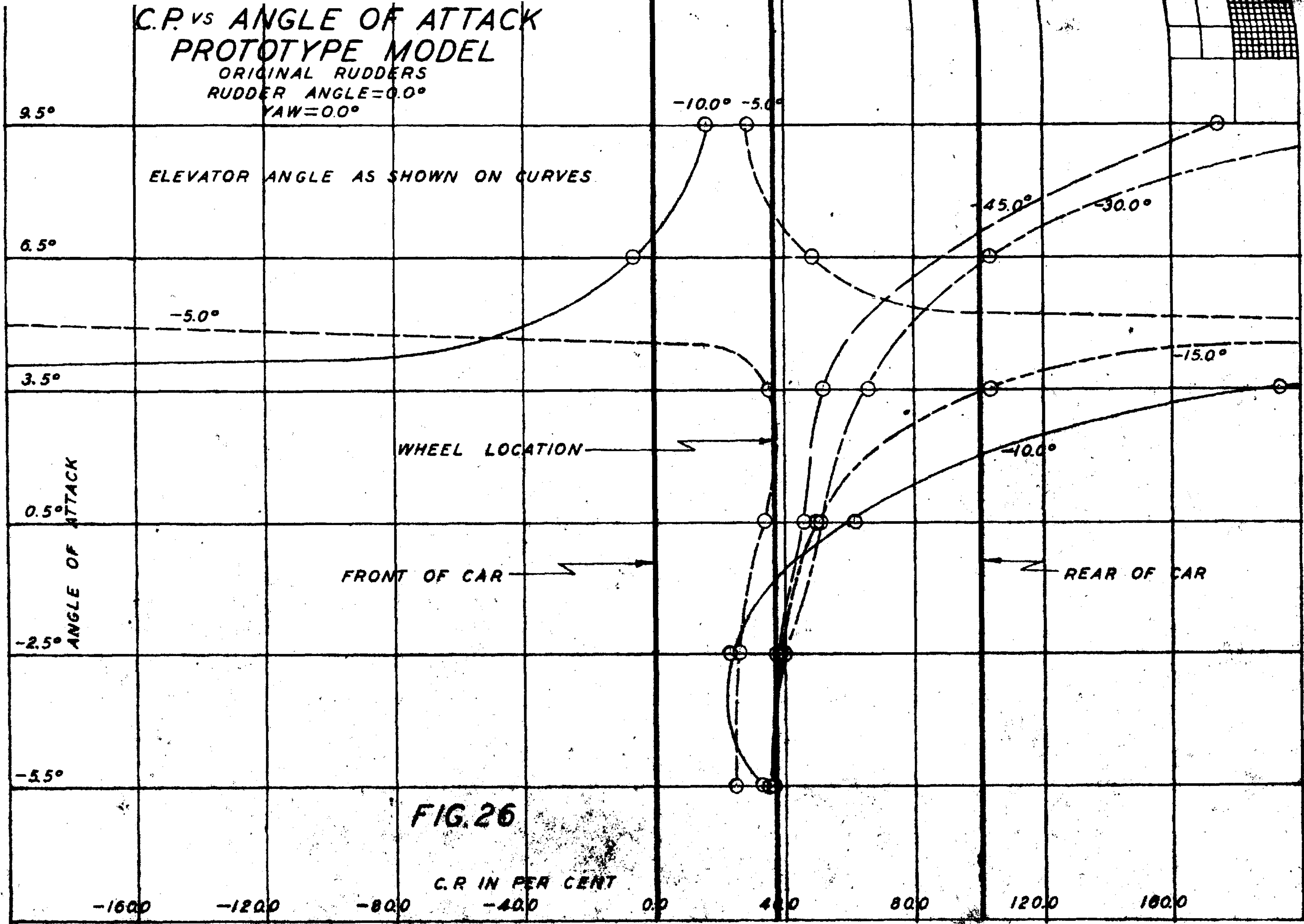
C.P. vs ANGLE OF ATTACK
PROTOTYPE MODEL
ORIGINAL RUDDERS
RUDDER ANGLE=0.0°
YAW=0.0°
ELEVATOR ANGLE AS SHOWN ON CURVES
-10.0°
-5.0°
-45.0°
-30.0°
-5.0°
-15.0°
-10.0°
WHEEL LOCATION
FRONT OF CAR
REAR OF CAR
9.5°
6.5°
3.5°
0.5°
-2.5°
-5.5°
ANGLE OF ATTACK
C.P. IN PER CENT
-160.0
-120.0
-80.0
-40.0
0.0
40.0
80.0
120.0
160.0

FIG. 26

simply displaced vertically by change in elevator setting. The most pronounced difference noticed in the C_D curves is the fact that they have a different general shape for positive and negative elevator settings indicating a change in flow conditions when the elevator passes from one side to the other of the zero setting. A peculiar shape is also noted for the curves which have a large positive setting (30 and 40 degrees). This is probably due to the fact that the flow over the whole body is stalled when the elevator is displaced to these large angles. Figure [illegible] brings out the fact, now well established in the aerodynamics of the airplane, that a change in elevator angle does not materially effect the longitudinal stability of the machine, but simply changes the angle of attack for trim. This condition is practically the same as that found in the airplane. A change in the setting of the fixed stabilizer simply causing the pitching moment curve to move vertically, the angle of trim is changed, but the general longitudinal stability is only slightly affected, if at all. Figure 28 shows a similar effect for the C_L curve. It is clear from these curves that no correction can be obtained for the unstable condition by the simple expedient of changing the incidence of the tail plane.

In Figure 27, C_D is plotted against elevator angle. As would be expected the minimum value of C_D occurs when the elevator is very near its neutral position. For the larger positive angles of attack of the model (6.5 and 9.5 degrees) C_D is at a minimum when the elevator is only about one degree from

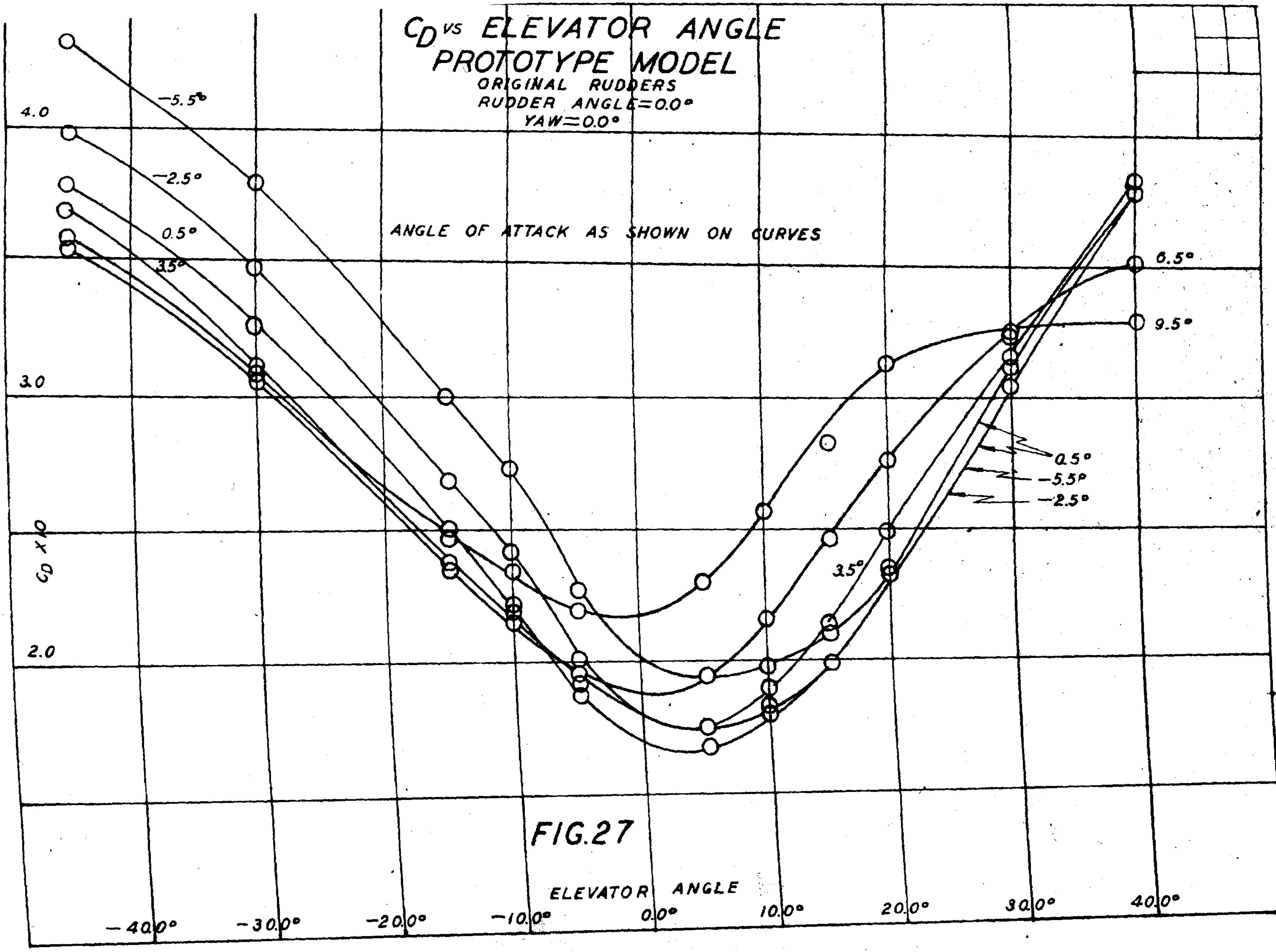

C_D vs ELEVATOR ANGLE
PROTOTYPE MODEL
ORIGINAL RUDDERS
RUDDER ANGLE=0.0°
YAW=0.0°
ANGLE OF ATTACK AS SHOWN ON CURVES
-5.5°
-2.5°
0.5°
3.5°
6.5°
9.5°
0.5°
-5.5°
-2.5°
3.5°
4.0
3.0
2.0
$C_D \times 10$
ELEVATOR ANGLE
-40.0°
-30.0°
-20.0°
-10.0°
0.0°
10.0°
20.0°
30.0°
40.0°

FIG.27

the zero setting while for the other angles of attack the minimum value of C_D occurs at about plus 4 degrees elevator setting.

In Figure 28 the lift coefficient C_L is plotted against elevator angle. The resulting curves illustrate the fact that large positive angles of attack for the elevator will not increase the value of the negative lift coefficient. Figure 29 shows the effect of rudder displacement on elevator control. The curves also illustrate the obvious fact that a deflected rudder increases the drag for any elevator setting. It is noted from these curves that C_L and C_m are both increased when the rudder is deflected to a large angle. This effect may be explained in this manner. The trailing edge of the elevator is cut away on each side so that the rudders may be moved.

Such mutilation of course materially reduces the effectiveness of the elevator as a control surface. When the rudders are deflected 30 degrees the inswinging rudder is almost against the side of the elevator. It would seem that this would improve the flow condition on that side and correct at least partially for the effect of the mutilation on that side. It must be admitted of course that the gap between the outswinging rudder and the elevator has been widened but the effect is minor since even in the neutral position this gap is so large that no appreciable shielding effect could be expected from the rudder. It is of interest to note the sudden change in lift when the elevator is displaced more than about plus 15 degrees. It would seem from the shape of the C_L curve in this region that the

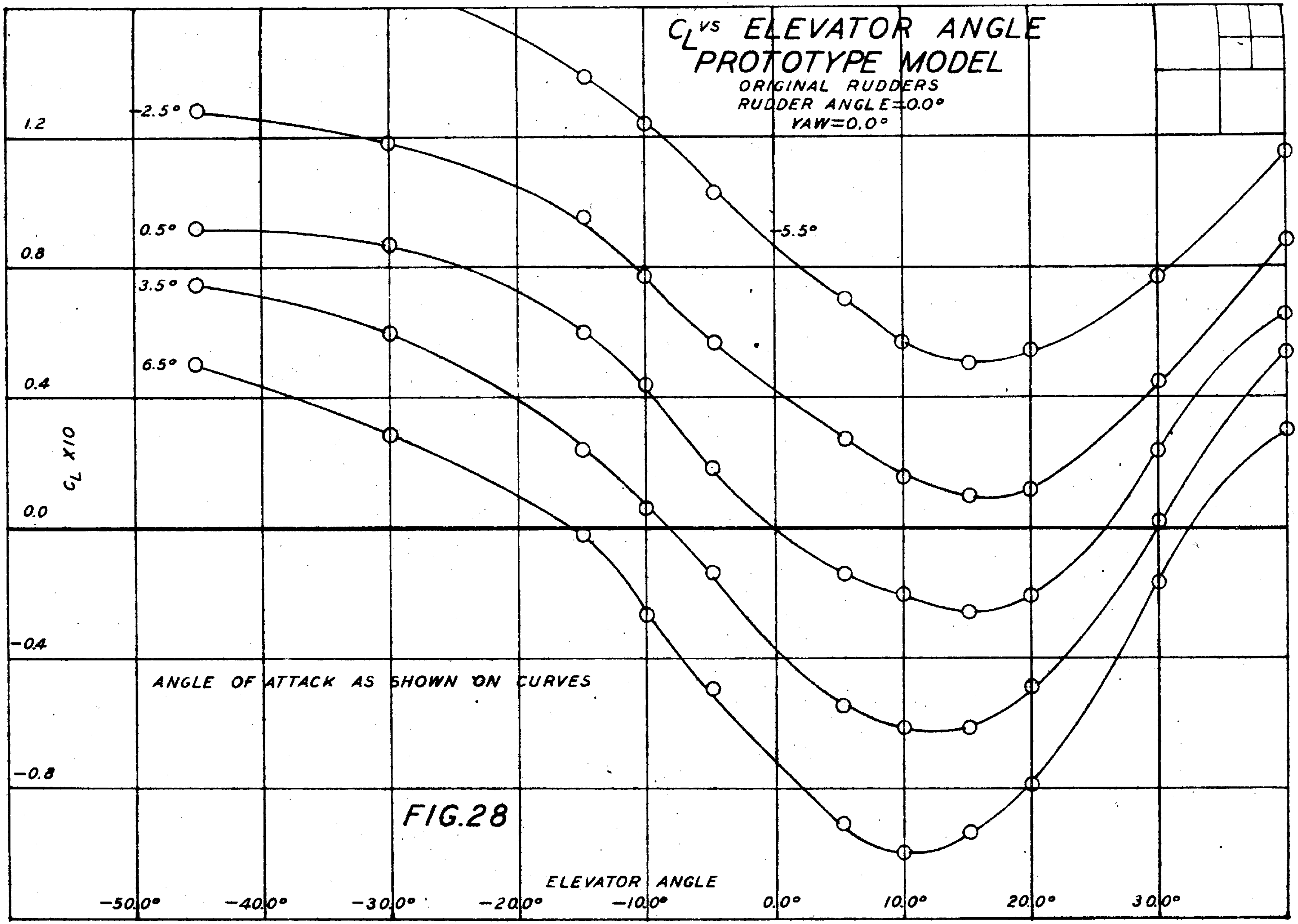
CL vs ELEVATOR ANGLE
PROTOTYPE MODEL
ORIGINAL RUDDERS
RUDDER ANGLE=0.0°
YAW=0.0°
-2.5°
0.5°
3.5°
6.5°
-5.5°
1.2
0.8
0.4
0.0
-0.4
-0.8
CL X10
ANGLE OF ATTACK AS SHOWN ON CURVES
ELEVATOR ANGLE
-50.0°
-40.0°
-30.0°
-20.0°
-10.0°
0.0°
10.0°
20.0°
30.0°

FIG.28

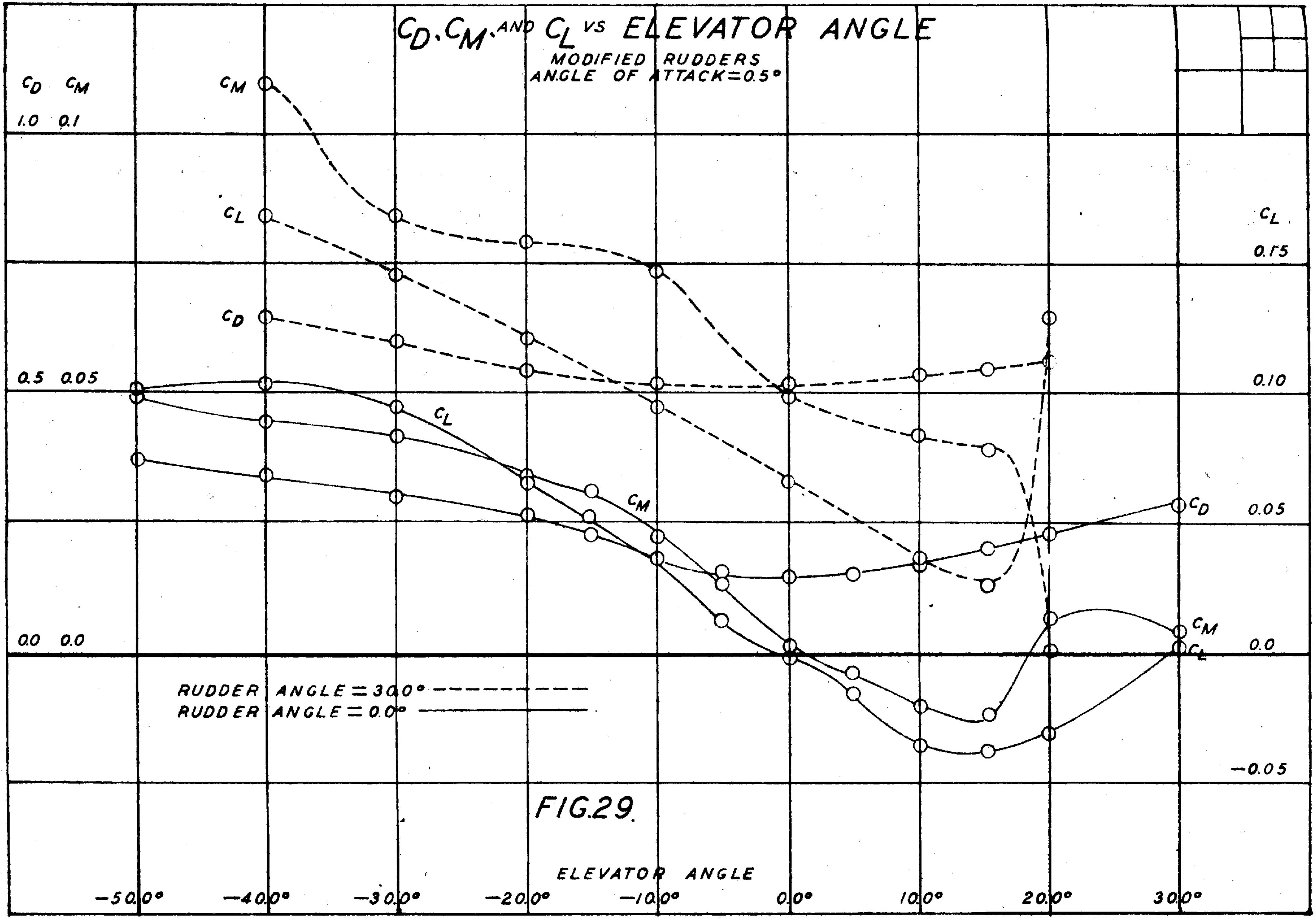

C_D, C_M, AND C_L VS ELEVATOR ANGLE
MODIFIED RUDDERS
ANGLE OF ATTACK = 0.5°
C_D C_M
1.0 0.1
0.5 0.05
0.0 0.0
C_L
0.15
0.10
0.05
0.0
-0.05
C_M
C_L
C_D
RUDDER ANGLE = 30.0°
RUDDER ANGLE = 0.0°
ELEVATOR ANGLE
-50.0° -40.0° -30.0° -20.0° -10.0° 0.0° 10.0° 20.0° 30.0°

FIG. 29.

proximity of the displaced rudder accentuates the increase in down load which occurs when the elevator stalls. The corresponding change in the C_m curve is to be expected and is a further illustration of the close relationship between the two curves. Attention is once more called to the fact that in the Roadplane as presently designed the positive elevator setting should not exceed 15 degrees to 18 degrees if smooth flow conditions are to be maintained. It may be said in regard to Figure 29 that a large rudder deflection has the same general effect on the balance of the machine as now designed as would a decrease in the angle of attack of the elevator. This effect has been noticed in the full sized machine as follows. When the full sized machine is running on two wheels a sudden rudder deflection always brings the nose up. Part of this effect is no doubt due to the increased drag moment but reference to Figure 29 shows that an increased down load on the body also occurs. The author believes that this effect could be partially corrected for if the elevator were made full width and the rudders were cut away to allow for clearance instead of the reverse arrangement which is now used.

Balance

In any discussion of the balance and stability characteristics of the Roadplane it is important to consider all the pitching moments which act on the machine. These moments may be classified as follows:

1. Aerodynamic pitching moments.
2. Pitching moments due to the weight of the machine.
3. Pitching moments due to the vertical accelerations of the machine.
4. Pitching moments due to the horizontal accelerations of the machine.
5. Pitching moments due to the angular acceleration of the rotating masses whose axes are not parallel to the plane of symmetry.
6. Pitching moments due to the friction on journals which do not lie in a plane parallel to the plane of symmetry.
7. Pitching moments due to rolling resistance.

In any practical application, item 6 is so small in comparison to the other items that it may be safely neglected.

Due to the many variables involved, the car will be analyzed for only one elevator setting and for the condition of zero yaw. It will also be assumed that the car is traveling in a straight path, with the rudders in their neutral position. Only longitudinal static stability will be considered in this analysis.

A free body for the driving wheels, and for the car less

FREE BODY OF ROADPLANE

GENERAL CASE

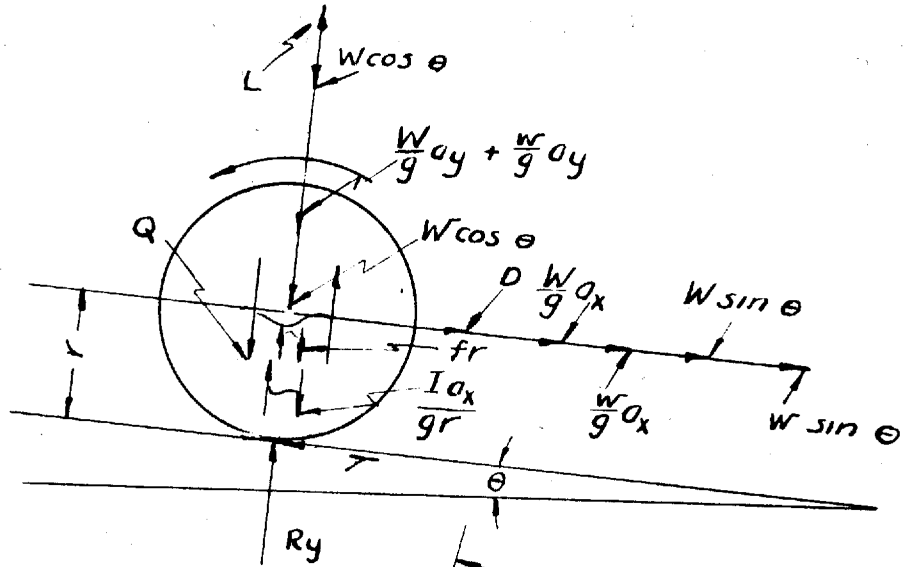

FIG. 30-a

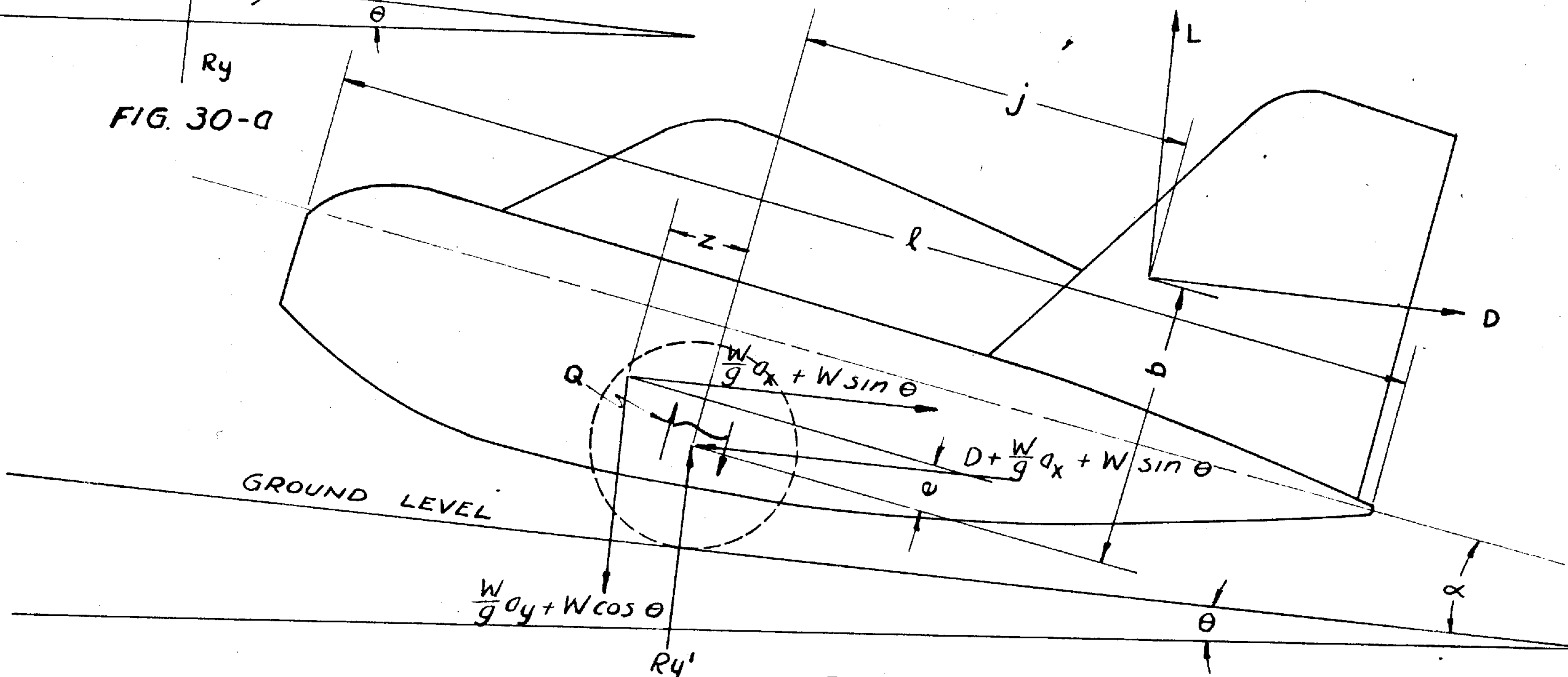

FIG. 30-b

wheels are shown in Figures 30-a and 30-b. These figures will apply equally well to any of the models discussed in this report as well as to the full scale machine. The analysis will be made on the basis of two wheeled operation in all cases.

Notation Used

X = axis taken parallel to road.

Y = axis taken perpendicular to road.

fr = Rolling friction couple assumed independent of speed.

$\frac{I\,a_x}{g\,r}$ = Acceleration couple involving the moment of inertia of the wheels and their angular acceleration. This couple becomes zero when the car is running at constant speed. In any case it is quite small.

T = Thrust force applied at point of contact of the wheel with the ground. This force decreases or changes direction when the car is decelerating.

Q = couple from motor applied at ring gear.

Ry = $\overline{Y}$ reaction from wheels on body.

Ry′ = Reaction from ground perpendicular to road.

= Length of car.

L = Aerodynamic lift assumed positive if acting down.

D = Aerodynamic drag assumed positive if acting to rear.

W = Weight of car less wheels and differential system.

w = Weight of wheels and differential system.

$\overline{W}$ = Total weight of machine.

Ay = Acceleration perpendicular to road surface.

Ax = Acceleration parallel to road surface.

e = Distance above the axle of the C.G. of the car less wheels and differential system.

b = Height of C. P. above axle.

g. = Acceleration due to gravity = 32.2 ft/sec.^{2}

r = Radius of wheels.

z = Longitudinal location of the C. G. of the car less wheels and differential system.

j = Longitudinal location of the C. P. with respect to the axle.

When the car is balanced on two wheels free bodies can be set up for any condition. Consider the condition where the longitudinal axes of the car makes a positive angle (angle of attack) with the surface of the road and where the road makes a positive slope angle with respect to the horizontal. In all cases the assumption is made that the relative wing blows parallel to the road surface.

Applying now the equations of Equilibrium, Figures 30-a and 30-b. Down forces plus, up forces minus. Rearward acting forces plus, forward acting forces minus. Clockwise moments plus, counter-clockwise moments minus.

$$T = D + \frac{\overline{W}a_x}{g} + \overline{W}\sin\Theta \qquad (1)$$

$$R_y = \overline{W}\cos\Theta + \frac{\overline{W}a_y}{g} - L \qquad (2)$$

$$Q = \frac{I}{g}x\frac{a_x}{r} + Tr + fr \qquad (3)$$

Substitution of (1) in (3)

$$Q = \frac{I}{g}x\frac{a_x}{r} + \left(D + \frac{\overline{W}a_x}{g} + \overline{W}\sin\Theta + f\right)r \qquad (4)$$

Consider now (Fig. 30-b)

$$R_{y_1} = W_x\cos\Theta + \frac{W_x a_y}{g} - L \qquad (5)$$

$$Lj\cos\alpha + Lb\sin\alpha - Db\cos\alpha + Dj\sin\alpha =$$

$$Q - W_x\left(\cos\Theta + \frac{a_y}{g}\right)(Z\cos\alpha - e\sin\alpha) + W_x\left(\sin\Theta + \frac{a_x}{g}\right)(Z\sin\alpha + e\cos\alpha) \qquad (6)$$

Substituting (4) in (6)

$$Lj \cos \alpha + Lb \sin \alpha - Db \cos \alpha + Dj \sin \alpha - Dr =$$

$$\frac{I}{g}\frac{a_x}{r} + \overline{W}r\left(\frac{a_x}{g} + \sin \Theta\right) - W\left(\cos \Theta + \frac{a_y}{g}\right)(Z \cos \alpha - e \sin \alpha)$$

$$+ W\left(\sin \Theta + \frac{a_x}{g}\right)(Z \sin \alpha + e \cos \alpha) + fr \qquad (7)$$

But

($Lj \cos \alpha + Lb \sin \alpha - Db \cos \alpha + Dj \sin \alpha - Dr$) is equal to the aerodynamic pitching moment acting on the car. Therefore these terms can be replaced by $\frac{1}{2}\rho SV^2C_M\ell$ where (S) is the plan area of the car, (ℓ) its length, and (C_M) is the pitching moment coefficient referred to an axis passing through the point of contact of the wheels with the ground. C_M as above referred to has been calculated with its proper signs for all the wind tunnel tests. Making this substitution in (7) we have:

$$\frac{1}{2}\rho SV^2C_M\ell = \frac{I}{g}\frac{a_x}{r} + \overline{W}r\left(\frac{a_x}{g} + \sin \Theta\right) + fr$$

$$+ W \cos \alpha \left(\frac{a_x e}{g} - \frac{a_y Z}{g}\right) + W \sin \alpha \left(\frac{a_x Z}{g} + \frac{a_y e}{g}\right)$$

$$+ We \sin (\Theta + \alpha) - WZ \cos (\Theta + \alpha) \qquad (8)$$

Equation (8) gives the aerodynamic pitching moment, or the aerodynamic pitching moment coefficient, required to balance a given Roadplane for any conditions of speed and road. Or if the aerodynamic characteristics are know from wind tunnel tests, the proper horizontal or vertical C.G. locations may be calculated for any specified set of operating conditions.

Equation (8) is determined for the condition where the car is going uphill and where the angle of attack is positive. It is also assumed that the accelerations are such that they cause reverse effective forces which act in a positive direction.

It is further assumed that the C. G. of the body is ahead of and above the axle. When any of these conditions change, equation (8) must be corrected as follows. When the sense of the acceleration is changed the signs of Ax and/or Ay must be changed. Cosine functions of $(\theta + \alpha)$ and/or θ do not change signs. When α, θ, and/or $(\theta + \alpha)$ become minus, the sine functions of α, θ, and/or $(\theta + \alpha)$ become minus. (Positive angles measured clockwise as shown). The factor (Z) changes sign only when the C. G. is back of the axle and the factor (e) changes sign only when the C. G. is below the axle. With these corrections the equation is perfectly general and will apply to any specified set of conditions.

It will be seen from equation (8) and Figure 30-a that contrary to first impressions, the motor does not exert any torque tending to pitch the body unless the wheels are restrained from moving by an externally applied couple. In this case the moment (Tr) is counteracted by the externally applied couple above mentioned and the motor couple (Q) is left free to pitch the body. The pitching of the car which exists at the lower driving speeds is due to the reverse effective forces resulting from the high horizontal accelerations occuring at these speeds. At the higher speeds where the horizontal accelerations are small, or zero, pitching is caused primarily by the aerodynamic forces acting on the car, by vertical accelerations due to road irregularities, by the rolling resistance of the wheels, and by hills. The weight will also exert a pitching moment even when the car is on a level road unless $Z = 0$. Equation (8) shows that the pitching moments acting on the Roadplane are of two general classes.

1. Aerodynamic pitching moments.

2. Pitching moments other than aerodynamic.

The important thing to note is that the pitching moments in class two are a function of the accelerations and not the speed. They are also fixed for any given machine unless the C. G. is shifted. It will be obvious as the discussion proceeds that the C. G. position for low speeds and high speeds must be different since at low speeds the possible accelerations are high and the necessary aerodynamic moments for balance are absent. It should be understood that the Roadplane can be operated successfully as a three wheeled machine at any speed, but its operation as a two wheeled machine is limited to the case where the machine is running at high speed on a good highway. It is also important that this speed be essentially constant. It will be interesting then, to investigate the Roadplane for a practical set of conditions.

Consider first the questions of acceleration and deceleration. Modern cars can decelerate as fast as 32.2 ft/sec^2. Equation (8) will reveal that it will be impossible to keep the Roadplane balanced on two wheels when it is subjected to decelerations of anything like this magnitude unless the car is running at an extremely high speed or unless its C. G. is located in a very peculiar position. Therefore when the brakes are applied or the motor is suddenly throttled the machine will cease to operate as a two wheeled vehicle. This condition is not a disadvantage since it is logical that in emergencies the operator will desire the added firmness and sense of security which comes with three wheeled operation. Contrary to preconceived impressions, the transition from two wheeled operation to three wheeled operation even at high speeds does not present any inherent dangers. The author has repeatedly made such transitions in the full scale machine without experiencing any fear, discomfort, or loss of control.

From the preceding discussion it will be seen that an arbitrary limit must be placed on the minimum speed and on the deceleration possible when the machine is operated as a two wheeled vehicle. For the purposes of this report these limits will be as follows; minimum speed for two wheeled operation 60.0 miles per hour. Maximum acceleration or deceleration along the path, 2 ft/sec^2. Since few cars canattain an acceleration of 2 ft/sec^2 when running at 60 miles per hour the limit referred to above really is a limit on deceleration only. It will also be assumed that no hills whose slope angle is greater than 3.5 degrees(6% grade) will be encountered. (Most states now limit their grades on high speed highways to 6%). Due to the varying influence of such factors as weight, springing and road surface, it becomes very difficult to place a limit on the maximum value of the vertical acceleration. Since the analysis is to be made for a well built machine running on a smooth surfaced high speed highway (Two wheel operation is not practical on poor roads) at a speed of 60 miles per hour, it will be assumed that at this speed the maximum possible value of the vertical acceleration will be 8.0 ft/sec². In dealing with the acceleration forces it will be logical to consider their effects as cumulative.

In a practical Roadplane the maximum possible value of α will not exceed $\pm 4.0°$. The C. G. of the body less wheels and differential system will be placed at a point zero inches ahead of the axle and one foot above it. Consider now the term $\frac{I}{g}\frac{a_x}{r}$. For the assumed acceleration and for a wheel of 12 inch radius whose moment of inertia = 37.8 lb. ft.², the term $\frac{I}{g}\frac{a_x}{r}$ becomes equal to 4.7 lbs.ft. The effect of such a couple is obviously negligible when compared to any of the other moments involved as will be seen shortly.

In the ordinary car the rolling resistance is equal to $0.0125\overline{W}$ lbs. Using this figure the factor (fr) can be replaced by $0.0125\overline{W}r$.

Writing equation (8) in its simplified form, we have

$$1/2\ SV^2C_M = \overline{W}(a_x/g + \sin\Theta + 0.0125)r + W\cos\alpha(ea_x/g - Za_y/g) + W\sin\alpha(Za_x/g + ea_y/g) + We\sin(\Theta + \alpha) - WZ\cos(\Theta + \alpha) \quad (9)$$

It will be obvious that for the case under consideration, the larger the value of $(\Theta + \alpha)$, the large the positive pitching moment. The worst case will occur when the car is going up hill with a large angle of attack and with (a_x) positive and (a_y) negative. Another bad condition will occur going down hill with (a_x) negative and (a_y) positive.

These conditions, however, are not practical in an actual case since even high performance cars cannot accelerate up a 6 percent grade while running at 60 m.p.h., conversely they can, but do not ordinarily decelerate when going down grade. For the above reasons it will be safe to assume that ($a_x = 0$) when going up or down a 6% grade and on other grades the value of (a_x) will be changed accordingly. The term (a_y) is a function of the road surface spring design and speed, it will be considered in all cases and will be given a sign such as to increase the magnitude of the adverse moments.

Consider the three extreme cases:

1. Car on level road accelerations maximum.
2. Car climbing a 6% grade ($a_x = 0$).
3. Car descending a 6% grade ($a_x = 0$).

It will be most instructive to consider the moments other than aerodynamic acting on the car under the above conditions. Since these moments are independent of speed they can readily be determined and compared with the aerodynamic moment for any speed. For the speed in question (60 miles per hour) it is desirable to see if balance is possible with the present design of machine. If balance is not possible the speed for balance can be determined or if such speed is too high, changes can be made in the basic design so as to increase the aerodynamic pitching moments available. In Figure 31 the pitching moments in lb. ft. acting on a 2400 lb. car are plotted against α for the three extreme cases just mentioned (w assumed =200 lbs., r, [redacted] and e =1.0 ft.). Figure 31 also shows the aerodynamic pitching moments in lbs. ft. acting on both the Prototype and the Tail Boom Models when running at 60.0 miles per hour. These curves bring out the fact that the Roadplane is basically unstable.

In the Prototype Model the aerodynamic pitching moments are also unstable in character, as before noted, so that the condition of unstability is increased instead of improved. This condition is noticeable in the operation of the full scale machine since two wheeled operation is possible only on a level road and then it is accomplished only by judicious use of elevator and throttle. Conditions are much better for the Tail Boom Model, but the corrective aerodynamic pitching moments are much too small. Before building the present full scale machine the author built a Tail Boom type of machine which had no body. This machine was aerodynamically stable and two wheeled operation was quite satisfactory when running at constant speeds on a level road.

Two ways of obtaining stability and balance present themselves:

1. Reduce adverse unstable moments acting on machine.
2. Increase slope of (Cm) curve.

Consider Method 1.

It will be seen that the weight of the Roadplane should be as small as possible and concentrated close to the driving axle. Rolling friction should also be kept at a minimum. The rotating masses should be light and the wheel radius should be as small as possible. In a practical machine improvement can be made in all of these items.

Consider Method 2.

The slope of the aerodynamic pitching moment curve can be increased as follows:

1. Longer tail and body.
2. Increased tail area.
3. Use a tail airfoil with a steeper (C_L) curve.
4. Improve body shape so as to steepen the (C_L) curve.
5. Increase aspect ratio of horizontal tail surface.
6. Move wheels further forward.
7. Incorporate an automatic control device to change angle of attack of elevator when car goes up or down hill or accelerates.

Practical considerations of size, comfort, and maneuverability eliminates from consideration items 1, 5, and 6. Considerable improvement can be obtained by the changes indicated in item 7. The use of such an automatic stabilizer when incorporated with the improvements indicated in items 2, 3, and 4, will, in the opinion of the author, not only solve the problem but will simplify the machine in that the driver will not be required to exercise any longitudinal control. Figure 32 shows a sketch of one form of automatic stabilizer which is extremely simple. In Figure 31 the aerodynamic pitching moments obtainable when such a device is used on the Prototype Model are plotted. It will be noted that correction is still not complete but the im-

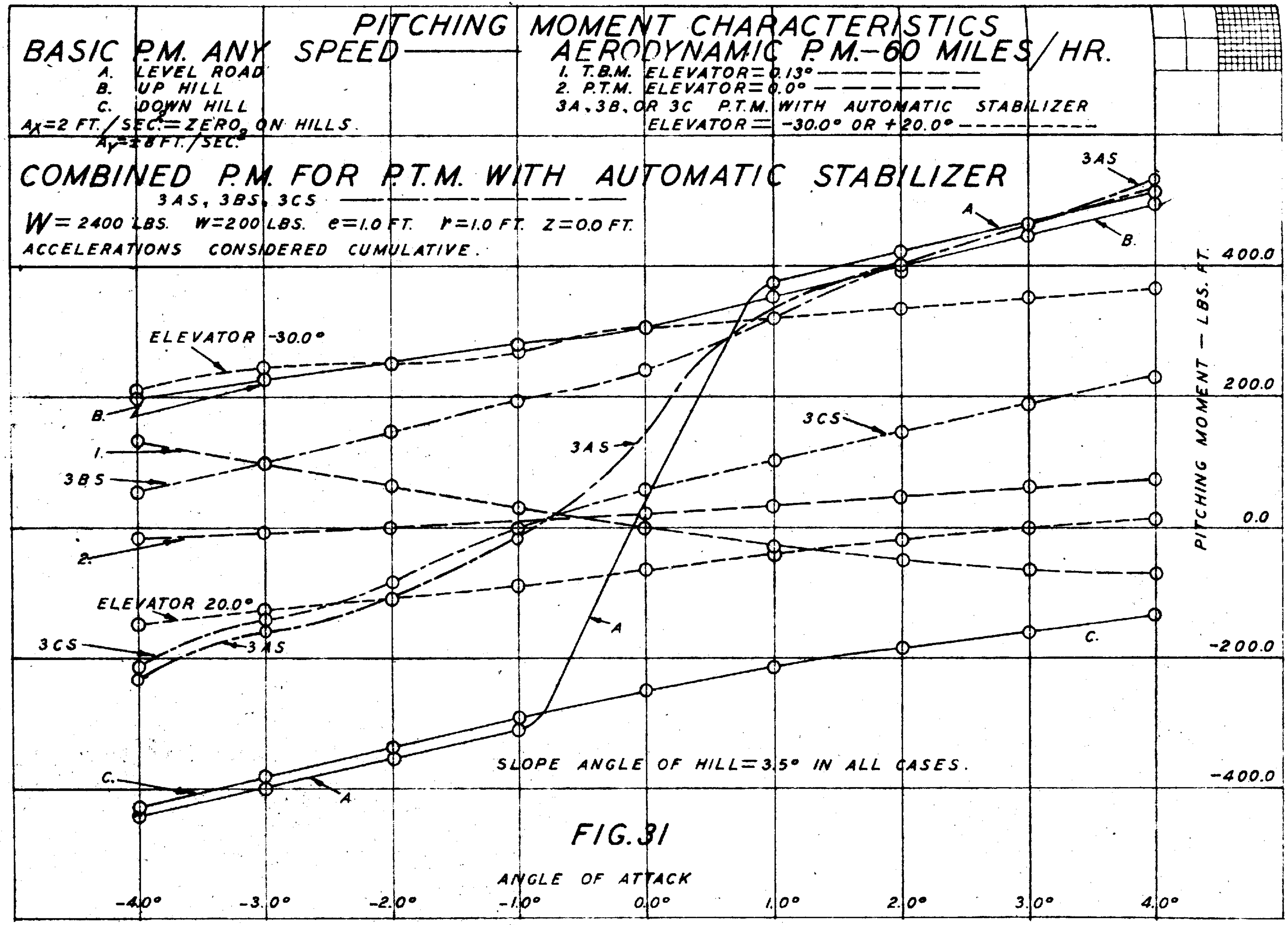
PITCHING MOMENT CHARACTERISTICS
BASIC P.M. ANY SPEED ——— AERODYNAMIC P.M.-60 MILES/HR.
A. LEVEL ROAD
B. UP HILL
C. DOWN HILL
Ax=2 FT./SEC.2=ZERO ON HILLS.
AY=28 FT./SEC.2
1. T.B.M. ELEVATOR=0.13°
2. P.T.M. ELEVATOR=0.0°
3A, 3B, OR 3C P.T.M. WITH AUTOMATIC STABILIZER
ELEVATOR= -30.0° OR +20.0°
COMBINED P.M. FOR P.T.M. WITH AUTOMATIC STABILIZER
3AS, 3BS, 3CS
W=2400 LBS. W=200 LBS. e=1.0 FT. r=1.0 FT. Z=0.0 FT.
ACCELERATIONS CONSIDERED CUMULATIVE.
ELEVATOR -30.0°
ELEVATOR 20.0°
3AS
3BS
3CS
A
B.
C.
1.
2.
SLOPE ANGLE OF HILL=3.5° IN ALL CASES.
PITCHING MOMENT — LBS. FT.
400.0
200.0
0.0
-200.0
-400.0
ANGLE OF ATTACK
-4.0°
-3.0°
-2.0°
-1.0°
0.0°
1.0°
2.0°
3.0°
4.0°

FIG. 31

provements mentioned under items 2, 3, and 4 when combined with this device should effect a complete cure.

In addition to this device it will be necessary to incorporate a device to shift the motor forward so that the machine will not buck at low speeds and when parking. Details of such a device will not be given in this report although the author has worked them out and they do not present any particular mechanical difficulty. It should be understood that the device for changing the location of the C. G. will not be used for control or balance but will simply be a two position device such that for rough roads or city driving the C. G. will be considerably ahead of the axle and for high speed driving the C. G. will be very near the axle as indicated in the preceding discussion.

AUTOMATIC STABILIZER FOR ROADPLANE

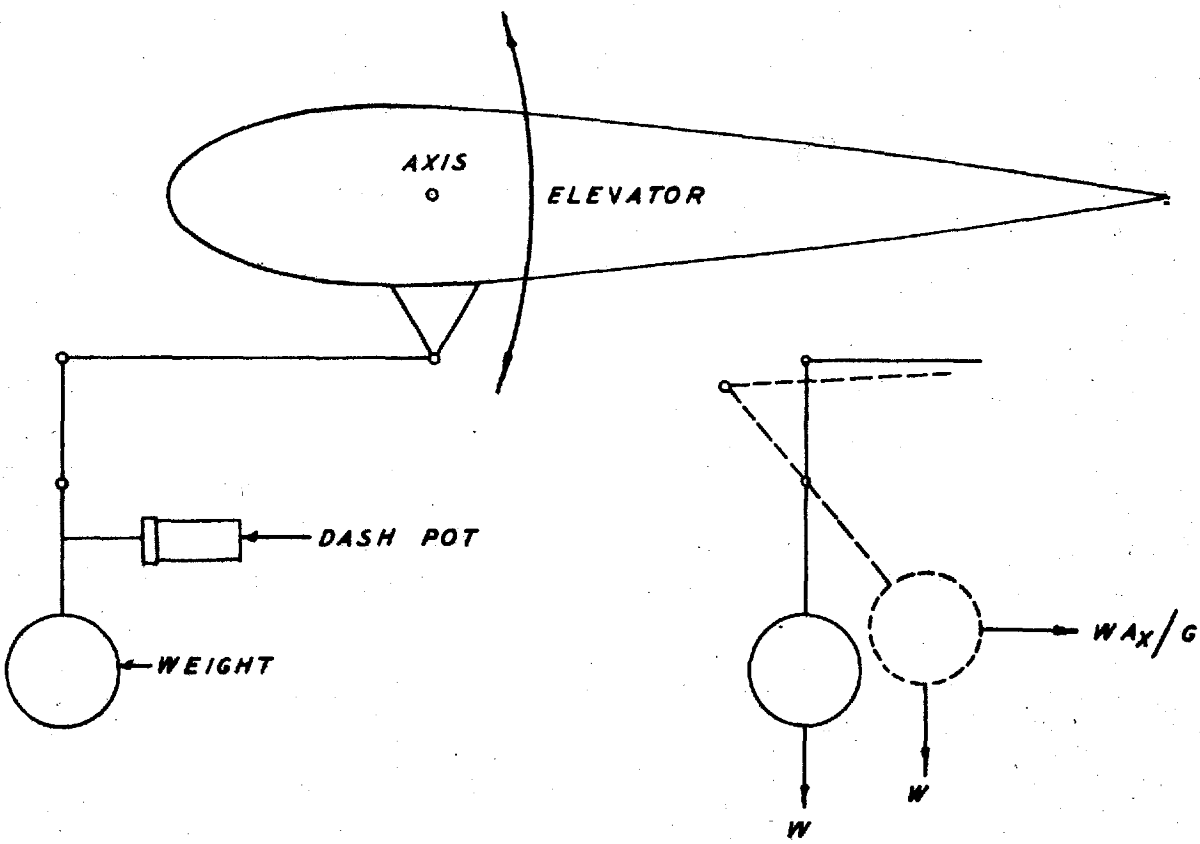

FIG. 32

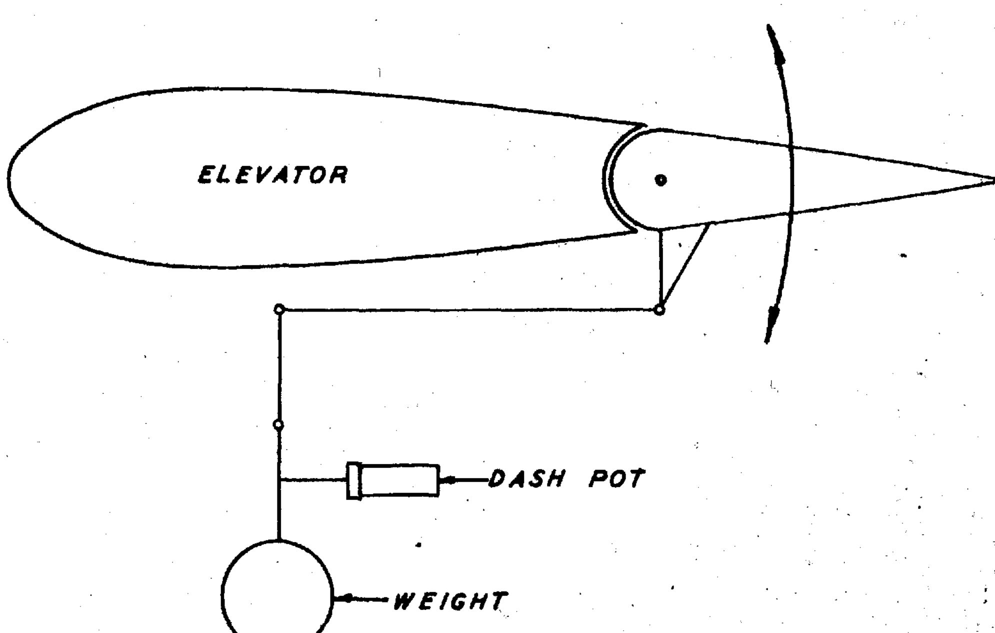

Yawing

In any type of vehicle it is of primary importance for the operator to be able to select a path of motion, maintain the vehicle in this path, or deviate from this path as desired. In a high speed machine it is also essential that the vehicle possess a certain degree of static stability or at least possess no static instability about the yawing axis. In addition to the above requirements dynamic stability about the yawing axis is desirable although not absolutely essential, if the operator is supplied with powerful controls. In high speed land vehicles the problems of directional control and stability become very complex since road friction forces, aerodynamic forces, and forces due to linear and angular accelerations all exert their influence. It would seem obvious that in a well designed machine an effort would be made to so correlate these varying factors that their harmful effects would be small and non-cumulative and their helpful effects would be utilized to the maximum advantage. Such a method of design is not, however, commonly used. Air forces except as they effect performance are consistently ignored and such factors as the effects of center of gravity location are considered almost solely from the standpoint of riding comfort.

It is customary to assume that no matter what external forces or couples are applied to the car that all harmful effects may be overcome by proper application of friction forces, acting at the point of contact of the wheels with the ground. It is also accepted without argument that a car must have four wheels and that it must be steered by the angular deflection of the two front wheels. When any suggestion is made to steer a car by any of the other ten known methods of steering, the intrepid one is looked upon aghast.

For example, when air steering is suggested, practically all automotive engineers are quick to point out the fact that air is a very tenuous and variable substance and therefore not suitable for a steering medium. These same engineers accept without question coefficients of friction which vary from 0.06 to 0.8 (depending on road conditions) and design their whole system of control around them.

In the discussion to follow, air steering will hold the center of the stage since the author has fairly complete data on this form of control. In 1100 miles of operation he has found it to be a practical and safe means of control for a road vehicle. In the design of future machines of the Roadplane type air steering would probably not be used, not because the author does not think that it can be made thoroughly practical, but simply because another form of steering is being investigated which is superior even to air steering and has the additional advantage of being much more simple and compact than either air steering or steering by the classical method of deflecting a wheel or wheels.

In discussing the yawing characteristics of the Roadplane it should be borne in mind that its operation is quite different from the airplane. The airplane operates practically all of the time in a relative wind produced solely by its own motion and therefore rarely operates under yawed flight conditions. In contrast to this condition, the Roadplane operates under yawed conditions most of the time. In view of this fact only slight directional stability is desired for the Roadplane, otherwise it will be too much affected by gusts and cross winds. A consideration of Figure 33 shows that both the Prototype Model and the Tail Boom Model Roadplanes are stable about a yawing axis. This stability is, in fact, too pronounced and should be reduced.

It would seem that the use of servo rudders would correct this situation since with the rudders floating into or nearly into the direction of the relative wind the slope of the (C_N) curve is actually reversed. A change in body shape or a relocation of the wheels would also have a corrective effect. The excessive stability shown in these curves is also present in the full scale machine since it tends to head into gusts unless restrained from doing so by the operator. The complete correction of this condition does not present any serious difficulty. Figure 34 shows the character of the cross wind force coefficients (C_C) for both types of machine. It will be noted that the (C_C) curves have essentially the same shape as the (C_N) curves, center of pressure locations are also shown in this figure as well as cross wind coefficients for the machine with floating rudders. Figure 35 shows the yawing moment coefficients (C_N) plotted against

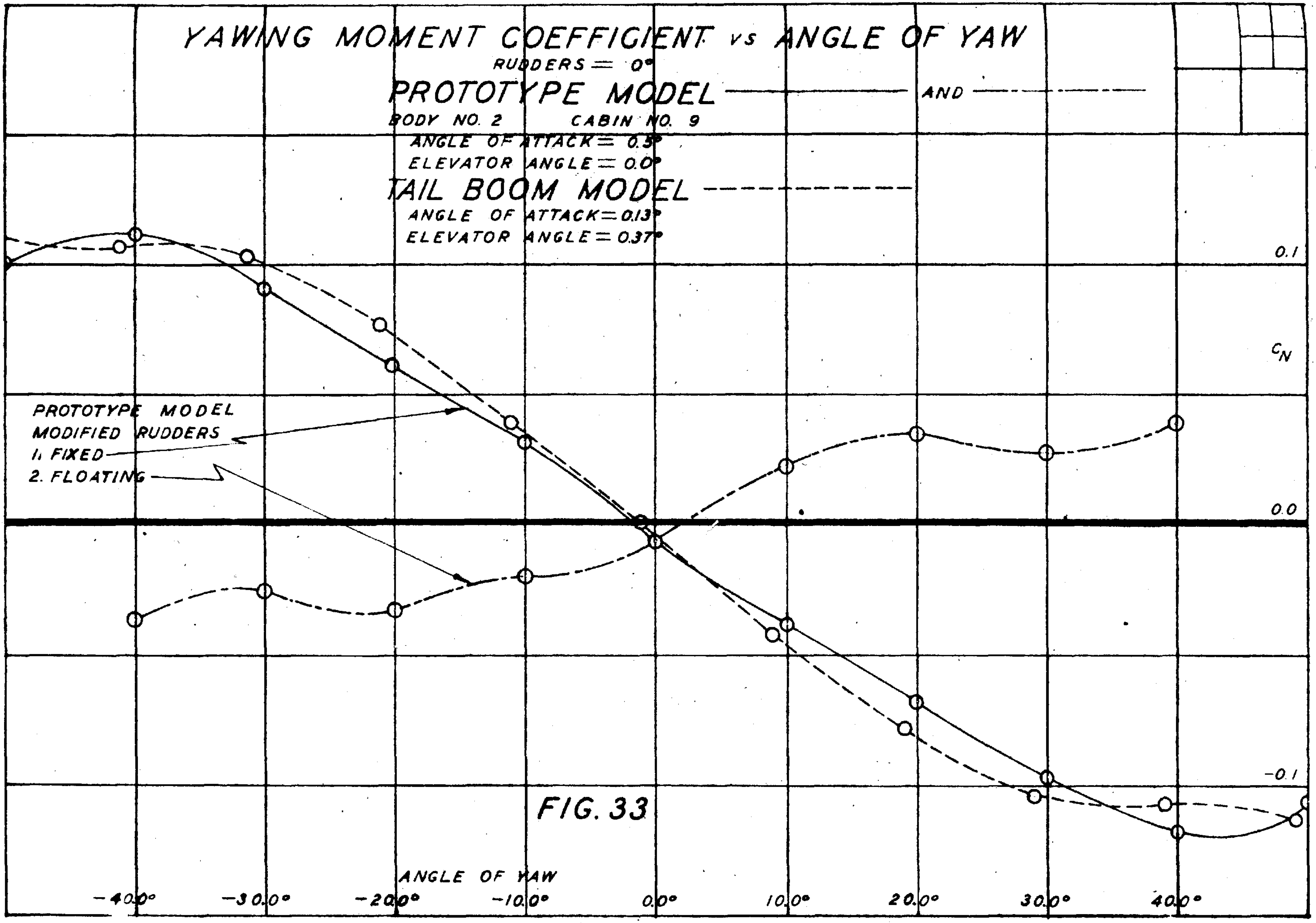

YAWING MOMENT COEFFICIENT vs ANGLE OF YAW
RUDDERS = 0°
PROTOTYPE MODEL AND
BODY NO. 2 CABIN NO. 9
ANGLE OF ATTACK = 0.5°
ELEVATOR ANGLE = 0.0°
TAIL BOOM MODEL
ANGLE OF ATTACK = 0.13°
ELEVATOR ANGLE = 0.37°
PROTOTYPE MODEL
MODIFIED RUDDERS
1. FIXED
2. FLOATING
0.1
C_N
0.0
-0.1
ANGLE OF YAW
-40.0°
-30.0°
-20.0°
-10.0°
0.0°
10.0°
20.0°
30.0°
40.0°

FIG. 33

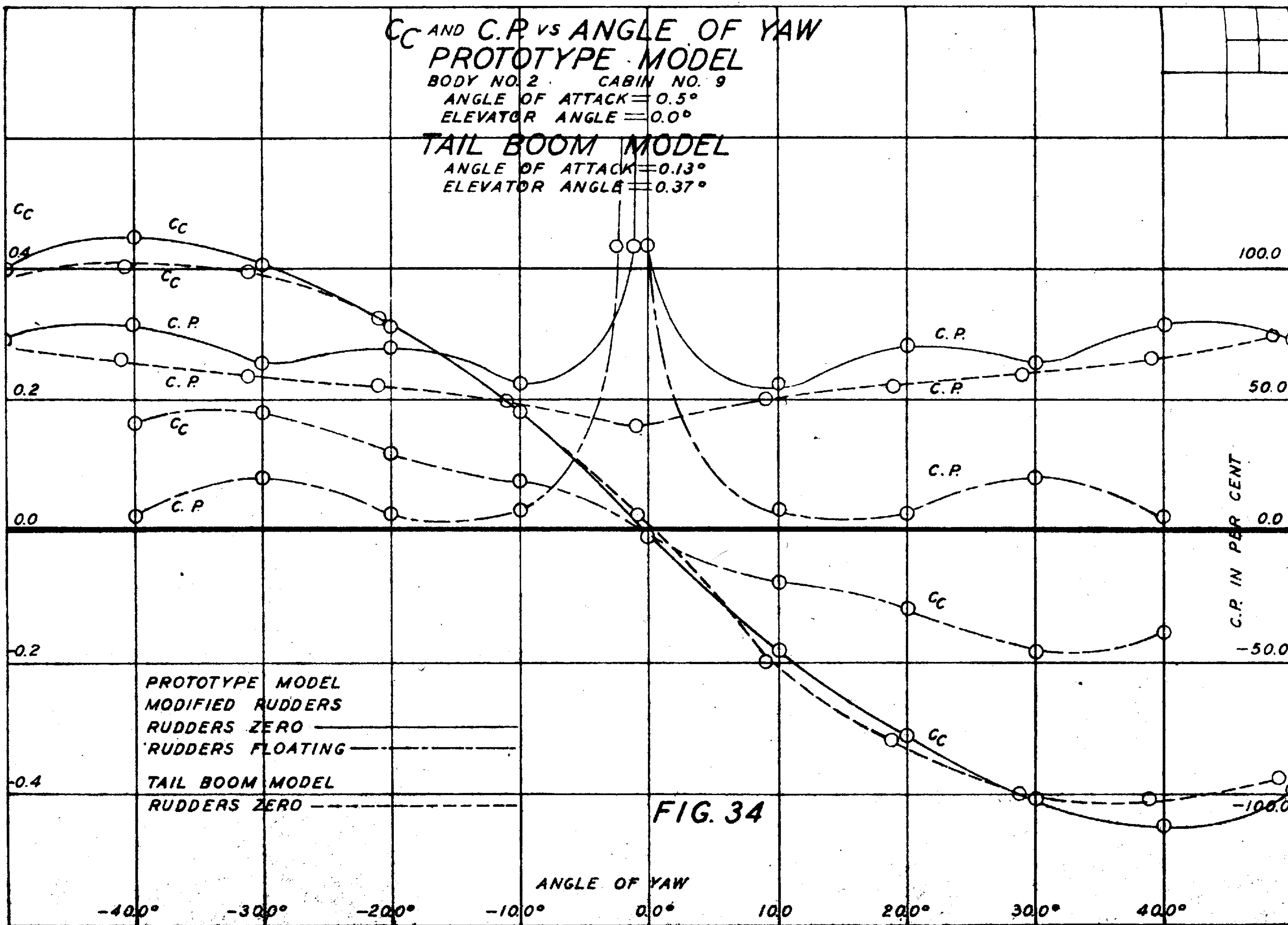

CC AND C.P. VS ANGLE OF YAW
PROTOTYPE MODEL
BODY NO. 2 CABIN NO. 9
ANGLE OF ATTACK = 0.5°
ELEVATOR ANGLE = 0.0°
TAIL BOOM MODEL
ANGLE OF ATTACK = 0.13°
ELEVATOR ANGLE = 0.37°
CC
C.P.
0.4
0.2
0.0
-0.2
-0.4
100.0
50.0
0.0
-50.0
-100.0
C.P. IN PER CENT
PROTOTYPE MODEL
MODIFIED RUDDERS
RUDDERS ZERO
RUDDERS FLOATING
TAIL BOOM MODEL
RUDDERS ZERO
ANGLE OF YAW
-40.0° -30.0° -20.0° -10.0° 0.0° 10.0 20.0° 30.0° 40.0°

FIG. 34

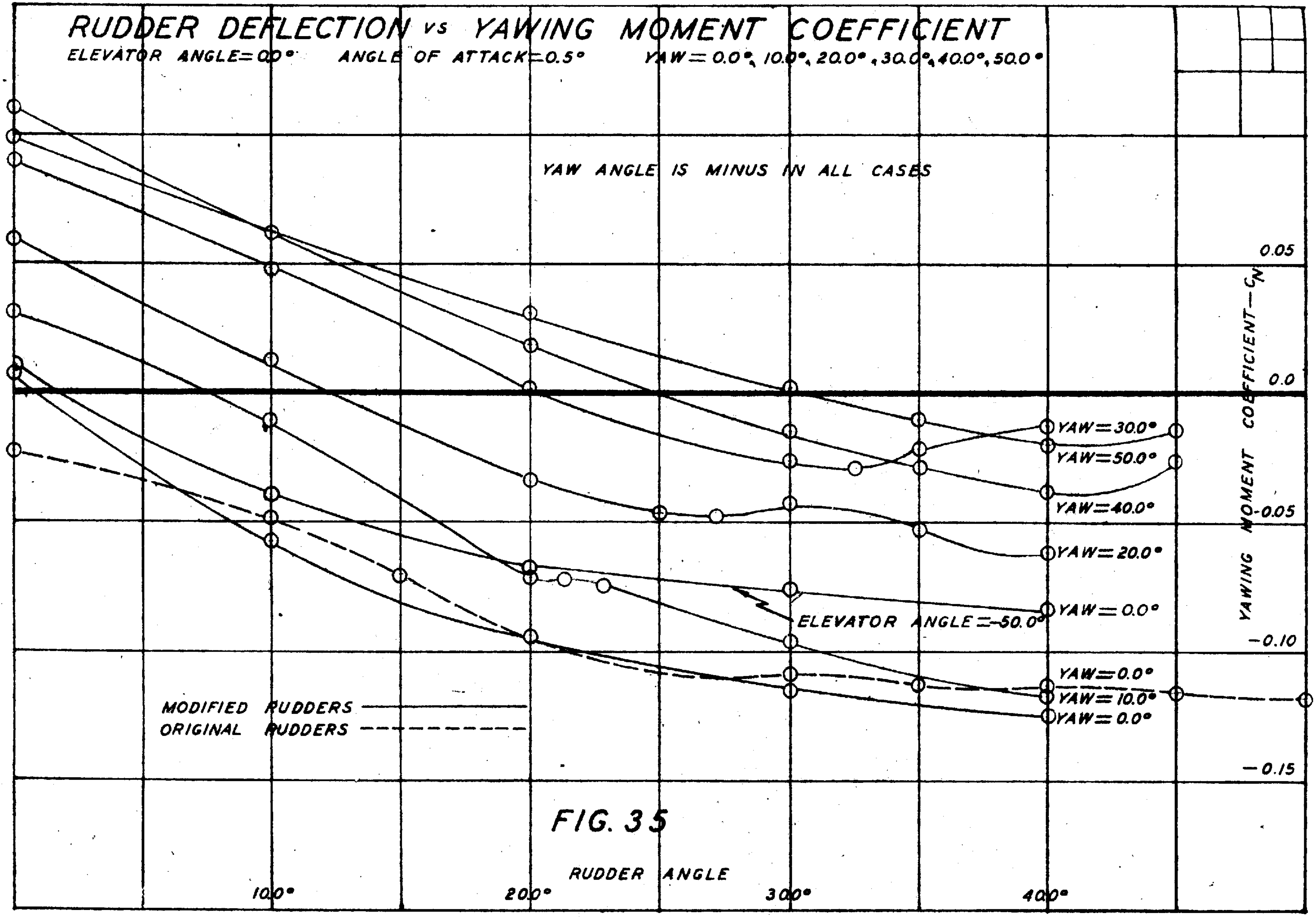
RUDDER DEFLECTION vs YAWING MOMENT COEFFICIENT
ELEVATOR ANGLE=0.0° ANGLE OF ATTACK=0.5° YAW=0.0°, 10.0°, 20.0°, 30.0°, 40.0°, 50.0°
YAW ANGLE IS MINUS IN ALL CASES
0.05
0.0
-0.05
-0.10
-0.15
YAWING MOMENT COEFFICIENT—C_N
YAW=30.0°
YAW=50.0°
YAW=40.0°
YAW=20.0°
YAW=0.0°
ELEVATOR ANGLE=-50.0°
YAW=0.0°
YAW=10.0°
YAW=0.0°
MODIFIED RUDDERS
ORIGINAL RUDDERS
RUDDER ANGLE
10.0°
20.0°
30.0°
40.0°

FIG. 35

rudder angle for angles of yaw up to and including 50°. It will be seen that the Prototype Model can be controlled even when the yaw is 50° since a rudder deflection of 30.5° will make $C_N = 0$ at this angle of yaw. Figure 36 illustrates this effect even more clearly. In this figure, rudder deflection is plotted against rudder angle for $C_N = 0$, with 30.5° rudder deflection full control is present up to 50° yaw. The cross wind force coefficients (C_c) for various angles of yaw are shown in Figure 37. It will be noted from these curves that (C_c) does not change direction regardless of the rudder setting, except where the yaw is less than 20°. With a 10° yaw, the cross wind coefficient (C_c) changes sign when the rudders are displaced to 16.0° the side centers of pressure will be at infinity for this yaw and rudder setting, as will be seen by reference to Figure 38 where side center of pressure locations are plotted for various angles of yaw.

In Figure 39 the cross wind force (C_c) and the side C.P. locations are plotted for the condition $C_N \doteq 0$. These curves show that the C.P. is directly opposite the wheels at all angles of yaw except zero yaw. This is a condition necessary for C_N to equal zero unless $C_c = 0$. At zero yaw the C.P. tends to infinity and C_c does equal zero, maintaining $C_N = 0$.

Figures 40 and 41 show the rolling moment coefficients (C_R) and the vertical side C.P. locations for various angles of yaw and various rudder settings. Under actual operating conditions the largest value of the rolling moment coefficient will occur when the rudders are displaced at 15°,

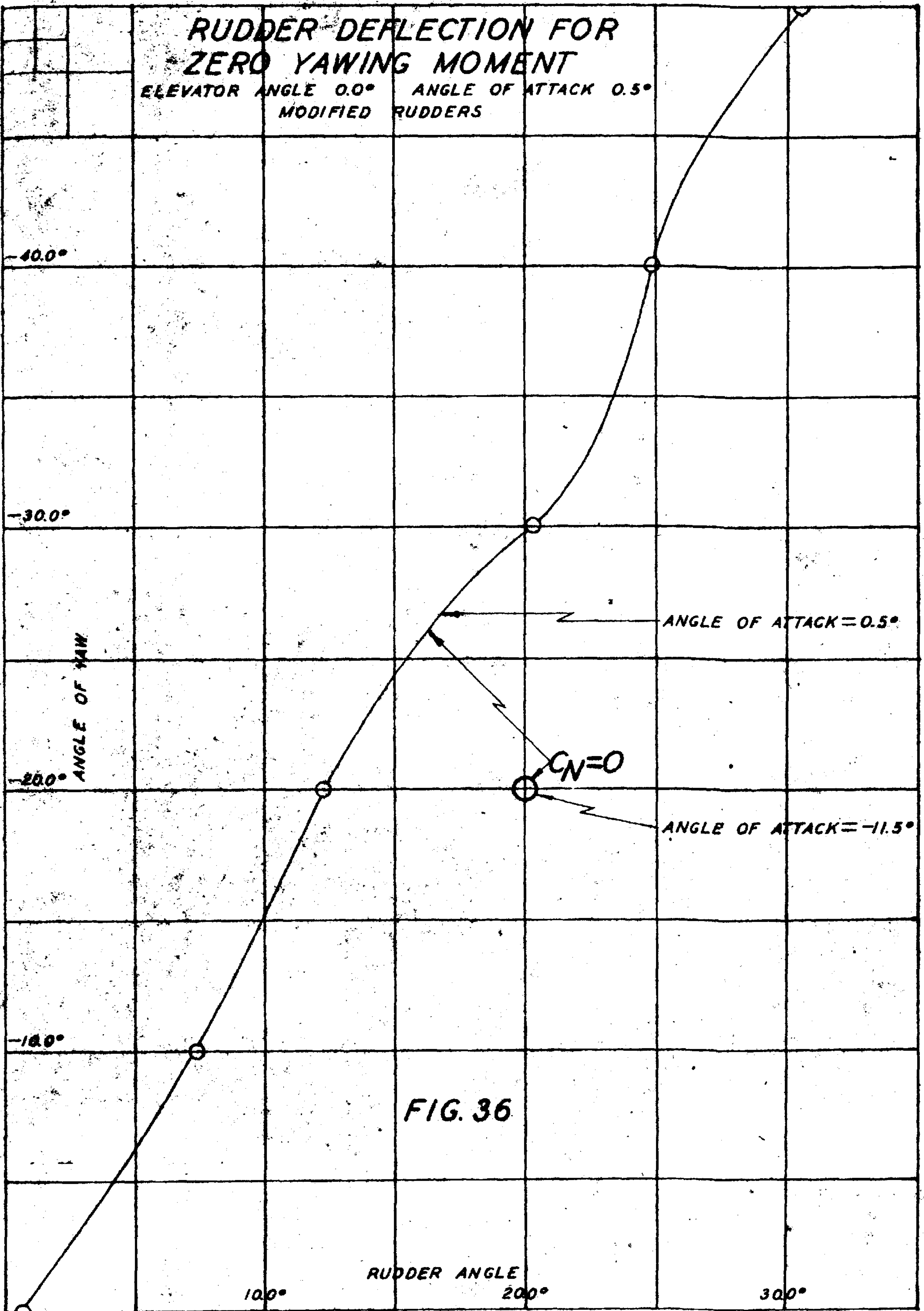
RUDDER DEFLECTION FOR ZERO YAWING MOMENT
ELEVATOR ANGLE 0.0° ANGLE OF ATTACK 0.5°
MODIFIED RUDDERS
-40.0°
-30.0°
-20.0°
-10.0°
ANGLE OF YAW
ANGLE OF ATTACK = 0.5°
$C_N = 0$
ANGLE OF ATTACK = -11.5°
RUDDER ANGLE
10.0°
20.0°
30.0°

FIG. 36

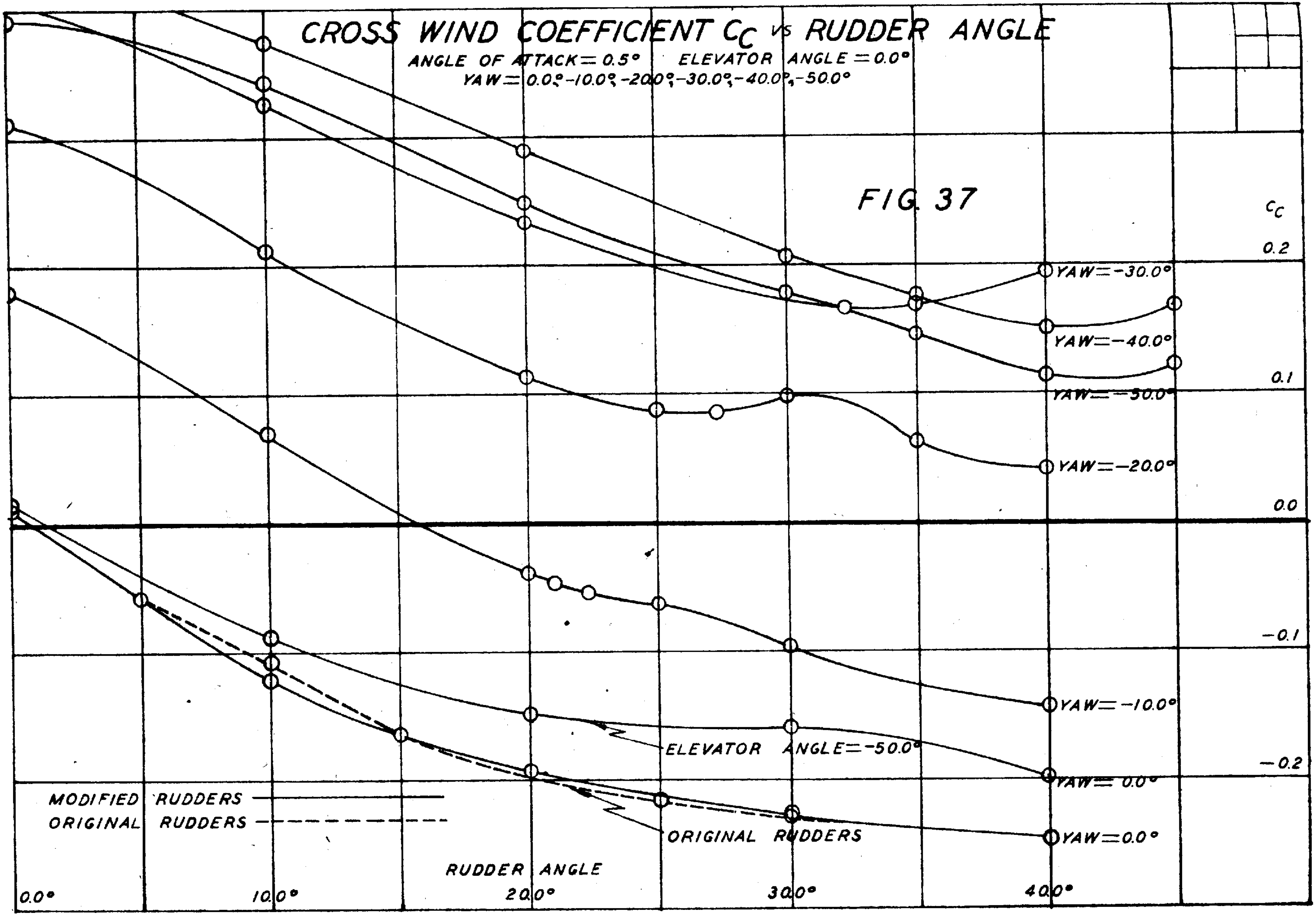
CROSS WIND COEFFICIENT C_C vs RUDDER ANGLE
ANGLE OF ATTACK = 0.5° ELEVATOR ANGLE = 0.0°
YAW = 0.0°, -10.0°, -20.0°, -30.0°, -40.0°, -50.0°
FIG. 37
C_C
0.2
0.1
0.0
-0.1
-0.2
YAW = -30.0°
YAW = -40.0°
YAW = -50.0°
YAW = -20.0°
YAW = -10.0°
ELEVATOR ANGLE = -50.0°
YAW = 0.0°
ORIGINAL RUDDERS
YAW = 0.0°
MODIFIED RUDDERS
ORIGINAL RUDDERS
RUDDER ANGLE
0.0°
10.0°
20.0°
30.0°
40.0°

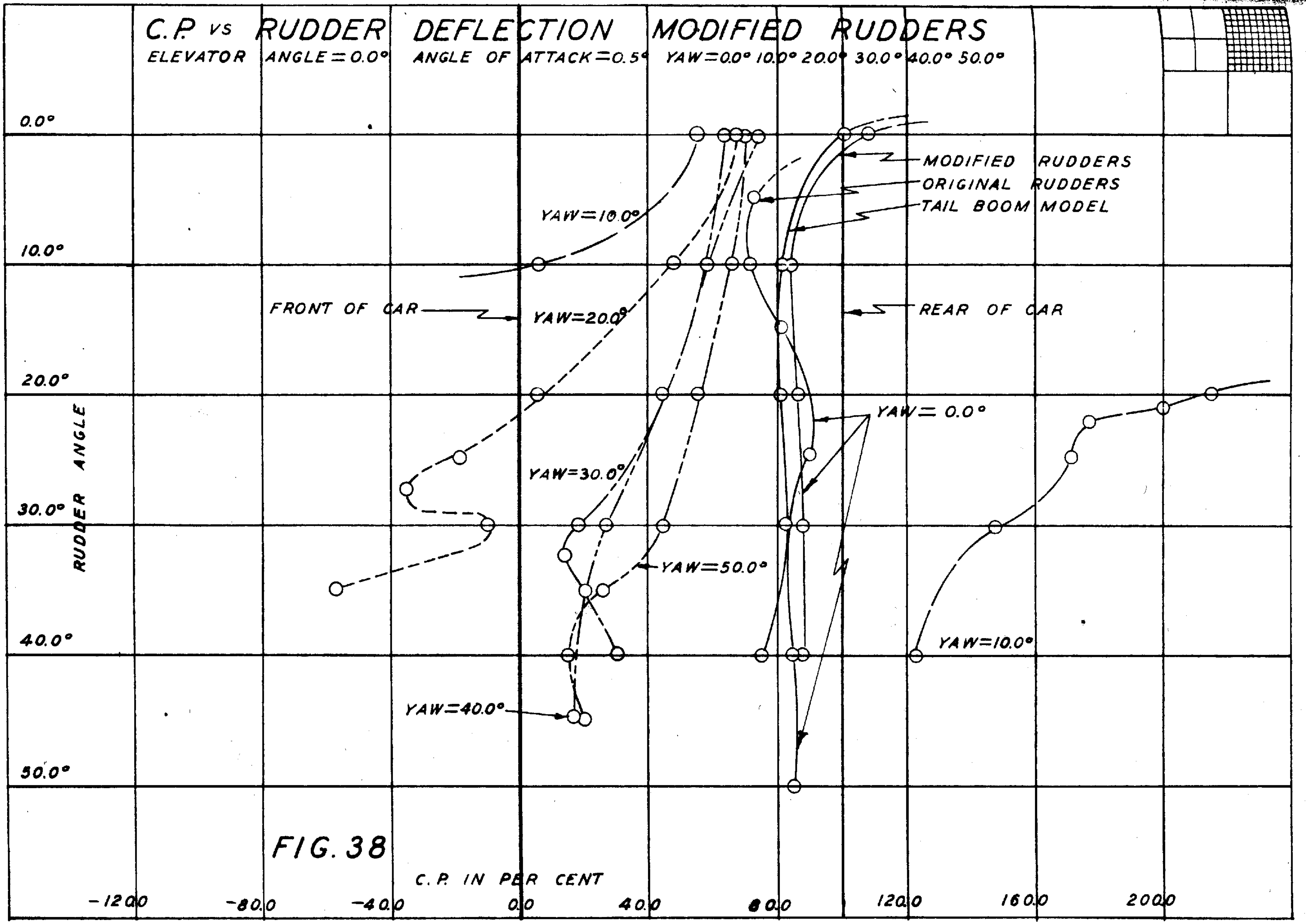
C.P. vs RUDDER DEFLECTION MODIFIED RUDDERS
ELEVATOR ANGLE = 0.0° ANGLE OF ATTACK = 0.5° YAW = 0.0° 10.0° 20.0° 30.0° 40.0° 50.0°
MODIFIED RUDDERS
ORIGINAL RUDDERS
TAIL BOOM MODEL
FRONT OF CAR
REAR OF CAR
YAW = 0.0°
YAW = 10.0°
YAW = 20.0°
YAW = 30.0°
YAW = 40.0°
YAW = 50.0°
RUDDER ANGLE
0.0°
10.0°
20.0°
30.0°
40.0°
50.0°
C.P. IN PER CENT
-120.0
-80.0
-40.0
0.0
40.0
80.0
120.0
160.0
200.0

FIG. 38

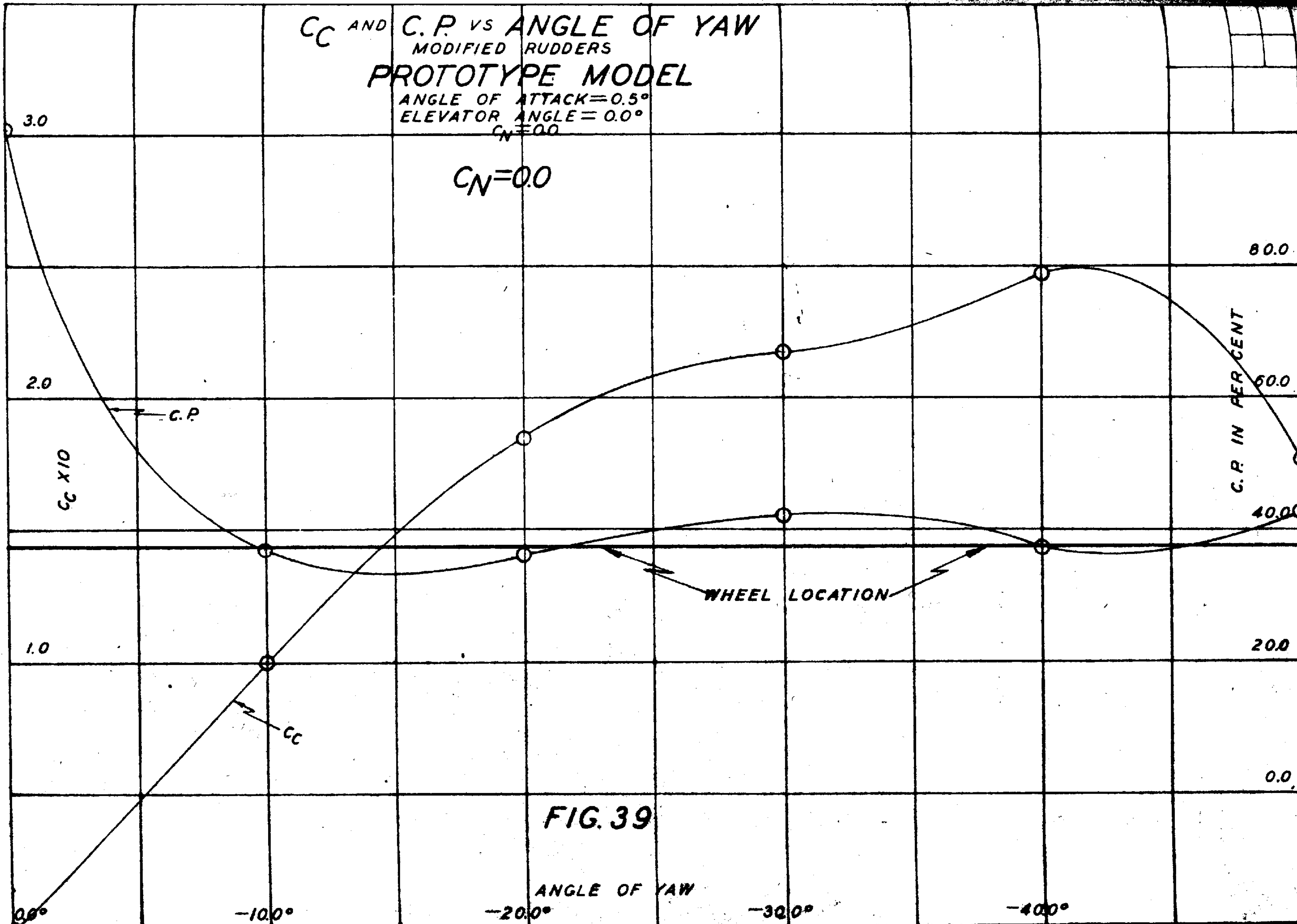
C_C AND C.P. VS ANGLE OF YAW
MODIFIED RUDDERS
PROTOTYPE MODEL
ANGLE OF ATTACK = 0.5°
ELEVATOR ANGLE = 0.0°
C_N = 0.0
C_N=0.0
3.0
2.0
1.0
80.0
60.0
40.0
20.0
0.0
C.P.
C_C X10
C.P. IN PER CENT
WHEEL LOCATION
C_C
ANGLE OF YAW
0.0°
−10.0°
−20.0°
−30.0°
−40.0°

FIG. 39

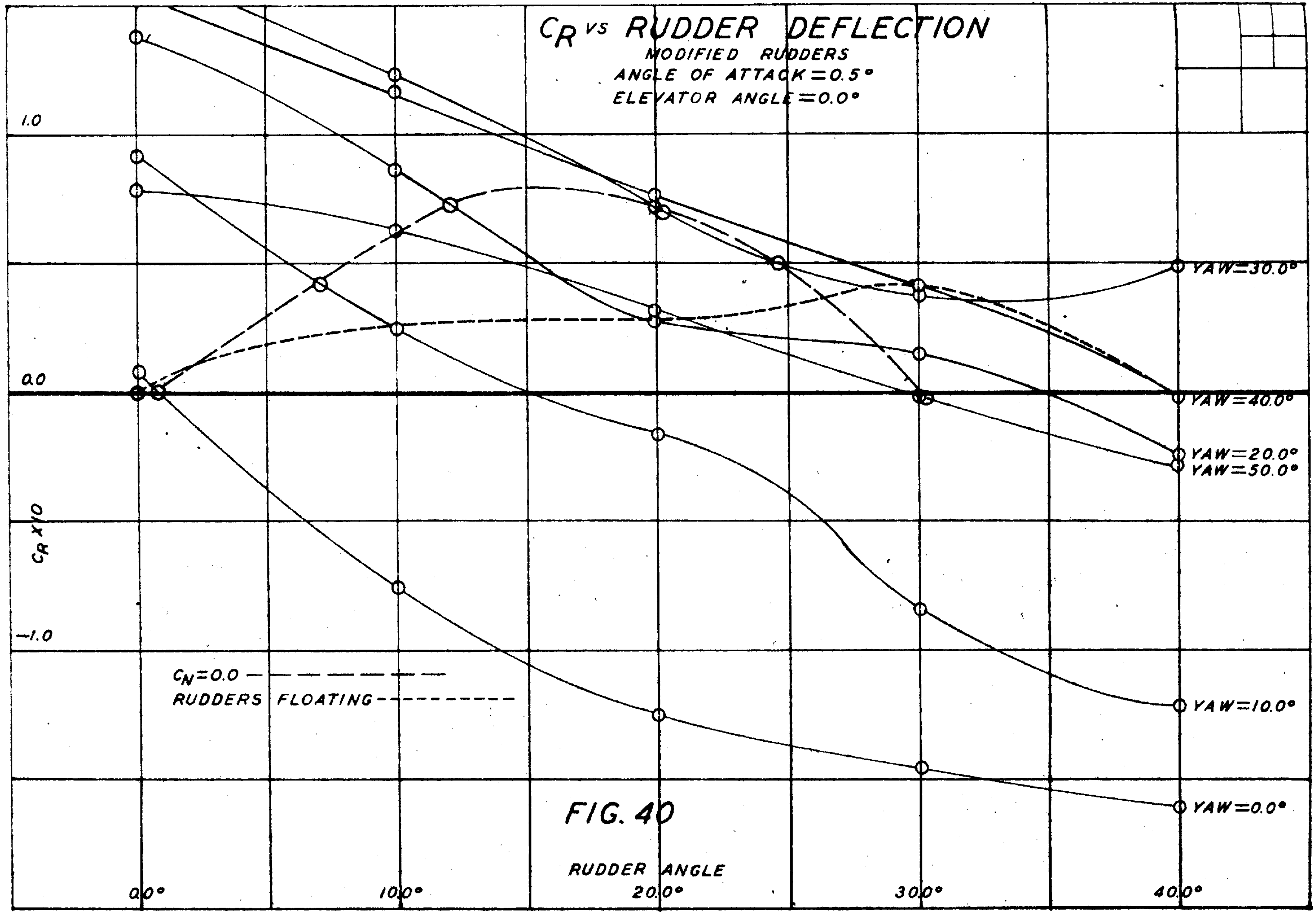
CR VS RUDDER DEFLECTION
MODIFIED RUDDERS
ANGLE OF ATTACK=0.5°
ELEVATOR ANGLE=0.0°
1.0
0.0
-1.0
CR X10
YAW=30.0°
YAW=40.0°
YAW=20.0°
YAW=50.0°
YAW=10.0°
YAW=0.0°
CN=0.0
RUDDERS FLOATING
RUDDER ANGLE
0.0°
10.0°
20.0°
30.0°
40.0°
FIG. 40

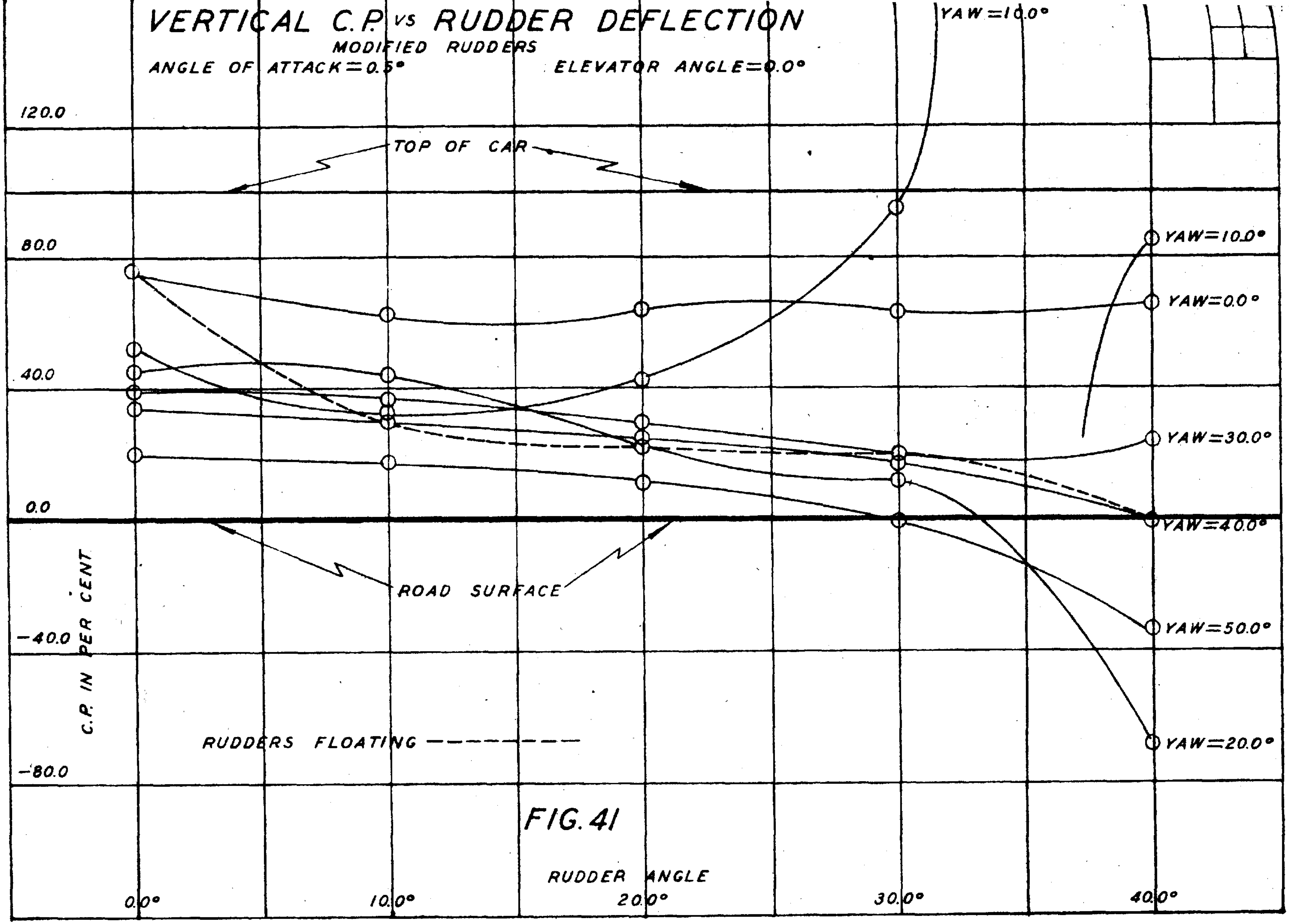

VERTICAL C.P. vs RUDDER DEFLECTION
MODIFIED RUDDERS
ANGLE OF ATTACK=0.5°
ELEVATOR ANGLE=0.0°
YAW=10.0°
120.0
TOP OF CAR
80.0
YAW=10.0°
YAW=0.0°
40.0
YAW=30.0°
0.0
YAW=40.0°
ROAD SURFACE
C.P. IN PER CENT
-40.0
YAW=50.0°
RUDDERS FLOATING
YAW=20.0°
-80.0
RUDDER ANGLE
0.0°
10.0°
20.0°
30.0°
40.0°

FIG. 41

the yaw being such that $C_N = 0$. For this condition C_R = 0.076 at 60 miles per hour, this will represent a rolling moment of $0.076 \times 0.001185 \times 77.5 \times 88^2 \times 14.58 = 788.0$ ft/lbs. This moment should cause no concern since the moment resisting it will amount to 3000 ft/lbs. for a 2000 pound car of 6 foot tread. At 100 miles per hour, the rolling moment would be increased to 2190 ft/lbs. in the extreme case above referred to. A further increase in speed would probably cause a dangerous condition since the effects of centrifugal forces must also be accounted for in case the condition referred to above occurred while the car was rounding a curve in a direction such that the centrifugal force moment had the same sense as the aerodynamic rolling moment.

In view of the preceding discussion, the reader may have some fear that the car may overturn when travelling at speeds greater than 100 miles per hour, unless it is observed that the extreme conditions just referred to occur only at a yaw angle of about 30°. In other words, the discussion is applied to the case where the machine is running at 100 miles per hour in a cross wind of 50 miles per hour. Under these conditions [redacted] an orthodox automobile is far from being safe, even if the cross wind forces acting on it were as small as those acting on the Roadplane.

In order to get a very approximate idea of the forces acting on a conventional automobile at high speeds consider the rolling moment acting on a Roadplane in a high wind when the rudders are in their neutral position (Such a condition could not actually occur in the Roadplane). Assume the yaw is 30 degrees and the velocity is 100 miles per hour. Rolling moment would equal $0.001185 \times 77.5 \times 147^2 \times 14.58 \times 0.17 = 4900$ ft. lbs. (Figure 40). This moment would overturn the ordinary car. Naturally this calculation is not strictly applicable to the conventional car since the coefficients are not the same but it gives an idea of the condition since in a cross wind the conventional car has no means of decreasing the magnitude of the cross wind forces. Contrast the condition to that in the Roadplane, where at large angles of yaw the cross wind coefficients may be reduced by about 65 percent,and at small angles of yaw proper rudder adjustments may reduce these coefficients to zero or even reverse their direction. (See Figure 37) In order to more accurately evaluate the forces and moments acting on the Roadplane in a steady turn refer to Figures 42-a and 42-b. These figures are free bodies for the Roadplane in a skidded turn.

Applying the equations of Equilibrium-

From Fig. 42-a

$$D \cos \alpha - C \sin \alpha - F_1 - F_2 + \frac{W}{g} \times \frac{V^2}{R} \times \sin \alpha = 0 \qquad (1)$$

$$D \sin \alpha + C \cos \alpha + F_3 - \frac{W}{g} \frac{V^2}{R} \times \cos \alpha = 0 \qquad (2)$$

$$(C \cos \alpha + D \sin \alpha)\left(C.P. - \frac{a}{L}\right) + \frac{W}{g} \frac{V^2}{R} \cos\alpha \left(\frac{a}{L} - \frac{h}{L}\right) \qquad (3)$$

$$- \frac{b}{2}F_1 + \frac{b}{2}F_2 = 0$$

From Fig. 42-b

$$-\frac{W}{g}\times\frac{V^2}{R}t\times\cos\alpha + W\frac{b}{2} - W_2 b + m\,(D\sin\alpha + C\cos\alpha) = 0 \quad (4)$$

$$(F_1 + F_2) = \frac{\eta HP\times 550 - 0.0125\,W\,V}{V} \quad (5)$$

$$(C\cos\alpha + D\sin\alpha)\left(C.P. - \frac{a}{L}\right) = N \quad (6)$$

$$m\,(D\sin\alpha + C\cos\alpha) = R.M. \quad (7)$$

There will be two general types of turn.

I. No skidding $\alpha = 0$

Possible limitations:

(a) Radial slipping starts.

(b) Inside wheel slips.

(c) HP insufficient to maintain speed in turn.

(d) See (b) below.

II. Turns involving a controlled skid.

Possible limitations:

(a) HP insufficient to maintain speed in turn.

(b) Control couples too small to maintain attitude necessary for the turn.

(c) Inside wheel slips.

The question of the car overturning is not involved in any type of power turn since before this occurs, the inside wheel must slip.

It will be observed that in a conventional car a skid of any character always changes or limits the steering couple which is being used to guide the car and therefore calls for a change in control setting. In many cases there is not sufficient time for the average operator to make this correction. In other cases

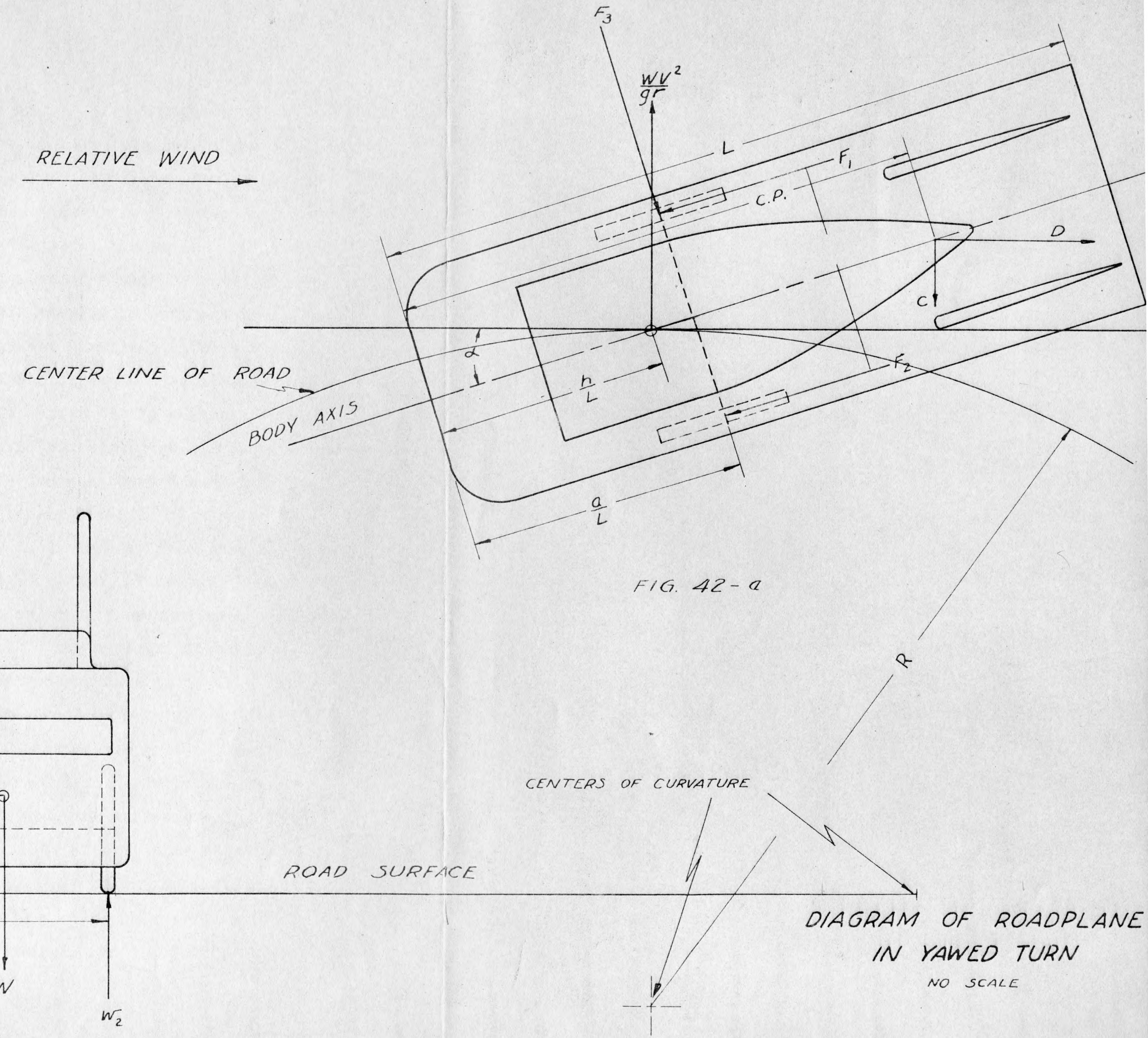

FIG. 42-a

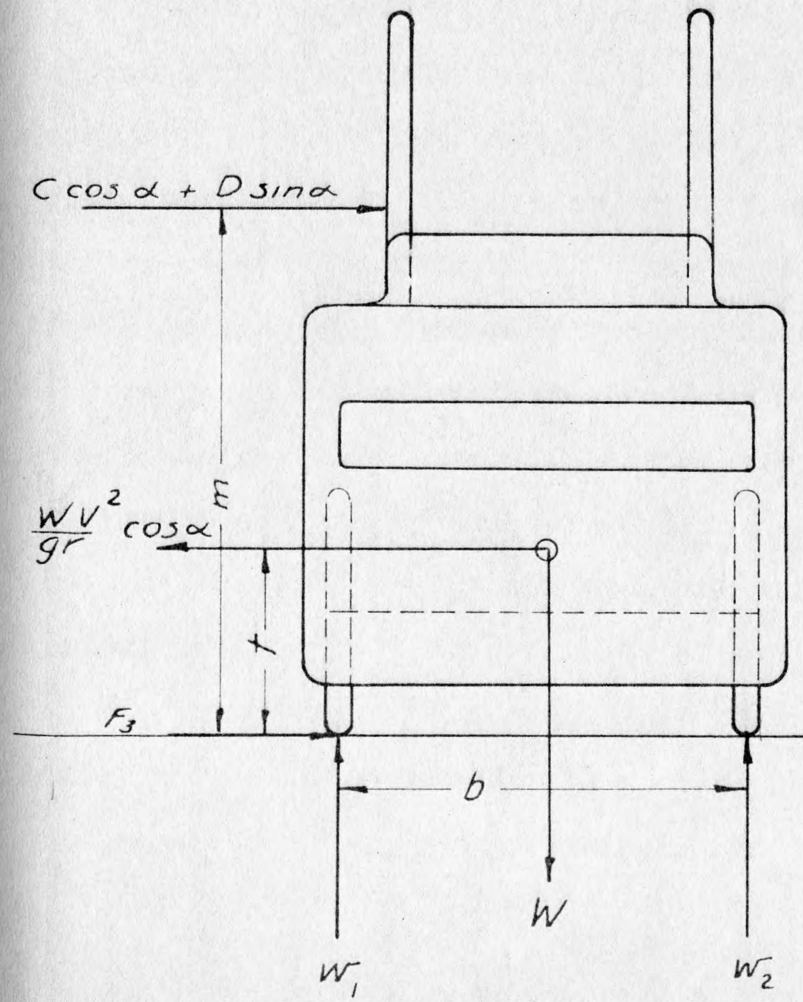

FIG. 42-b

DIAGRAM OF ROADPLANE IN YAWED TURN

NO SCALE

the skid can be stopped only by abandoning the contemplated maneuver, which means, of course, that the operator must practically surrender the control of the car. In all cases in a conventional car the correction for a skid calls for a rapid manipulation of the controls in a manner which is not natural to the average driver. Due to the above factors, the average person thinks of a skid as a catastrophe which must be avoided at all costs. In contrast to this condition a class B turn in the Roadplane,(i.e. a skidded turn, which does not involve slipping of the inside wheel) does not destroy the effectiveness of the controls or prevent them from being even further deflected. The only control moments which are effected are those due to $\frac{b}{2} F_1$ and $\frac{b}{2} F_2$, and in order for the desired radius of turn to be maintained or even decreased, it is only necessary for the operator to open the throttle. This, of course, requires some experience but is not as awkward as unnatural manipulation of the steering wheel. The average driver is afraid of a skid principally because once he is in a skid the selected radius of turn cannot be maintained. In the Roadplane this is not the case, the driver has the choice of continuing the turn and the skid by simply opening the throttle, or he can stop the skid and allow the radius of turn to increase. The skid is thus seen to be an emergency range of control into which the operator may enter with perfect assurance, knowing that even though he has exceeded the practical minimum radius of turn he can still continue his contemplated maneuver and, if necessary, even further tighten his turn at the same time maintaining full and complete control.

Needless to say, the skid is not a desirable maneuver to enter under ordinary conditions, even with the Roadplane. It is obvious, of course, that a high velocity skid may cause overturning, in case one of the tires should roll off or should strike an obstruction. A sudden change in coefficient of friction will also cause trouble. In addition to these facts, the Roadplane while in a skidded turn makes a considerable yaw angle with respect to its direction of motion and is, therefore, in some danger of striking another vehicle. It will also be obvious that skidded turns are expensive maneuvers since they cause heavy wear on the tires and also a large expenditure of power, if any appreciable speed is to be maintained. Under favorable conditions the operator need not exercise any special ability to make these turns except that he should be careful with the use of the throttle since in these maneuvers the steering control is effected to an appreciable extent by the throttle setting.

Rewriting equations (1) - (5) in coefficient form:

$$0.001185\ A\ V^2 C_D \cos\alpha - 0.001185\ S\ V^2 C_c \sin\alpha + \frac{W}{g}\frac{V^2}{R} x \sin\alpha = F_1 + F_2 \qquad (1)$$

$$\frac{W}{g}\frac{V^2}{R}\cos\alpha - 0.001185\ A\ V^2\ C_D \sin\alpha - 0.001185\ S\ V^2 C_c \cos\alpha = F_3 \qquad (2)$$

$$0.001185\ S\ L\ V^2 C_N + \frac{W}{g}\frac{V^2}{R} \cos\alpha \left(\frac{a}{L} - \frac{h}{L}\right) + \frac{b}{2} F_2 = \frac{b}{2} F_1 \qquad (3)$$

$$0.001185\ S\ L\ C_R V^2 + \frac{Wb}{2} - \frac{W}{g}\frac{V^2}{R} t \cos\alpha = w_2 b \qquad (4)$$

$$F_1 + F_2 = \frac{\eta HP \times 550 - 0.0125\ W\ V}{V} \qquad (5)$$

In any turn the minimum radius of turn will be obtained when:

(A) The BHP available from the motor is insufficient to meet the power requirements for the turn.

(B) When the HP is sufficient the turn may be limited by the fact that the weight w_2 may not be sufficient to allow the development of the force F_2 necessary to make the turn.

$$R = \frac{W\ V^2 \sin\alpha}{g\left[\eta HP\ 550 - 0.0125\ W\ V - 0.001185\ (A\ C_D \cos\alpha - SC_c \sin\alpha)V^3\right]} \qquad (8)$$

For a given HP, speed and yaw angle the above equation will give the minimum radius of turn provided the weight w_2 on the inside wheel is sufficient to prevent slipping.

Combining equations (1) and (3)

$$0.001185\ V^2 (A\ C_D \cos\alpha - S\ C_c \sin\alpha)\frac{b}{2} + \frac{W}{g}\frac{V^2}{R} \sin\alpha\ \frac{b}{2} =$$

$$F_2 b + 0.001185\ S\ L\ V^2 C_N + \frac{W}{g}\frac{V^2}{R} \cos\alpha \left(\frac{a}{L} - \frac{h}{L}\right) \qquad (9)$$

From (4) when slipping starts $\mu w_2\ b = F_2\ b$

$$F_2 b = 0.001185\ S\ L\ C_R V^2 \mu + \frac{W\mu b}{2} - \frac{W}{g}\frac{V^2}{R} \times t\mu \cos\alpha \qquad (10)$$

$$R = \frac{W\ V^2}{g}\left[\frac{\cos\alpha\left[\left(\frac{a}{L} - \frac{h}{L}\right) - t\mu\right] - \frac{b}{2}\sin\alpha}{0.001185\ V^2\left(\frac{bAC_D}{2}\cos\alpha - \frac{bSC_c}{2} \times \sin\alpha - SLC_N - SL\mu C_R\right) - \frac{Wb\mu}{2}}\right] \qquad (11)$$

Equation (11) gives the absolute minimum value for a turn of any character. For a non-skidded turn, $\alpha = 0$. Equation (2) will also give the radius of any skidded turn, provided the angle of yaw is known or vica versa since when skidding exists, $F_3 = \mu W$. Equation (2) cannot be used to obtain the minimum radius of a skidded turn since it contains no factors involving the HP of the motor or the weight on the inside wheel, the two factors which control the minimum radius of skidded turn. Equation (2) cannot be used to determine the radius of a non-skidded turn unless F_3 is known, since in this character of turn, $F_3 < \mu W$. This equation can, of course, be used if the car is just on the point of skidding and when so used will determine the minimum value of R for a non-skidded turn.

From Equation (3) it is seen that the applied aerodynamic yawing moment necessary to make a turn of any radius is:

$$N = \frac{b}{2}(F_1 - F_2) - \frac{W}{g}\frac{V^2}{R}\cos\alpha\left(\frac{a}{L} - \frac{h}{L}\right) \qquad (12)$$

In a non-skidded turn ($\alpha = 0$) and $\frac{F_1}{F_2} = \frac{R - \frac{b}{2}}{R + \frac{b}{2}}$ since the propelling or thrust forces are divided in the differential in inverse proportion to the R.P.M. of the wheels. Under these conditions, we may write from equations (1) and (12)

$$N = -\frac{b^2\ 0.001185\ A\ V^2 C_D}{4\ R} - \frac{W}{g} x \frac{V^2}{R}\left(\frac{a}{L} - \frac{h}{L}\right) \qquad (13)$$

This equation indicates that the aerodynamic moment necessary to turn the car is very materially affected by the C.G. location and when this location is directly over the wheels the moment above referred to is equal to the drag of the car times one fourth of the square of the wheel tread divided by the radius of the turn. It will also be observed that if the C.G. of the car is behind the wheels, it has an unstable effect on the turn since the higher the speed or the smaller the radius, the less effort is required to make the turn. This effect is very noticeable in the full scale machine. When the C.G. is moved back, the machine becomes very sensitive and it is very difficult to avoid overcontrol. The same effect is common to airplanes and gives rise to the phenomena known as ground looping. Airplanes with their C.G.'s far back of the wheels will ground loop badly on the least provocation.

Collecting the Equations for non-skidded turns:

I. Applied moment necessary to make a non-skidded turn of any radius.

$$N = \pm \frac{0.001185AV^2C_Db^2}{4\ R} \pm \frac{W}{g} x \frac{V^2}{R} x \left(\frac{a}{L} - \frac{h}{L}\right)$$

II. Minimum non-skidded turn, radial slipping just starting.

$$R = \frac{WV^2}{g(0.001185SC_cV^2 + \mu W)}$$

III.

$$R = \frac{WV^2}{g}\left[\frac{\frac{a}{L} - \frac{h}{L} - t\mu}{0.001185V^2\left(\frac{AC_Db}{2} - SLC_N - \mu SLC_R\right) - \frac{Wb\mu}{2}}\right]$$

Minimum non-skidded turn in which traction may be maintained on inside wheel. Minimum R is determined for a non-skidded turn by Equation II or III whichever gives the larger value.

IV. From Equation (8) it is seen that R = 0 when there is no skid which simply means that the BHP available is not a limiting factor to the radius of a turn so long as skidding does not exist. Rewriting Equation (8):

$$gR\eta HP550 - 0.0125WVgR - 0.001185AC_DV^3gR = 0$$

$$\eta HP550 = 0.0125WV + 0.001185AC_DV^3$$

$$\eta HP = \frac{(0.0125W + 0.001185AC_DV^3)V}{550}$$

This Equation is the standard power equation for an automobile on a level road and shows that except for the effect of the increased aerodynamic drag due to the rudder displacement, the HP required is not effected by the radius of a non-skidded turn.

Collecting Equations for skidded turns:

From Equation (2)

$$\text{(A)} \quad R = \frac{WV^2\cos\alpha}{g\mu W + 0.001185V^2g(AC_D\sin\alpha + SC_c\cos\alpha)}$$

This Equation applied to any turn and determines transition from a non-skidded turn to a skidded turn when ($\alpha = 0$), at this point R is the maximum value for a skidded turn or the minimum value for a non-skidded turn.

$$\text{(B)} \quad R_{Min.} = \frac{WV^2}{g}\left[\frac{\cos\alpha\left[\left(\frac{a}{L} - \frac{h}{L}\right) - t\mu\right] - \frac{b}{2}\sin\alpha}{0.001185V^2\left(\frac{AC_Db}{2}\cos\alpha - \frac{SC_cb}{2}\sin\alpha - SLC_N - SL\mu C_R\right) - \frac{Wb\mu}{2}}\right]$$

(C)

$$R_{Min.} = \frac{WV^2 \sin\alpha}{g[\eta HP550 - 0.0125WV - 0.001185\,(AC_D\cos\alpha - SC_c\sin\alpha)V^3]}$$

The largest value of R obtained by the use of equations (B) and (C) will give the minimum possible radius for a skidded turn.

Consider now the practical application of these formulae. For the purpose a hypothetical car will be used, which has the same aerodynamic characteristics of the Prototype Model tested in the tunnel and is exactly sixteen times the size of this model. Its principal characteristics will be assumed to be as follows:

$L = 13.875$ ft. $S = 77.5$ sq.ft. $A = 23.60$ sq.ft.

$W = 2400$ lbs. $b = 4.66$ ft. $\mu = 0.5$

C.G. assumed 3 ft. above ground line.

Assume all turns are made with a maximum rudder deflection of 30° and use this rudder setting in order to determine the coefficients C_D, C_c, and C_R.

$\frac{a}{L} = 37.3$ percent $(\frac{a}{L} - \frac{h}{L}) = 0.5$ ft.

η = efficiency of drive from engine to wheels = 0.90

Rolling friction losses = 0.0125 W lbs.

Sea level and standard conditions $\frac{1}{2}\rho = 0.001185$

$g = 32.2$ ft./sec.^{2} BHP = 50.0

All velocities are in ft./sec.

Skidded Turns

Applied to this particular car the equations are as follows:

(A) $$R = \frac{2660\,V^2 \cos\alpha}{42800 + V^2(C_D \sin\alpha + 3.28C_c \cos\alpha)}$$

(B) $$R_{Min.} = 1143\left[\frac{2.33 \sin\alpha + \cos\alpha}{C_D \cos\alpha - 3.28C_c \sin\alpha - 19.5C_N - 9.77C_R - \frac{42200}{V^2}}\right]$$

(C) $$R_{Min.} = \frac{74.5V^2 \cos\alpha}{24750 - 30V - 0.028(C_D \cos\alpha - 3.28C_c \sin\alpha)V^2}$$

Normal Turns. No Skid.

I. Will be discussed later.

II.
$$R_{Min.} = \frac{74.5V^2}{0.0918C_c V^2 + 1200} = \frac{812V^2}{C_c + 13070}$$

III.
$$R_{Min.} = 74.5V^2\left[\frac{-1.0}{0.001185V^2(-178) - 1400}\right]$$

$$= \frac{74.5V^2}{0.211V^2 + 1400}$$ = 284 ft. when car is going 60 miles per hour.

Equation III does not really determine the minimum radius of non-skidded turn but simply determines what the radius would be before slipping started on the inside wheel. This equation is, therefore, not strictly applicable since radial skidding always starts before such slipping starts. For the minimum radius of non-skidded turn refer to Equation II.

For the sake of simplicity only steady non-skidded flat turns of 60 miles per hour and 100 miles per hour will be investigated.

60 miles per hour.

$$R_{Min.} = \frac{812 \times \overline{88}^2}{C_c \times 88^2 + 13070} = \frac{812}{C_c + 1.688} = \frac{812}{0.2292 + 1.688}$$

$$= 557.0 \text{ ft.}$$

100 miles per hour.

$$R_{Min.} = \frac{812}{-0.2292 + 1.3070} = \frac{812}{1.0778} = 755.0 \text{ ft.}$$

Consider Equation I:

I. Required yawing moment for minimum non-skidded turn.

$NR = -\ 37.333V^2$

$NR = -\ 288500$ lb.ft.^{2}

$N = -\ 518.0$ lbs.ft. for 60 miles per hour.

$N = -\ 1062$ lb.ft. for 100 miles per hour.

The preceding equations with their applications give a fairly comprehensive idea of the possibilities and limitations of air control. It will be observed that due to the outward acting air force, the minimum radius of non-skidded turn will be slightly more than that for the conventional car. However, this turn will still be sufficiently small for any normal condition. It will also be noted that when the coefficient of friction is very low due to slippery roads, the Roadplane can still maintain a very small radius of controlled turn by simply changing into a skidded turn. In fact, the absolute minimum radius of controlled turn is much smaller on the Roadplane than on the conventional car since control practically disappears on the conventional car when skidding starts.

Performance

One of the most important factors to consider in the design of a streamlined car is the question of performance. Determination of performance involves a consideration of the following general items.

1. Aerodynamic drag.
2. Rolling resistance.
3. Drive gear efficiency.
4. Gear ratio.
5. Brake horsepower available from the motor.
6. Specific fuel consumption of the motor.
7. Weight of the car.

It has been the practice in many cases to compute the drag of a small model in the wind tunnel, allow 0.0125W or some similar figure for the rolling resistance, assume some figure for the drive gear efficiency, calculate the top speed obtainable from a given horsepower, and compare the results with the actual performance of a full scale machine much to the latter's disadvantage. In most cases the question of yawed operation is not even considered, even though a motor car in ordinary service operates under yawed conditions most of the time. The author must admit that in this report he has followed part of the procedure just outlined but at this point he wishes to make it clear that where performance figures are worked up on the basis of wind tunnel tests that these figures are for illustrative purposes only. They are directly comparable only when dealing with tests made by the author or others on similar size models tested under similar conditions. They may also be used to indicate in a general way certain effects which may result from streamlining.

In addition to the tunnel tests the author made full scale road tests on one model of the Roadplane. Due to the exceedingly poor condition of the small motor used in this machine the performance was calculated on the assumption that the machine was equipped with a V-8 motor of 80.0 BHP. In this calculation no unscientific assumptions were made and the results are based on resistance data actually obtained from road tests on the full scale machine. In view of this fact the author feels that the calculated performance of the full scale machine is directly comparable to the measured, or calculated, performance of any other full scale machine provided such performance was determined from road tests and not wind tunnel tests.

Consider now the question of drag. Figure 43 shows the drag coefficient (C_D) for the Prototype Model for various angles of yaw and various rudder settings. These coefficients are referred to wind axes. As would be expected the drag increases with yaw at a very rapid rate and for any angle of yaw the drag is a minimum when the rudders are displaced to an angle just about 5 degrees less than the yaw angle.

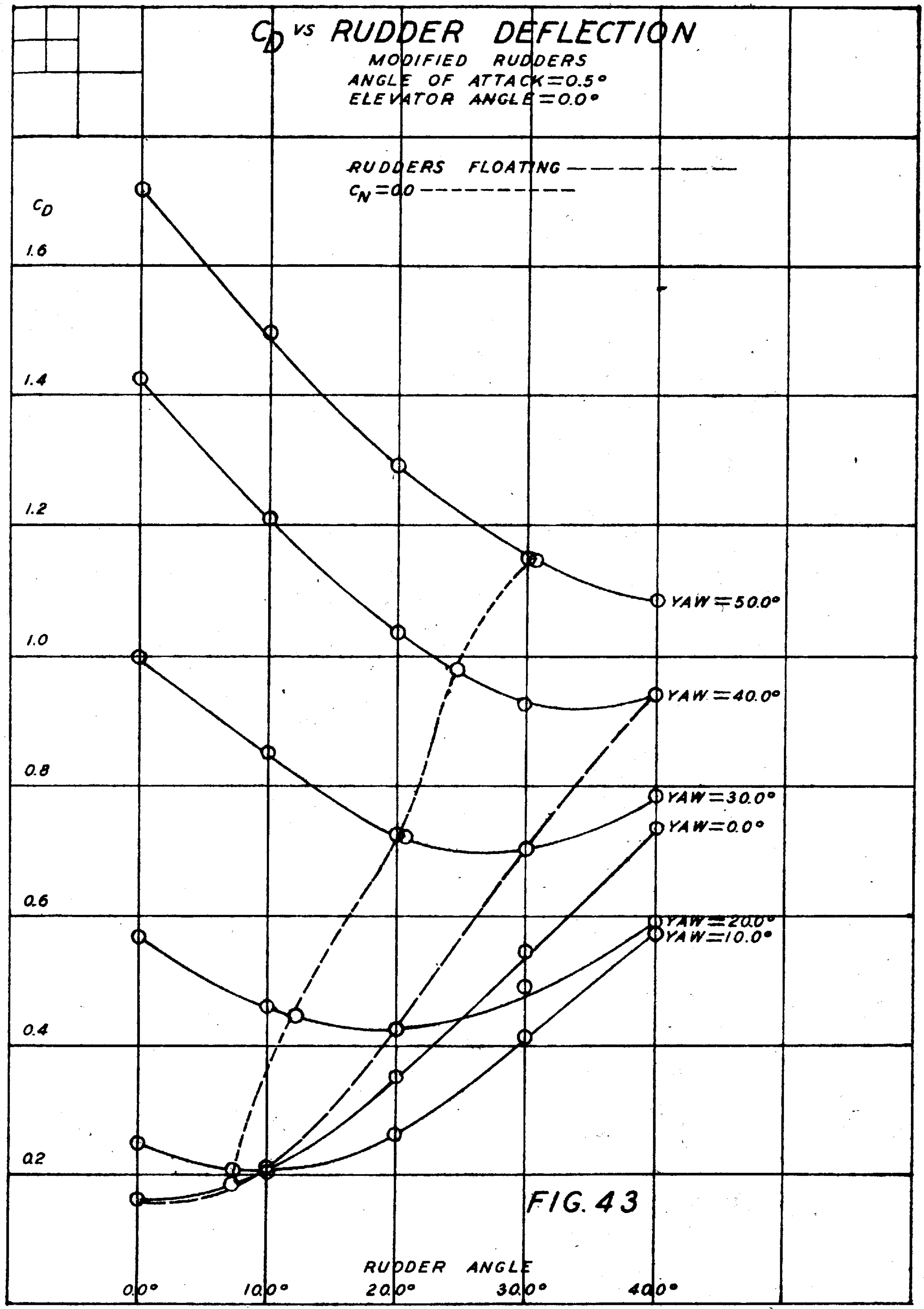

C_D vs RUDDER DEFLECTION
MODIFIED RUDDERS
ANGLE OF ATTACK=0.5°
ELEVATOR ANGLE=0.0°
RUDDERS FLOATING
C_N=0.0
C_D
1.6
1.4
1.2
1.0
0.8
0.6
0.4
0.2
YAW=50.0°
YAW=40.0°
YAW=30.0°
YAW=0.0°
YAW=20.0°
YAW=10.0°
RUDDER ANGLE
0.0°
10.0°
20.0°
30.0°
40.0°

FIG. 43

Figure 43 also shows the effect of rudder displacement on the drag coefficient. At zero yaw the drag is increased about four times when the rudder is displaced to 40 degrees. Consider for a moment the case of the ordinary car. Since the ordinary car has no rudders the effect of yaw can be estimated (coefficients would of course have different values) by reading up the ordinate for rudder angle =0. Such an analysis shows that in a cross wind the Roadplane operates at a much smaller drag than does the ordinary car due to the change in flow conditions caused by the rudders. In order to bring this and another important fact out in a more forceful fashion refer to Figure 44. In this figure the drag coefficients are referred to body axes instead of wind axes. The coefficients along these axes are plotted both as coefficients and as a % of the minimum value of $(C_D)_{\text{wind axis}}$. In addition to the curves for the Roadplane a curve for the stripped model of the Shenandoah (Reference 6) is shown. This curve is used for purposes of comparison since it represents the drag characteristics of a very excellent streamline shape.

Looking at the curves for the Shenandoah and the Tail Boom Model it will be seen that both curves have the same general shape and that the drag coefficient referred to body axes decreases with increasing angle of yaw. This decrease is so pronounced that at 43 degrees on the airship and 56 degrees on the Tail Boom Model the drag forces become propulsive forces. This effect is a familiar one in aeronautics

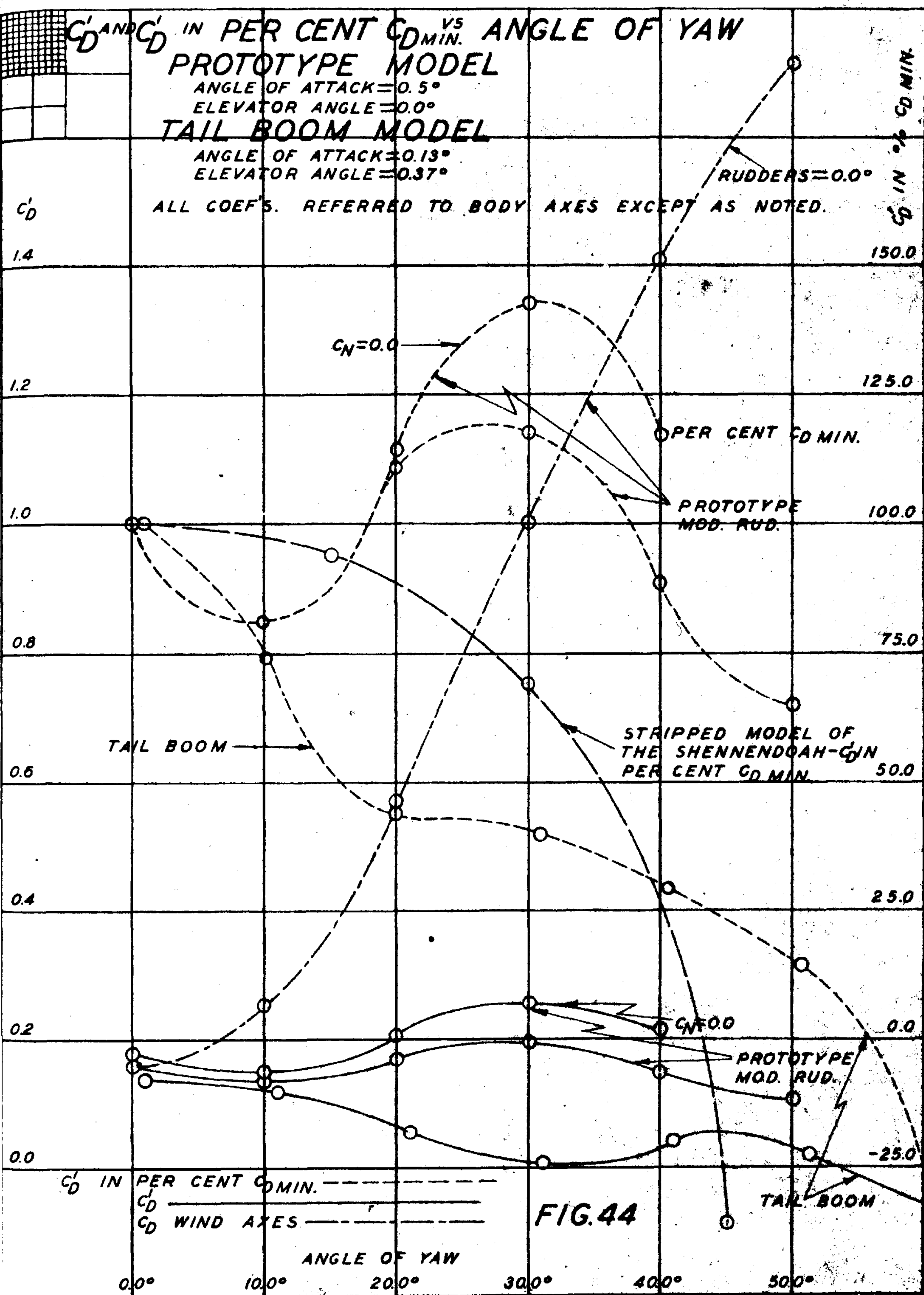

C'D AND C'D IN PER CENT CD MIN. VS ANGLE OF YAW
PROTOTYPE MODEL
ANGLE OF ATTACK = 0.5°
ELEVATOR ANGLE = 0.0°
TAIL BOOM MODEL
ANGLE OF ATTACK = 0.13°
ELEVATOR ANGLE = 0.37°
RUDDERS = 0.0°
ALL COEF'S. REFERRED TO BODY AXES EXCEPT AS NOTED.
C'D
C'D IN % CD MIN.
1.4
1.2
1.0
0.8
0.6
0.4
0.2
0.0
150.0
125.0
100.0
75.0
50.0
25.0
0.0
-25.0
CN=0.0
PER CENT CD MIN.
PROTOTYPE MOD. RUD.
STRIPPED MODEL OF THE SHENNENDOAH-C'D IN PER CENT CD MIN.
TAIL BOOM
CN=0.0
PROTOTYPE MOD. RUD.
TAIL BOOM
C'D IN PER CENT CD MIN.
C'D
CD WIND AXES
ANGLE OF YAW
0.0°
10.0°
20.0°
30.0°
40.0°
50.0°

FIG. 44

and is used to advantage in such applications as the autogyro. The effect is produced, of course, by the action of the cross wind force. In a shape streamlined in plan form this force is really a lift force and leans forward when the model is yawed. Its forward acting component reduces the drag force acting along the body axis and when large angles are reached the forward acting component of the lift force may even be larger than the rearward acting component of the drag force. This effect is illustrated in Figure 44.

In the Prototype Model which is only slightly streamlined in plan form the effect is much less and is completely obliterated at 20 degree yaw due probably to a stalled condition occuring on the leeward side of the car at this angle. It will be noted that the effect appears again at 40 degrees yaw. The conventional car or even a car streamlined in elevation only, would probably have characteristics much worse than the Prototype Model. This phenomemon illustrates a very important fact which may be stated as follows. Vehicles which operateunder yawed conditions (namely automobiles) benefit more by streamlining in plan than in elevation.

In Figure 45 the BHP, torque, and specific fuel consumption of a V-8-82 Horsepower motor are plotted against R.P.M. These curves with the exception of the specific fuel consumption curve, were furnished by the manufacturer. The specific fuel consumption curve was plotted in on a percentage basis from another motor. It should, however, be quite accurate as the specific fuel consumption of all modern motors varies only

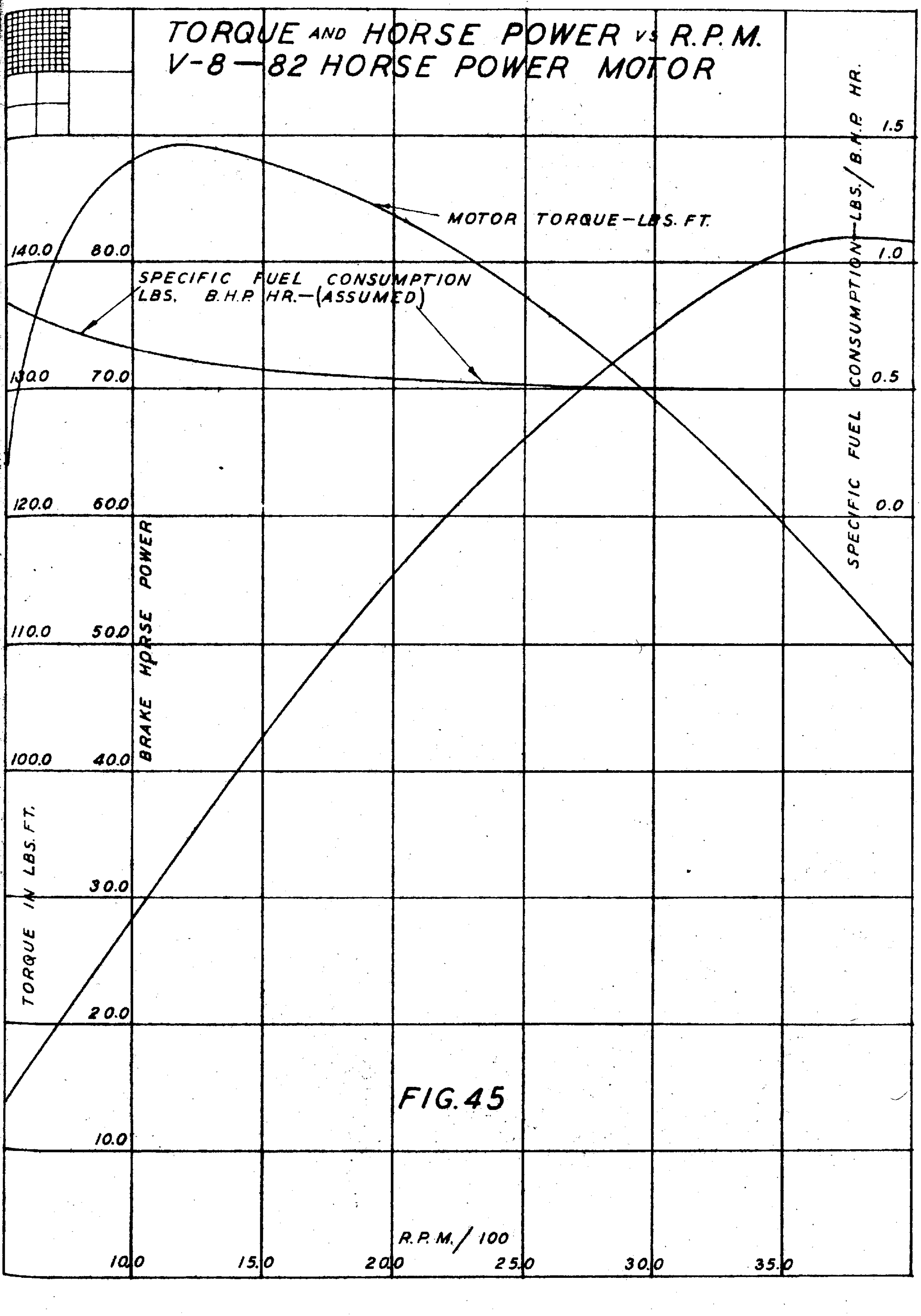
TORQUE AND HORSE POWER vs R.P.M.
V-8—82 HORSE POWER MOTOR
MOTOR TORQUE—LBS. FT.
SPECIFIC FUEL CONSUMPTION
LBS. B.H.P. HR.—(ASSUMED)
TORQUE IN LBS. FT.
BRAKE HORSE POWER
SPECIFIC FUEL CONSUMPTION—LBS./B.H.P. HR.
140.0
130.0
120.0
110.0
100.0
80.0
70.0
60.0
50.0
40.0
30.0
20.0
10.0
1.5
1.0
0.5
0.0
R.P.M./100
10.0
15.0
20.0
25.0
30.0
35.0

FIG. 45

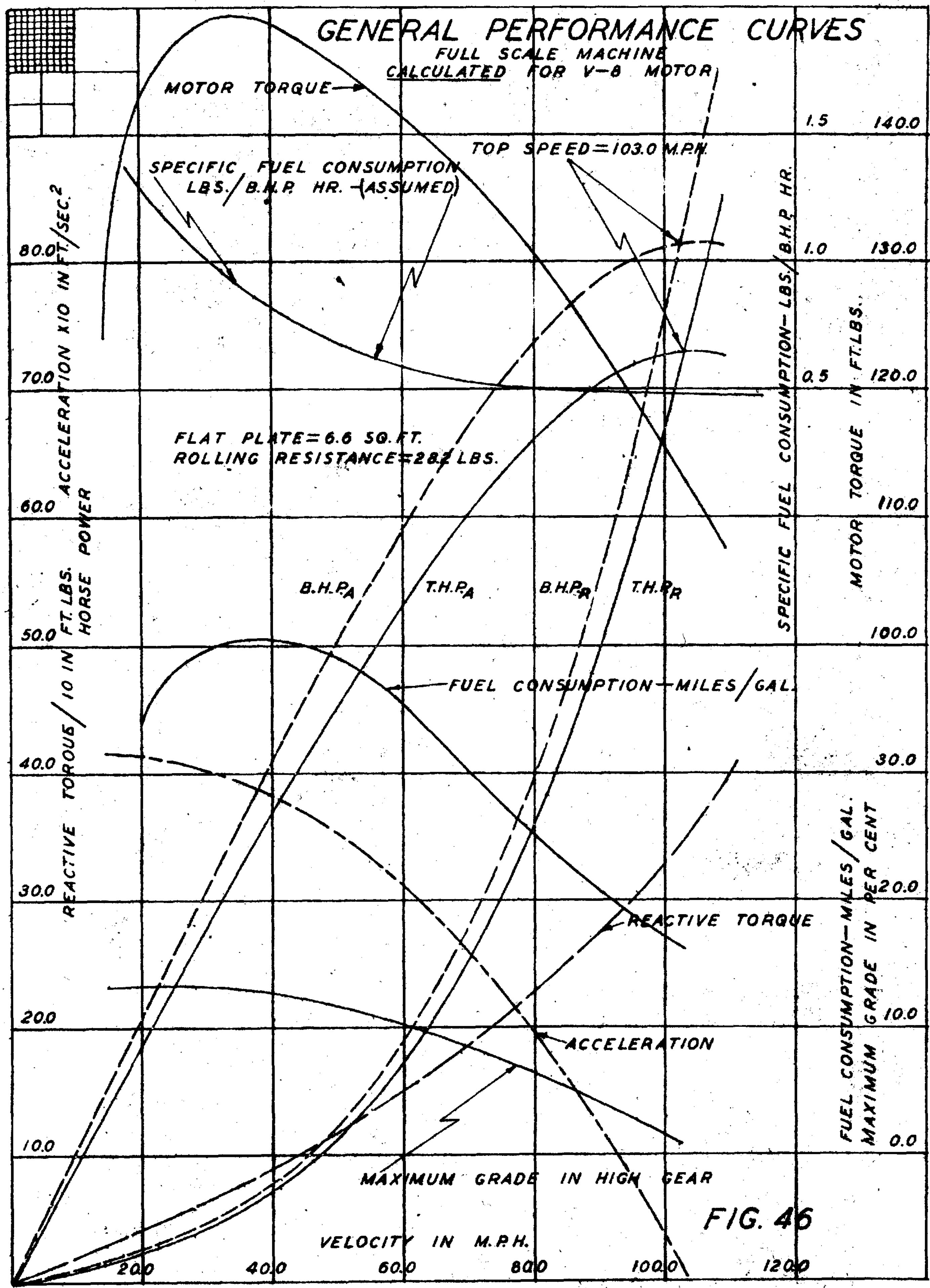
GENERAL PERFORMANCE CURVES
FULL SCALE MACHINE
CALCULATED FOR V-8 MOTOR
MOTOR TORQUE
TOP SPEED=103.0 M.P.H.
SPECIFIC FUEL CONSUMPTION
LBS./B.H.P. HR.-(ASSUMED)
FLAT PLATE=6.6 SQ.FT.
ROLLING RESISTANCE=282 LBS.
B.H.P.A
T.H.P.A
B.H.P.R
T.H.P.R
FUEL CONSUMPTION-MILES/GAL.
REACTIVE TORQUE
ACCELERATION
MAXIMUM GRADE IN HIGH GEAR
VELOCITY IN M.P.H.
20.0
40.0
60.0
80.0
100.0
120.0
10.0
20.0
30.0
40.0
50.0
60.0
70.0
80.0
ACCELERATION X10 IN FT./SEC.2
REACTIVE TORQUE/10 IN FT.LBS.
HORSE POWER
SPECIFIC FUEL CONSUMPTION-LBS./B.H.P. HR.
0.5
1.0
1.5
MOTOR TORQUE IN FT.LBS.
100.0
110.0
120.0
130.0
140.0
FUEL CONSUMPTION-MILES/GAL.
MAXIMUM GRADE IN PER CENT
0.0
10.0
20.0
30.0

FIG. 46

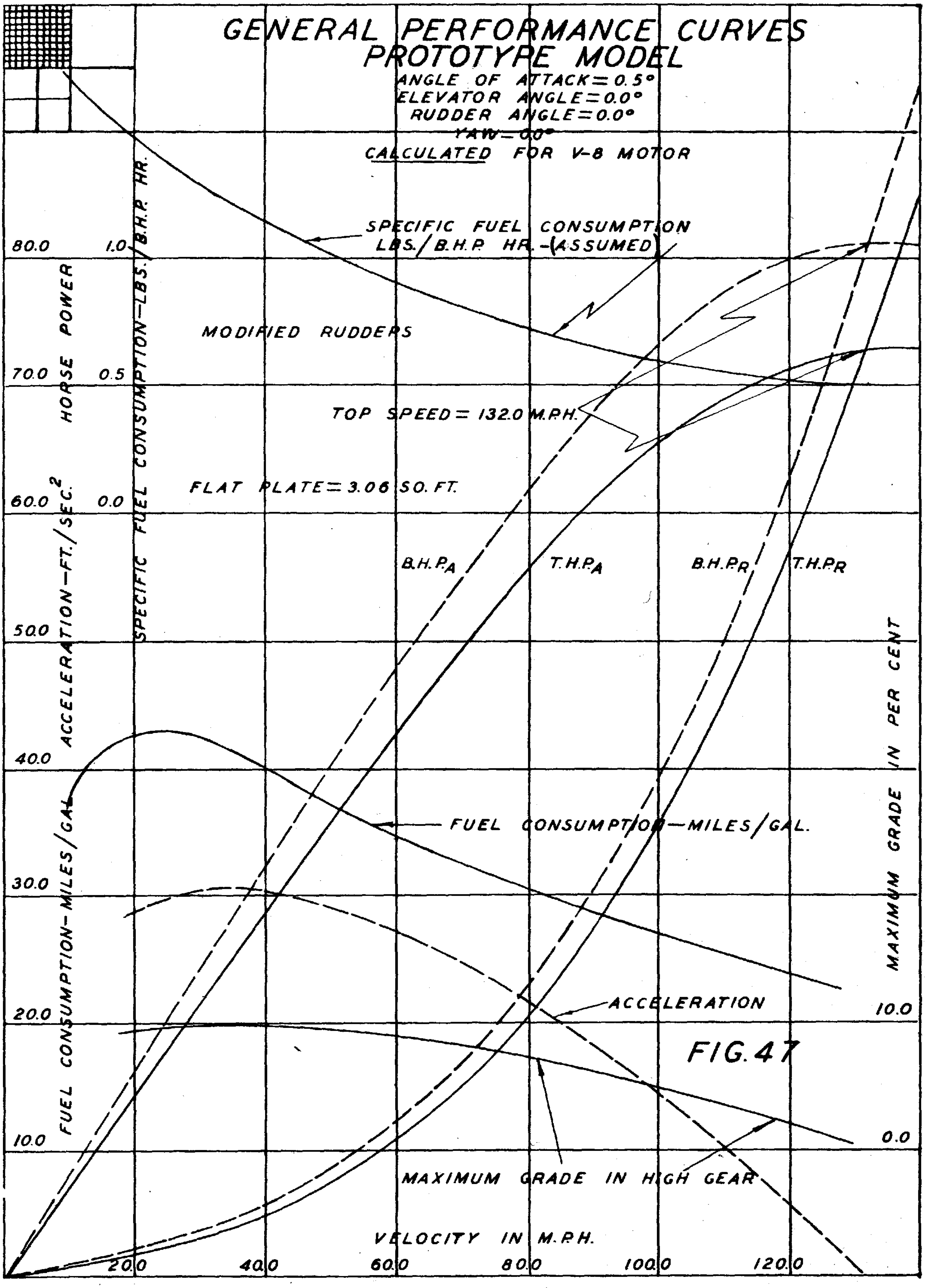
GENERAL PERFORMANCE CURVES
PROTOTYPE MODEL
ANGLE OF ATTACK = 0.5°
ELEVATOR ANGLE = 0.0°
RUDDER ANGLE = 0.0°
YAW = 0.0°
CALCULATED FOR V-8 MOTOR
SPECIFIC FUEL CONSUMPTION LBS./B.H.P. HR.-(ASSUMED)
MODIFIED RUDDERS
TOP SPEED = 132.0 M.P.H.
FLAT PLATE = 3.06 SQ. FT.
B.H.P.A
T.H.P.A
B.H.P.R
T.H.P.R
FUEL CONSUMPTION-MILES/GAL.
ACCELERATION
MAXIMUM GRADE IN HIGH GEAR
VELOCITY IN M.P.H.
HORSE POWER
SPECIFIC FUEL CONSUMPTION-LBS./B.H.P. HR.
ACCELERATION-FT./SEC.²
FUEL CONSUMPTION-MILES/GAL
MAXIMUM GRADE IN PER CENT
80.0
70.0
60.0
50.0
40.0
30.0
20.0
10.0
1.0
0.5
0.0
10.0
0.0
20.0
40.0
60.0
80.0
100.0
120.0
FIG. 47

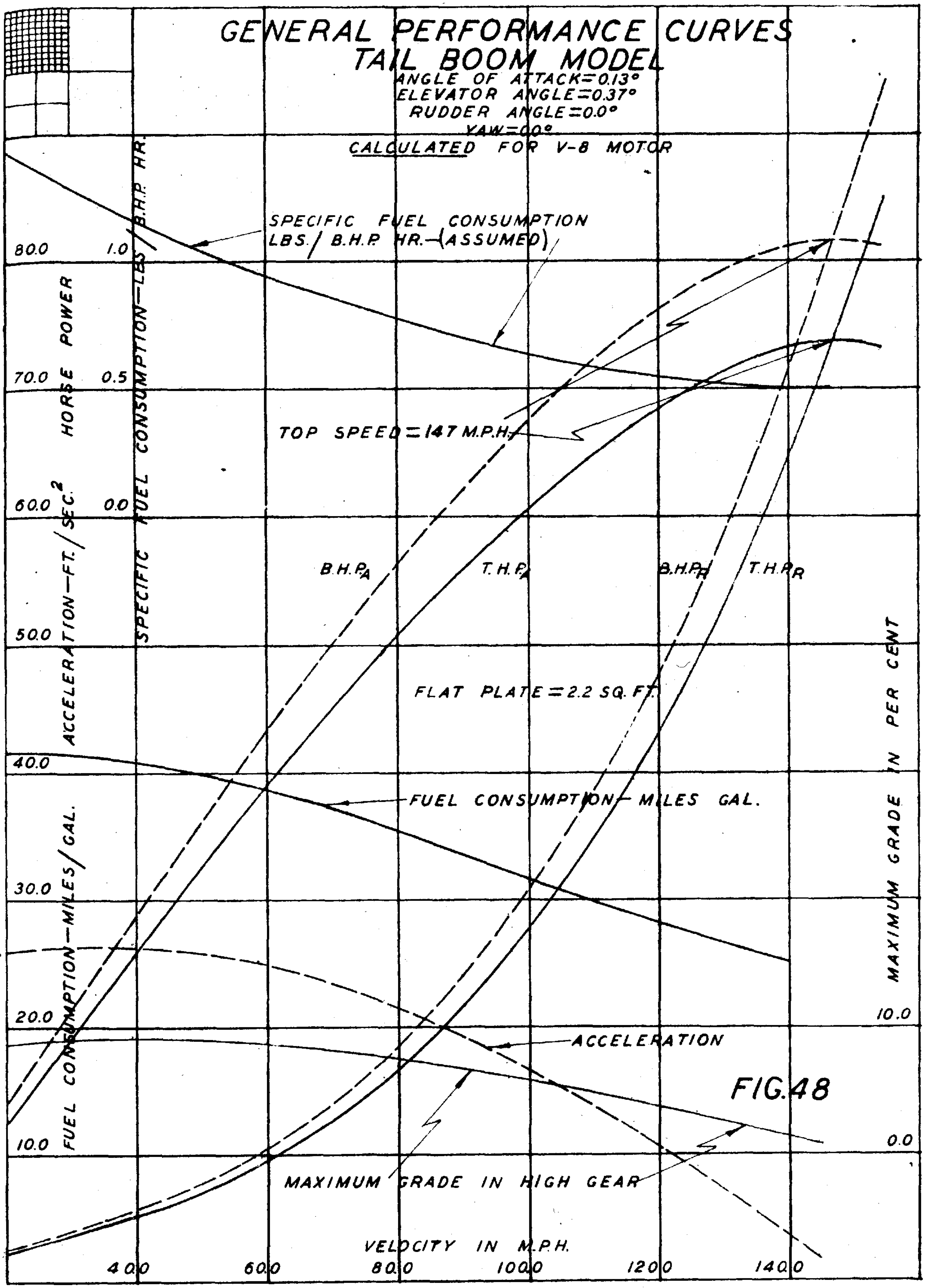
GENERAL PERFORMANCE CURVES
TAIL BOOM MODEL
ANGLE OF ATTACK=0.13°
ELEVATOR ANGLE=0.37°
RUDDER ANGLE=0.0°
YAW=0.0°
CALCULATED FOR V-8 MOTOR
SPECIFIC FUEL CONSUMPTION LBS./B.H.P. HR.-(ASSUMED)
TOP SPEED=147 M.P.H.
B.H.P.A
T.H.P.A
B.H.P.R
T.H.P.R
FLAT PLATE=2.2 SQ. FT.
FUEL CONSUMPTION-MILES GAL.
ACCELERATION
MAXIMUM GRADE IN HIGH GEAR
VELOCITY IN M.P.H.
HORSE POWER
SPECIFIC FUEL CONSUMPTION-LBS./B.H.P. HR.
ACCELERATION-FT./SEC.²
FUEL CONSUMPTION-MILES/GAL.
MAXIMUM GRADE IN PER CENT
80.0
70.0
60.0
50.0
40.0
30.0
20.0
10.0
1.0
0.5
0.0
10.0
0.0
40.0
60.0
80.0
100.0
120.0
140.0

FIG. 48

slightly. This consumption curve is, if anything, conservative since it was taken from tests on a motor several years old.

The curves in Figure 45 are transferred to Figures 46, 47, and 48 with proper selection of gear ratios so that top speed and maximum BHP will coincide. Figures 46, 47, and 48 show the top speed, power required at any speed, acceleration at any speed, fuel consumption in miles per gallon at any speed. These curves are plotted from data obtained from wind tunnel tests on the Tail Boom and Prototype Models and on data obtained from road tests on the full scale machine. (See Appendix III). Figures 47 and 48 are calculated for a machine which weighs 2400 pounds, has an assumed drive gear efficiency of 90%, and a rolling resistance of 0.0125W lbs. Figure 46 is plotted for the full scale machine which weighed 2337 pounds with operator and passenger, and which had a rolling resistance of 28.2 pounds and an equivalent flat plate parasite area of 6.6 square feet. The drive gear efficiency was assumed to be 90%. Figure 46 is the only Figure which can justifiably be considered on a comparative basis with other full scale machines. This figure shows a maximum fuel consumption of 40.1 miles per gallon at 40.0 miles per hour and a top of speed of 103.0 miles per hour. From this figure it will be seen that the car can climb a 14% grade in high gear at any speed between 20 and 38 miles per hour. The maximum acceleration in high gear is approximately 4.0 ft/sec^2. The maximum acceleration occurs at 20 miles per hour. Note that at 60 miles per hour the acceleration in high gear has dropped to 3 ft/sec^2. It is of interest to see that the fuel consumption is 25 miles per gallon at 80 miles per hour and 17 miles per gallon at 100 miles per hour. Referring to Figures 47 and 48 several factors appear to be startling. In Figure 47 the equivalent flat plate parasite area is 3.06 sq. ft., and in Figure 48 it is 2.2 sq.ft. In spite of this difference there is little variation in the fuel consumption. In fact, the best fuel consumption is very little better than for the full scale machine which had a flat plate of 6.6 sq.ft. In regard to speed, the better streamlined model has the higher top speed, 147 miles per hour against 132 miles per hour. This would, of course, be expected. Note that the car with the lowest air resistance suffered slightly in regard to hill climbing ability and very markedly in regard to accelerating ability in high gear. The fuel economy at high speeds is excellent in all models. From these curves it appears that at 100 miles per hour the full scale machine (flat plate 6.6) could make 17 miles to the gallon, the Prototype Model (flat plate 3.06) could make 27 miles to the gallon and the Tail Boom Model (flat plate 2.2) could make 31.5 miles per gallon. The explanation for the poor hill climbing and acceleration on the highly streamlined models is quite obvious and has been noted by other observers. (References 1 and 7). In brief, a gear ratio suitable for top speed on a highly streamlined model is entirely unsuited for the lower speeds. The ideal solution to this problem will be found in the installation of a continously variable transmission. Such a device is discussed at length in References 1 and 7. The poor fuel economy at the lower speeds is due to the fact that the motor is called upon to develop such a small percent of its total power that it is inefficient. In other words, the motor is simply too large to drive a car of this type at low speeds and still operate at an economical point on its specific fuel consumption curve.

Notice, however, the wonderful economy at the high speeds. When and if cars are built so that their flat plate coefficients do not exceed 2, 3, or 4 sq.ft., they should be supplied with a special transmission to take care of the large speed range possible and extremely good fuel economy should not be expected at the lower speeds unless small motors are used and the top speed limited to 80 or 100 miles per hour.

CONCLUSION

1. Air steering at speeds beyond 30 miles per hour is a definite possibility.

2. A car of moderate length can be given excellent streamline characteristics without putting the motor in the rear.

3. Individual wheel brakes can be used on a road vehicle safely and effectively after the operator has become accustomed to their use.

4. An air controlled car can be operated in cross winds.

5. A properly designed air steered car is practically unaffected by passing vehicles.

6. Assuming usual operating conditions, streamlining in plan form is superior to streamlining in elevation.

7. At 100 miles per hour the aerodynamic moments on a vehicle which has a large angle of yaw are too large to be safely ignored.

8. Very finely streamlined vehicles should have a special type of transmission if they are to develop their maximum effectiveness.

9. The fuel economy possible with correct streamlining is very high especially at the higher speeds.

10. The basic pitching moment characteristics of a Roadplane are unstable. This instability is particularly bad when the car is running on a hill or is accelerating.

11. The basic pitching moment characteristics of a Roadplane are functions solely of the inclination of the road, the

pitch, and the accelerations of the vehicle.

12. The Prototype Model Roadplane is aerodynamically unstable about a pitching **axis** and the Tail Boom Model is stable.

13. If two wheeled operation is to be considered it is essential that a Roadplane be made as light as possible unless extreme length is allowable.

14. In the types of Roadplanes so far tested, stability and balance cannot be obtained about a pitching axis when the machine is on <u>steep hills</u> or is experiencing <u>accelerations</u> of any appreciable magnitude, unless a speed of 60 miles per hour is considerably exceeded or special balancing devices are used.

15. In an air steered Roadplane side forces due to cross winds can be considerably reduced by the use of the rudders.

16. In an air steered Roadplane the minimum radius of non skidded turn slightly exceeds the minimum radius of turn for a conventional car.

17. A Roadplane should be able to make skidded turns under full control.

18. In any vehicle which is not supported at, at least two points along its longitudinal axis, the center of gravity should be ahead of the point of support.

19. In any road vehicle, if dependence is placed on the classical methods of steering it is essential that an appreciable amount of weight be kept on the rear wheels at all times.

20. When the weight of a vehicle is located directly over the axes of rotation, the moment necessary to maintain a normal turn, (neglecting friction) is equal to one quarter of the aerodynamic drag divided by the radius of the turn and multiplied by the square of the wheel tread.

21. Any road vehicle designed to operate at high speeds should have neutral or very slight aerodynamic stability about a yawing axis.

22. In an air controlled Roadplane satisfactory aerodynamic directional control can be obtained at air speeds as low as thirty miles per hour.

23. In the opinion of the author the case for the three wheeled car with conventional steering and with the third wheel located in the rear is practically hopeless. In this type of car a rear C. G. location does not give sufficient moment to prevent overturning and a forward C. G. location renders the car uncontrollable, when the brakes are applied on a high speed turn.

24. In the opinion of the author the Roadplane offers considerable promise as a high speed land vehicle and its possibilities should be further investigated.

APPENDICES

APPENDIX I

A. Constant Data
B. Experimental Data

APPENDIX II

Reduction of Data

APPENDIX III

References

APPENDIX IV

Acknowledgements

APPENDIX I

A. Constant Data

B. Experimental Data

PART A

CONSTANT DATA

A. PROJECTED FRONTAL AREA-CAR AXIS HORIZONTAL

1. Body Type	Wind Tunnel Model sq.in.	Full Scale Machine sq.ft.
a. Tail Boom Model	11.75	20.80
b. Prototype Model		
(1) Body No. 1 Cabin No. 1	12.94	23.20
(2) Body No. 1 Cabin No. 2	12.94	23.20
(3) Body No. 2 Cabin No. 2	12.74	22.63
(4) Body No. 2 Cabin No. 3	12.74	22.63
(5) Body No. 2 Cabin No. 4	12.86	22.90
(6) Body No. 2 Cabin No. 5	12.86	22.90
(7) Body No. 2 Cabin No. 6	12.99	23.22
(8) Body No. 2 Cabin No. 7	12.88	23.00
(9) Body No. 2 Cabin No. 8	12.68	22.45
(10) Body No. 2 Cabin No. 9	12.68	22.45
(11) Body No. 2 without cabin	10.46	18.60
(12) Body No. 2 Cabin No. 9 (modified tail)	13.26	23.60
(13) Body No.n2 without cabin or tail	8.80	15.64
(14) Body No. 2 without cabin (modified tail)	10.60	18.85
c. Full Scale Machine		23.50

B. AREA IN PLAN VIEW-CAR AXIS HORIZONTAL

1. Body Type	Wind Tunnel Model sq.in.	Full Scale Machine sq.ft.
a. Tail Boom Model	34.68	61.60
b. Prototype Model		
(1) Body No. 1 Cabins No. 1-2	43.76	77.80
(2) Body No. 2 Cabins No. 1-9	43.52	77.50
(3) Body No. 2 Cabin No. 9 (modified tail)	43.52	77.50
c. Full Scale Machine		72.50

C. LENGTH CAR-AXIS HORIZONTAL

1. Body Type	Wind Tunnel Model in.	Full Scale Machine ft.-in.
a. Tail Boom Model	11.53	15-5
b. Prototype Model		
(1) All Forms	10.40	13-10.5
c. Full Scale Machine	14	14-7

D. DYNAMIC PRESSURE

q = 75.8 mm. of alcohol @ specific gravity 0.807

E. AERODYNAMIC TARES ON BALANCE SUPPORT

1. Tail Boom Model
   a. Lift = 30.0 gms.
   b. Drag = 103.5 gms.
   c. P.M.F.= -3.0 gms.
   d. Y.M.F.= Assumed 0.0 gms.
   e. R.M.F.= " 0.0 gms
   f. C.W.F.= " 0.0 gms.

2. Prototype Model
   a. Lift = 20.0 gms.
   b. Drag = 100.0 gms.
   c. P.M.F.= -2.5 gms.
   d. Y.M.F.= 8.5 gms.
   e. R.M.F.= 4.0 gms.
   f. C.W.F.= 4.0 gms.

3. Prototype Model Body No. 2 Without Cabin (modified tail)
   a. Lift = 25.0 gms.
   b. Drag = 99.0 gms.
   c. P.M.F.= -2.0 gms.
   d. Y.M.F.= 9.0 gms.
   e. R.M.F.= 3.0 gms.
   f. C.W.F.= 6.0 gms.

F. AVERAGE BAROMETRIC PRESSURE

736.77 mm. Mercury

G. AVERAGE ROOM TEMPERATURE

31.36° Centigrade

H. AVERAGE SEA LEVEL VELOCITY

70.0 Miles per Hour

I. REYNOLDS NUMBER BASED ON OVERALL LENGTH

a. Tail Boom Model - 594,000
b. Prototype Model - 500,000

PART B

EXPERIMENTAL DATA

Table XIII

Constant Speed Coasting Tests

Hill No.I
Length 1200 feet
Slope Angle 1 -44'
Loaded Weight of Machine 2337 lbs.

Wind Calm

Run No.	Speed-ometer M.P.H.	Time 1st Half Sec.	Time Finished Sec.	Time 2nd Half Sec.	Average Speed 1st Half M.P.H.	Average Speed 2nd Half M.P.H.
1	---	7.5	15.0	7.5	45.4	45.5
2	---	7.2	14.8	7.6	47.2	44.8
3	---	8.0	15.8	7.8	42.5	43.6
4	---	8.1	16.0	7.9	42.0	43.0
5	---	7.8	15.2	7.4	43.6	46.0
6	---	7.3	14.6	7.3	46.6	46.6
7	---	7.1	14.6	7.5	47.9	45.4
Total					315.2	314.8
Average					45.0	45.0

Average Coasting Speed 45 mi/hr

Driver Moodie
Timer Mullooney
Helper Whitlock

Propelling Component= 2337 X 0.0303 = 70.8 lbs.

Table XIV

Constant Speed Coasting Tests

Hill No. II
Length 1000 feet
Slope Angle 2 --8'
Loaded weight of Machine 2343 lbs.

Wind Calm

Run No.	Speedometer Start M.P.H.	Time 1st Half Sec.	Time Finished Sec.	Time 2nd Half Sec.	Average Speed 1st Half M.P.H.	Average Speed 2nd Half M.P.H.
1	50.0	8.2	16.2	8.0	49.8	51.0
2	52.0	7.8	15.4	7.6	52.35	53.7
3	54.0	7.6	15.2	7.6	53.70	53.7
4	50.0	8.1	15.8	7.7	50.4	53.0
5	55.0	7.3	15.0	7.7	55.9	53.0
6	54.0	7.6	15.2	7.6	53.7	53.7
7	55.0	7.3	15.0	7.7	55.9	53.0
8	55.0	7.5	15.2	7.7	54.4	53.0
Total	425.0				426.15	424.1
Average	53.2				53.25	53.1

Average Coasting Speed 53.12 mi/hr

Driver Moodie
Timer Craig
Helper Brandau

Propelling Compoment = 2343 X 0.0373 = 87.5 lbs.

Table XV

Fuel Consumption

Road Tests Full Scale Machine

Distance Covered 8280 ft. each way

Gas Used Ethyl Specific Gravity 6.154 lb/gal.

All Data Based on Round Trip

Morning Run

Miles per hr.	Elapsed time (Round trip) Min.	Sec.	Weight Gas Used Grams	Miles per Gallon
17.45	10	46.5	232.5	37.70
18.10	10.	24.0	228.0	38.40
20.00	9	24.0	225.5	38.85
22.55	8	20.0	224.5	39.00
22.80	8	15.0	228.5	38.20
22.60	8	20.0	227.5	38.50
30.50	6	10.0	240.5	36.40
38.50	4	53.0	267.0	32.70
38.25	4	55.0	262.5	33.40

Afternoon Run

Miles per hr.	Elapsed Time (Round Trip) Min	Sec	Weight Gas Used Grams	Miles per Gallon
19.50	9	28.0	218.0	40.20
28.90	6	44.0	225.0	38.90
34.60	5	27.0	237.5	36.90
43.40	4	20.0	287.5	30.50
46.21	4	05.0	304.5	28.80

Table XVIII and XIX

PROTOTYPE MODEL--MODIFIED RUDDERS
BODY NO.2 CABIN NO.9
Elevator angle 0.0 Degrees
Yaw angle 0.0 Degrees
Rudder angle 0.0 Degrees

BODY ONLY

Angle of attack in degrees	Lift coef. C_L	Drag coef. C_D	Equivalent Flat Plate Parasite Area in Sq. Ft.	Pitching Moment Coef. C_m
-8.5	0.1308	0.2345	2.87	-0.00633
-5.5	0.0785	0.1755	2.15	-0.00139
-2.5	0.0436	0.1440	1.76	0.00466
0.5	0.0145	0.1295	1.58	0.01233
3.5	-0.0145	0.1267	1.55	0.02350
6.5	-0.0494	0.1410	1.73	0.03120
9.5	-0.0785	0.1640	2.01	0.03720

Table XVI

DRAG CHARACTERISTICS OF VARIOUS MODELS
Angle of attack 0.5 Degrees
Elevator angle 0.0 Degrees
Rudder angle 0.0 Degrees

Body No.	Cabin No.	Frontal Area in Sq. Ft.	Drag Coef. C_D	Equivalent Flat Plate Parasite Area in Sq. Ft.	Pitching Moment Coef. C_m
1	1	23.00	0.2388	4.32	18.67
1	2	23.00	0.2155	3.90	16.83
2	2	22.62	0.1977	3.49	15.42
2	3	22.62	0.1807	3.19	14.10
2	4	22.83	0.1850	3.32	14.47
2	5	22.83	0.1713	3.12	13.40
2	6	23.02	0.1765	3.20	13.78
2	7	22.85	0.1958	3.52	15.30
2	7*	22.85	0.1690	3.04	13.20
2	8	22.50	0.1690	2.96	13.19
2	9	22.50	0.1699	2.98	13.28
2	9M	23.55	0.1662	3.06	13.00
T.B.M.	#	20.85	0.1349	2.20	10.52

Note: *Elevator set at 7.5 Degrees
#Tail Boom Model -- Angle of attack 0.13 Degrees and Elevator angle 0.37 Degrees

Table XVII

LIFT AND L/D CHARACTERISTICS OF VARIOUS MODELS

Angle of attack 0.5 Degrees
Elevator angle 0.0 Degrees
Rudder angle 0.0 Degrees

Body No.	Cabin No.	Plan Area in Sq. Ft.	Lift Coef. C_L	L/D
1	1	77.8	0.0347	0.492
1	2	77.8	0.0376	0.590
2	2	77.5	0.0116	0.201
2	3	77.5	------	-----
2	4	77.5	------	-----
2	5	77.5	0.0058	0.115
2	6	77.5	0.0116	0.221
2	7	77.5	0.0174	0.302
2	7*	77.5	-0.0145	-0.291
2	8	77.5	0.0000	0.000
2	9	77.5	0.0029	0.0588
2	9M	77.5	-0.0058	-0.115
T.B.M.#		61.7	-0.00732	-0.1575

<u>Note</u>: *Elevator set at 7.5 Degrees
#Tail Boom Model--Angle of attack 0.13 Degrees and Elevator angle 0.37 Degrees

Table XXXIX

PROTOTYPE MODEL--MODIFIED RUDDERS

BODY NO.2 CABIN NO.9

Elevator angle 0.0 Degrees
Angle of attack 0.5 Degrees
Yawing moment coefficient C_n 0

Yaw angle in degrees	Rudder angle in degrees	Cross wind coef. C_c	Longitudinal side C.P. in % of car length
0.0	0.75	0.0000	100.3
-10.0	7.40	0.1000	37.0
-20.0	12.20	0.185	36.0
-30.0	20.30	0.218	42.0
-40.0	24.90	0.247	37.0
-50.0	30.50	0.177	42.5

Table XVIII and XIX

PROTOTYPE MODEL--MODIFIED RUDDERS

BODY NO.2 CABIN NO.9
Elevator angle 0.0 Degrees
Yaw angle 0.0 Degrees
Rudder angle 0.0 Degrees

BODY PLUS CABIN

Angle of attack in degrees	Lift coef. C_L	Drag coef. C_D	Equivalent Flat Plate Parasite Area in Sq. Ft.
-8.5	0.1280	0.2093	3.42
-5.5	0.0698	0.1653	2.70
-2.5	0.0378	0.1480	2.42
0.5	0.0116	0.1378	2.25
3.5	-0.0233	0.1426	2.33
6.5	-0.0464	0.1536	2.51
9.5	-0.0753	0.1838	3.00

COMPLETE MODEL LESS ELEVATORS

Angle of attack in degrees	Lift coef. C_L	Drag coef. C_D	Equivalent Flat Plate Parasite Area in Sq. Ft.	Pitching Moment Coef. C_m
-8.5	0.1309	0.2180	4.02	-0.00555
-5.5	0.0755	0.1823	3.36	-0.00414
-2.5	0.0320	0.1660	3.06	-0.00040
0.5	0.0087	0.1660	3.06	-0.00580
3.5	-0.0378	0.1613	2.97	-0.01003
6.5	-0.0726	0.1738	3.20	-0.01448
9.5	-0.1162	0.2023	3.73	-0.01945

COMPLETE MODEL

Angle of attack in degrees	Lift coef. C_L	Drag coef. C_D	Equivalent Flat Plate Parasite Area in Sq. Ft.	Pitching Moment Coef. C_m
-8.5	0.1480	0.2360	4.35	0.001117
-5.5	0.0843	0.1940	3.57	-0.000865
-2.5	0.0407	0.1768	3.26	-0.000500
0.5	-0.0058	0.1662	3.06	0.003360
3.5	-0.0436	0.1680	3.10	0.007600
6.5	-0.0813	0.1825	3.36	0.010850
9.5	-0.0122	0.2130	3.93	0.012120

Table XX

TAIL BOOM MODEL
Rudder angle 0.0 Degrees
Yaw angle 0.0 Degrees

ELEVATOR ANGLE 0.13 DEGREES

Angle of attack in degrees	Lift coef. C_L	Pitching moment coef. C_m	Drag coef. C_D	Longitudinal side C.P. in % of car length
-8.87	0.1534	0.03750	0.1985	47.8
-5.87	0.0878	0.02320	0.1580	47.8
-2.87	0.0366	0.00921	0.1413	39.0
0.13	-0.00732	-0.00112	0.1349	79.0
3.13	-0.0585	-0.00774	0.1380	49.5
6.13	-0.1097	-0.00227	0.1530	53.6
9.13	-0.01534	-0.0289	0.1765	51.0

Table XX

PROTOTYPE MODEL--ORIGINAL RUDDERS
BODY NO.2 CABIN NO.9
Elevator angle 0.0 Degrees
Rudder angle 0.0 Degrees
Yaw angle 0.0 Degrees

Angle of attack in degrees	Lift coef C_L	Pitching moment coef. C_m	Drag coef. C_D	Longitudinal side C.P. in % of car length
-5.5	0.0843	-0.00087	0.1940	0.00000
-2.5	0.0407	-0.00050	0.1768	------
0.5	-0.0058	0.00336	0.1662	------
3.5	-0.0436	0.00760	0.1680	------
6.5	-0.0813	0.01085	0.1825	------
9.5	-0.1220	0.01212	0.2130	------

Tables XXI --XXVI

PROTOTYPE MODEL--ORIGINAL RUDDERS

BODY NO.2	CABIN NO.9
Rudder angle	0.0 Degrees
Yaw angle	0.0 Degrees

ELEVATOR ANGLE -45 DEGREES

Angle of attack in degrees	Lift Coef. C_L	DRAG Coef. C_D	Pitching Moment Coef. C_m	Longitudinal side C.P. in % of car length
-5.5	0.160	0.434	0.0207	34.8
-2.5	0.125	0.398	0.0212	36.0
0.5	0.090	0.378	0.0289	45.0
3.5	0.0726	0.368	0.0374	51.2
6.5	0.0494	0.363	0.0474	89.6
9.5	0.0232	0.358	0.0530	74.4

ELEVATOR ANGLE -30 DEGREES

Angle of attack in degrees	Lift Coef. C_L	Drag coef. C_D	Pitching Moment Coef. C_m	Longitudinal side C.P. in % of car length
-5.5	0.1625	0.379	0.0187	35.7
-2.5	0.1190	0.346	0.0235	40.5
0.5	0.0842	0.325	0.0302	49.5
3.5	0.0581	0.311	0.0347	65.0
6.5	0.0280	0.305	0.0403	113.4
9.5	-0.0028	0.310	0.0456	-873.1

ELEVATOR ANGLE -15 DEGREES

Angle of attack in degrees	Lift Coef. C_L	Drag Coef. C_D	Pitching Moment Coef. C_m	Longitudinal side C.P. in % of car length
-5.5	0.136	0.300	0.0132	34.6
-2.5	0.0930	0.267	0.0174	39.2
0.5	0.0581	0.249	0.0212	49.1
3.5	0.0232	0.237	0.0268	103.1
6.5	-0.00290	0.235	0.0267	-404.1
9.5	-0.0407	0.245	0.0305	-355.1

Tables XXI -- XXVI

PROTOTYPE MODEL--ORIGINAL RUDDERS

BODY NO.2	CABIN NO.9
Rudder angle	0.0 Degrees
Yaw angle	0.0 Degrees

ELEVATOR ANGLE -10 DEGREES

Angle of attack in degrees	Lift Coef. C_L	Drag Coef. C_D	Pitching Moment Coef. C_m	Longitudinal side C.P. in % of car length
-5.5	0.1220	0.272	0.00896	32.1
-2.5	0.0755	0.241	0.0118	22.1
0.5	0.0435	0.222	0.0137	61.3
3.5	0.0058	0.214	0.0217	194.7
6.5	-0.0261	0.219	0.0244	-7.2
9.5	-0.0663	0.2333	0.0301	14.6

ELEVATOR ANGLE -5 DEGREES

Angle of attack in degrees	Lift Coef. C_L	Drag Coef. C_D	Pitching Moment Coef. C_m	Longitudinal side C.P. in % of car length
-5.5	0.1018	0.226	0.000452	25.2
-2.5	0.0552	0.201	0.00621	27.9
0.5	0.0174	0.186	0.0102	34.4
3.5	-0.0145	0.185	0.0141	34.5
6.5	-0.0494	0.195	0.0166	47.1
9.5	-0.090	0.218	0.0216	27.4

ELEVATOR ANGLE 5 DEGREES

Angle of attack in degrees	Lift Coef. C_L	Drag Coef. C_D	Pitching Moment Coef. C_m	Longitudinal side C.P. in % of car length
-5.5	0.0697	0.193	-0.0116	5.0
-2.5	0.0261	0.175	-0.00797	-30.2
0.5	-0.0145	0.167	-0.00369	127.6
3.5	-0.0552	0.174	0.00241	50.9
6.5	-0.0900	0.193	0.00604	42.7
9.5	-0.1280	0.228	0.00755	41.8

Tables XXI -- XXVI

PROTOTYPE MODEL--ORIGINAL RUDDERS

BODY NO.2	CABIN NO.9
Rudder angle	0.0 Degrees
Yaw angle	0.0 Degrees

ELEVATOR ANGLE 10 DEGREES

Angle of attack in degrees	Lift Coef. C_L	Drag Coef. C_D	Pitching Moment Coef. C_m	Longitudinal side C.P. in % of car length
-5.5	0.0552	0.196	-0.0126	-8.8
-2.5	0.01452	0.181	-0.0123	-114.1
0.5	-0.02033	0.178	-0.00923	132.0
3.5	-0.0610	0.188	-0.00336	60.3
6.5	-0.0988	0.215	0.00252	47.3
9.5	-0.1368	0.256	0.00543	44.3

ELEVATOR ANGLE 15 DEGREES

Angle of attack in degrees	Lift Coef. C_L	Drag Coef. C_D	Pitching Moment Coef. C_m	Longitudinal side C.P. in % of car length
-5.5	0.0493	0.208	-0.00755	-1.6
-2.5	0.0087	0.199	-0.0119	-323.1
0.5	-0.0261	0.197	-0.00827	109.9
3.5	-0.0610	0.213	-0.0024	61.3
6.5	-0.0930	0.244	0.00101	51.4
9.5	-0.1280	0.281	0.00504	46.1

ELEVATOR ANGLE 20 DEGREES

Angle of attack in degrees	Lift Coef. C_L	Drag Coef. C_D	Pitching Moment Coef. C_m	Longitudinal side C.P. in % of car length
-5.5	0.0522	0.233	-0.0163	-18.8
-2.5	0.0116	0.231	-0.0119	-175.6
0.5	-0.0208	0.232	-0.00504	131.9
3.5	-0.0493	0.249	0.000112	67.1
6.5	-0.0784	0.275	0.00514	51.2
9.5	-0.1131	0.312	0.0094	45.3

Tables XXI -- XXVI

PROTOTYPE MODEL--ORIGINAL RUDDERS

BODY NO.2	CABIN NO.9
Rudder angle	0.0 Degrees
Yaw angle	0.0 Degrees

ELEVATOR ANGLE 30 DEGREES

Angle of attack in degrees	Lift Coef. C_L	Drag Coef. C_D	Pitching Moment Coef. C_m	Longitudinal side C.P. in % of car length
-5.5	0.0755	0.302	-0.00582	7.3
-2.5	0.0436	0.302	-0.00408	-12.4
0.5	0.0232	0.310	0.00274	-24.7
3.5	0.0029	0.314	0.0115	-194.9
6.5	-0.0174	0.322	0.0192	27.2
9.5	-0.0436	0.324	0.0235	27.5

ELEVATOR ANGLE 40 DEGREES

Angle of attack in degrees	Lift Coef. C_L	Drag Coef. C_D	Pitching Moment Coef. C_m	Longitudinal side C.P. in % of car length
-5.5	0.1130	0.377	-0.00268	16.3
-2.5	0.0872	0.376	0.00353	16.6
0.5	0.0640	0.382	0.013	23.2
3.5	0.0523	0.377	0.0223	37.5
6.5	0.0291	0.350	0.0232	64.8
9.5	-0.0174	0.327	0.0309	-28.1

Tables XXI -- XXVI

PROTOTYPE MODEL--MODIFIED RUDDERS

BODY NO.2	CABIN NO.9
Rudder angle	0.0 Degrees
Yaw angle	0.0 Degrees

ELEVATOR ANGLE ZERO DEGREES

Angle of attack in degrees	Lift Coef. C_L	Drag Coef. C_D	Pitching Moment Coef. C_m	Longitudinal side C.P. in % of car length
-5.5	0.0843	0.1940	-0.000865	----
-2.5	0.0407	0.1768	-0.000502	----
0.5	-0.0058	0.1662	0.00336	----
3.5	-0.0436	0.1680	0.00760	----
6.5	-0.0813	0.1825	0.01085	----
9.5	-0.1220	0.2130	0.01212	----

ELEVATOR ANGLE 15 DEGREES

Angle of attack in degrees	Lift Coef. C_L	Drag Coef. C_D	Pitching Moment Coef. C_m	Longitudinal side C.P. in % of car length
-5.5	0.0522	0.202	-0.0196	23.0
-2.5	0.0058	0.186	-0.0140	-390.1
0.5	-0.0348	0.184	-0.0115	100.9
3.5	-0.0697	0.1930	-0.00458	60.3
6.5	-0.1103	0.2387	0.00207	48.5
9.5	-0.1390	0.2710	0.00441	46.1

Table XXIV

TAIL BOOM MODEL

Rudder angle	0.0 Degrees
Yaw angle	0.0 Degrees

ELEVATOR ANGLE 0.13 DEGREES

Angle of attack in degrees	Longitudinal side C.P. in % of car length
-8.87	47.8
-5.87	47.8
-2.87	39.0
0.13	79.0
3.13	49.5
6.13	53.6
9.13	51.0

PROTOTYPE MODEL--ORIGINAL RUDDERS

BODY NO.2	CABIN NO.9
Rudder angle	0.0 Degrees
Yaw angle	0.0 Degrees

	ELEVATOR ANGLE 5 DEGREES	ELEVATOR ANGLE -5 DEGREES
Angle of attack in degrees	Longitudinal side C.P. in % of car length	Longitudinal side C.P. in % of car length
-5.5	5.0	25.2
-2.5	-30.2	27.9
0.5	127.6	34.4
3.5	50.9	34.5
6.5	42.7	47.1
9.5	41.8	27.4

Tables XXVII and XXVIII
PROTOTYPE MODEL--ORIGINAL RUDDERS

BODY NO.2 CABIN NO.9
Rudder angle 0.0 Degrees
Yaw angle 0.0 Degrees

ANGLE OF ATTACK -5.5 DEGREES

Elevator angle in degrees	Pitching Moment Coef. C_m	Lift Coef. C_L	Drag Coef. C_D	Longitudinal side C.P. in % of car length
-45.0	0.0207	0.160	0.434	34.8
-30.0	0.0187	0.1625	0.379	35.7
-15.0	0.0132	0.136	0.300	34.6
-10.0	0.00896	0.122	0.272	32.1
-5.0	0.000452	0.1018	0.226	25.2
5.0	-0.0116	0.0697	0.193	5.0
10.0	-0.0126	0.0552	0.196	-8.8
15.0	-0.00755	0.0493	0.208	-1.6
20.0	-0.0163	0.0522	0.233	-18.8
30.0	-0.00582	0.0755	0.302	7.3
40.0	-0.00268	0.1130	0.377	16.3

ANGLE OF ATTACK -2.5 DEGREES

Elevator angle in degrees	Pitching Moment Coef. C_m	Lift Coef. C_L	Drag Coef. C_D	Longitudinal side C.P. in % of car length
-45.0	0.0212	0.125	0.398	36.0
-30.0	0.0235	0.1190	0.346	40.5
-15.0	0.0174	0.0930	0.267	39.2
-10.0	0.0118	0.0755	0.241	22.1
-5.0	0.00621	0.0552	0.201	27.9
5.0	-0.00797	0.0261	0.175	-30.2
10.0	-0.0123	0.0145	0.181	-114.1
15.0	-0.0119	0.0087	0.199	-323.1
20.0	-0.0119	0.0116	0.231	-175.6
30.0	-0.00408	0.0436	0.302	-12.4
40.0	-0.00353	0.0872	0.376	16.3

Tables XXVII and XXVIII

PROTOTYPE MODEL--ORIGINAL RUDDERS

BODY NO.2	CABIN NO.9
Rudder angle	0.0 Degrees
Yaw angle	0.0 Degrees

ANGLE OF ATTACK 0.5 DEGREES

Elevator angle in degrees	Pitching Moment Coef. C_m	Lift Coef. C_L	Drag Coef. C_D	Longitudinal side C.P. in % of car length
-45.0	0.0289	0.090	0.378	45.0
-30.0	0.0302	0.0842	0.325	49.5
-15.0	0.0212	0.0581	0.249	49.1
-10.0	0.0137	0.0435	0.222	61.3
-5.0	0.0102	0.0174	0.186	34.4
5.0	-0.00369	-0.0145	0.167	127.6
10.0	-0.00923	-0.0203	0.178	132.0
15.0	-0.00827	-0.0261	0.197	109.9
20.0	-0.00504	-0.0208	0.232	131.9
30.0	0.00274	0.0232	0.310	-24.7
40.0	0.013	0.064	0.382	23.2

ANGLE OF ATTACK 3.5 DEGREES

Elevator angle in degrees	Pitching Moment Coef. C_m	Lift Coef. C_L	Drag Coef. C_D	Longitudinal side C.P. in % of car length
-45.0	0.0374	0.0726	0.368	51.2
-30.0	0.0347	0.0581	0.311	65.0
-15.0	0.0268	0.0232	0.237	103.1
-10.0	0.0217	0.0058	0.214	194.7
-5.0	0.0141	-0.0145	0.185	34.5
5.0	0.00241	-0.0552	0.174	50.9
10.0	-0.00336	-0.061	0.188	60.3
15.0	-0.0024	-0.0610	0.213	61.3
20.0	0.000112	-0.0493	0.249	67.1
30.0	0.0115	0.0029	0.314	-194.9
40.0	0.0223	0.0523	0.377	37.5

Tables XXVII and XXVIII

PROTOTYPE MODEL--ORIGINAL RUDDERS

BODY NO.2	CABIN NO.9
Rudder angle	0.0 Degrees
Yaw angle	0.0 Degrees

ANGLE OF ATTACK 6.5 DEGREES

Elevator angle in degrees	Pitching moment coef. C_m	Lift coef. C_L	Drag coef. C_D	Longitudinal side C.P. in % of car length
-45.0	0.0474	0.0494	0.363	89.6
-30.0	0.0403	0.0280	0.305	113.4
-15.0	0.0267	-0.0029	0.235	-404.1
-10.0	0.0244	-0.0261	0.219	-7.2
-5.0	0.0166	-0.0494	0.195	47.1
5.0	0.00604	-0.0900	0.193	42.7
10.0	0.00252	-0.0988	0.215	47.3
15.0	0.00101	-0.0930	0.244	51.4
20.0	0.00514	-0.0784	0.275	51.2
30.0	0.0192	-0.0174	0.322	27.2
40.0	0.0232	0.0291	0.350	64.8

ANGLE OF ATTACK 9.5 DEGREES

Elevator angle in degrees	Pitching moment coef. C_m	Lift coef. C_L	Drag coef. C_D	Longitudinal side C.P. in % of car length
-45.0	------	-----	0.358	174.4
-30.0	0.0456	-----	0.310	-873.1
-15.0	0.0305	-----	0.245	-355.1
-10.0	0.0301	-----	0.233	14.6
-5.0	0.0216	-----	0.218	27.4
5.0	0.00755	-----	0.228	41.8
10.0	0.00543	-----	0.256	44.3
15.0	0.00504	-----	0.281	46.1
20.0	0.0094	-----	0.312	45.3
30.0	0.0235	-----	0.324	27.5
40.0	0.0309	-----	0.327	-28.1

Table XXIX

PROTOTYPE MODEL--MODIFIED RUDDERS

BODY NO.2	CABIN NO.9
Angle of attack	0.5 Degrees
Yaw angle	0.0 Degrees

RUDDER ANGLE ZERO DEGREES

Elevator angle in degrees	Pitching moment coef. C_m	Lift coef. C_L	Drag coef. C_D	Longitudinal side C.P. in % of car length
-60.0	0.047	0.1076	0.419	56.7
-50.0	0.0498	0.1017	0.382	63.2
-40.0	0.0467	0.1047	0.358	61.0
-30.0	0.0422	0.0958	0.302	62.1
-20.0	0.0349	0.0668	0.258	66.3
-15.0	0.0324	0.0552	0.240	69.7
-10.0	0.0232	0.0348	0.195	70.1
-5.0	0.0143	0.0145	0.170	65.9
0.0	0.00336	-0.0058	0.1662	----
5.0	-0.0029	-0.0174	0.166	110.5
10.0	-0.00949	-0.0348	0.185	95.9
15.0	-0.0105	-0.0378	0.206	97.1
20.0	0.0084	-0.0319	0.236	106.3
30.0	0.00609	0.0058	0.272	-137.9
40.0	0.012	0.0343	0.296	20.7

Table XXIX

RUDDER ANGLE THIRTY DEGREES

Elevator angle in degrees	Pitching moment coef. C_m	Lift coef. C_L	Drag coef. C_D	Longitudinal side C.P. in % of car length
-60.0	0.103	0.1685	0.715	62.4
-40.0	0.1032	0.1710	0.660	74.0
-30.0	0.0846	0.1450	0.605	77.9
-20.0	0.0796	0.1220	0.556	74.9
-10.0	0.0746	0.0958	0.527	68.9
0.0	0.0494	0.0639	0.527	73.7
10.0	0.0426	0.0378	0.538	64.4
15.0	0.0409	0.0290	0.550	64.4
20.0	0.0008	0.1300	0.570	11.5

Table XXXIII

PROTOTYPE MODEL-MODIFIED RUDDERS

BODY NO. 2 CABIN NO. 9

Elevator angle 0.0 Degrees
Angle of attack 0.5 Degrees
Rudders floating

Yaw angle in degrees	Rudder angle in degrees	Yawing moment coef. C_n	Cross wind coef. C_c	Longitudinal side C.P. in % of car length
-40.0	40.0	-0.0381	0.1490	3.8
-30.0	30.0	-0.0263	0.1766	19.5
-20.0	20.0	-0.0340	0.1120	4.9
-10.0	10.0	-0.0208	0.0692	6.3
0.0	0.0	0.00762	-0.0107	107.4
10.0	-10.0	0.0208	-0.0692	6.3
20.0	-20.0	0.0340	-0.1120	4.9
30.0	-30.0	0.0263	-0.1766	19.5
40.0	-40.0	0.0381	-0.1490	3.8

Table XXXVI

PROTOTYPE MODEL-MODIFIED RUDDERS

BODY NO. 2 CABIN NO. 9

Elevator angle 0.0 Degrees
Angle of attack 0.5 Degrees
Pitch angle 0.0 Degrees
Yawing moment coef. $C_n = 0$

Yaw angle in degrees	Rudder angle in degrees
0.0	0.75
-10.0	7.40
-20.0	12.20
-30.0	20.30
-40.0	24.90
-50.0	30.50

Tables XXXIII and XXXIV

PROTOTYPE MODEL--MODIFIED RUDDERS

BODY NO.2 CABIN NO.9

Angle of attack	0.5	Degrees
Elevator angle	0.0	Degrees
Rudder angle	0.0	Degrees

Yaw angle in degrees	Yawing moment coef. C_n	Cross wind coef. C_c	Longitudinal side C.P. in % of car length
-50.0	0.09820	0.3870	70.3
-40.0	0.11200	0.4410	75.4
-30.0	0.09050	0.4040	62.6
-20.0	0.06030	0.3080	67.6
-10.0	0.03150	0.1790	54.8
0.0	0.00762	-0.0107	107.4
10.0	-0.03150	-0.1790	54.8
20.0	-0.06030	-0.3080	67.6
30.0	-0.09050	-0.4040	62.6
40.0	-0.11200	-0.4410	75.4
50.0	-0.09820	-0.3870	70.3

TAIL BOOM MODEL

Angle of attack	0.13	Degrees
Elevator angle	0.37	Degrees
Rudder angle	0.0	Degrees

Yaw angle in degrees	Yawing moment coef. C_n	Cross wind coef. C_c	Longitudinal side C.P. in % of car length
-51.0	0.11110	0.3710	
-41.0	0.10670	0.3910	74.6
-31.0	0.10150	0.3870	63.25
-21.0	0.07680	0.3130	57.6
-11.0	0.03990	0.1820	53.4
-1.0	0.00184	0.01896	49.5
9.0	-0.03990	-0.1820	36.9
19.0	-0.07680	-0.3130	49.5
29.0	-0.10150	-0.3870	53.4
39.0	-0.10670	-0.3910	57.6
49.0	-0.11110	-0.3710	63.25
			74.6

Tables XXXV, XXXVII and XXXVIII

PROTOTYPE MODEL
BODY NO.2 CABIN NO.9
Angle of attack 0.5 Degrees
Pitch angle 0.0 Degrees
Elevator angle 0.0 Degrees

YAW ZERO DEGREES
Original Rudders

Rudder angle in degrees	Yawing moment coefficient C_n	Cross wind coefficient C_c	Longitudinal side C.P. in % of car length
5.0	-0.0227	-0.0593	75.1
10.0	-0.0499	-0.1070	73.3
15.0	-0.0719	-0.1645	80.4
20.0	-0.0888	-0.1935	82.7
25.0	-0.1097	-0.2140	88.0
30.0	-0.1085	-0.2310	83.6
40.0	-0.1135	-0.2456	83.0
45.0	-0.116		82.8
50.0	-0.117		82.3

YAW ZERO DEGREES
Modified Rudders

Rudder angle in degrees	Yawing moment coef. C_n	Cross Wind coef. C_c	Longitudinal side C.P. in % of car length
0.0	0.00762	0.0107	107.4
10.0	-0.057	-0.1216	83.6
20.0	-0.0948	-0.1940	85.8
30.0	-0.115	-0.2292	87.0
40.0	-0.125	-0.2460	87.5

YAW ZERO DEGREES
Modified Rudders
Elevator angle -50.0 degrees

Rudder angle in degrees	Yawing moment coef. C_n	Cross wind coef. C_c	Longitudinal side C.P. in % of car length
0.0	0.00955	0.013	100.1
10.0	-0.0395	-0.088	81.3
20.0	-0.0674	-0.147	80.8
30.0	-0.0745	-0.158	84.5
40.0	-0.0839	-0.197	76.5

Tables XXXV, XXXVII and XXXVIII

PROTOTYPE MODEL
MODIFIED RUDDERS
BODY NO.2 CABIN NO.9
Angle of attack 0.5 Degrees
Pitch angle 0.0 Degrees
Elevator angle 0.0 Degrees

YAW TEN DEGREES

Rudder angle in degrees	Yawing moment coef. C_n	Cross wind Coef. C_c	Longitudinal side C.P. in % of car length
0.0	0.0315	0.1790	54.8
10.0	-0.0208	0.0692	6.3
20.0	-0.0707	-0.0397	214.9
21.25	-0.072	-0.0446	200.9
22.5	-0.0751	-0.0538	177.9
25.0	-0.0805	-0.0622	168.9
30.0	-0.0964	-0.0883	147.9
40.0	-0.117	-0.1410	122.6

YAW TWENTY DEGREES

Rudder angle in degrees	Yawing moment coef. C_n	Cross wind Coef. C_c	Longitudinal side C.P. in % of car length
0.0	0.0603	0.3080	67.6
10.0	0.0139	0.2124	43.85
20.0	-0.0340	0.1120	4.9
25.0	-0.0469	0.0877	-19.1
27.5	-0.0488	0.0852	-36.5
30.0	-0.0436	0.0990	- 9.7
35.0	-0.0545	0.0610	-57.1
40.0	-0.0622	0.0403	-126.1

YAW THIRTY DEGREES

Rudder angle in degrees	Yawing moment coef. C_n	Cross wind Coef. C_c	Longitudinal side C.P. in % of car length
0.0	0.0905	0.4040	62.6
10.0	0.0475	0.3240	59.7
20.0	0.0012	0.2300	42.5
30.0	-0.0263	0.1766	19.5
32.5	-0.0307	0.1657	15.6
35.0	-0.0223	0.1680	21.5
40.0	-0.0133	0.1930	30.0

Tables XXXV, XXXVII and XXXVIII

PROTOTYPE MODEL
MODIFIED RUDDERS
BODY NO.2 CABIN NO.9
Angle of attack 0.5 Degrees
Pitch angle 0.0 Degrees
Elevator angle 0.0 Degrees

YAW FORTY DEGREES

Rudder angle in degrees	Yawing moment coef. C_n	Cross wind coef. C_c	Longitudinal side C.P. in % of car length
0.0	0.112	0.4410	75.4
10.0	0.0655	0.3710	59.9
20.0	0.0188	0.2870	45.4
30.0	-0.0147	0.2072	27.6
35.0	-0.0279	0.1764	21.8
40.0	-0.0381	0.1490	3.8
45.0	-0.0253	0.1678	17.3

YAW FIFTY DEGREES

Rudder angle in degrees	Yawing moment coef. C_n	Cross wind coef. C_c	Longitudinal side C.P. in % of car length
0.0	0.0982	0.3870	70.3
10.0	0.0628	0.3400	65.4
20.0	0.0312	0.2450	56.6
30.0	0.00104	0.1783	45.8
35.0	-0.0105	0.1457	25.9
40.0	-0.0208	0.1123	15.6
45.0	-0.0134	0.1200	19.6

Tables XL and XLI

PROTOTYPE MODEL--MODIFIED RUDDERS

BODY NO.2	CABIN NO.9
Angle of attack	0.5 Degrees
Elevator angle	0.0 Degrees

	YAW ZERO DEGREES		YAW TEN DEGREES	
Rudder angle in degrees	Rolling Moment Coef. C_r	Vertical side C.P. in % of car height	Rolling Moment Coef. C_r	Vertical side C.P. in % of car height
0.0	0.0082	75.5	0.0937	52.1
10.0	0.0756	62.0	0.0242	34.8
20.0	0.1250	64.2	-0.0171	43.0
30.0	0.1456	63.3	-0.0836	94.3
40.0	0.1605	65.4	-0.1215	85.8

	YAW TWENTY DEGREES		YAW THIRTY DEGREES	
Rudder angle in degrees	Rolling Moment Coef. C_r	Vertical side C.P. in % of car height	Rolling Moment Coef. C_r	Vertical side C.P. in % of car height
0.0	0.1375	44.5	0.1610	39.6
10.0	0.0855	44.0	0.1211	37.6
20.0	0.0269	23.9	0.0708	30.6
30.0	0.0121	12.2	0.0355	20.3
40.0	-0.0268	-66.2	0.0473	24.4

	YAW FORTY DEGREES		YAW FIFTY DEGREES	
Rudder angle in degrees	Rolling Moment Coef. C_r	Vertical side C.P. in % of car height	Rolling Moment Coef. C_r	Vertical side C.P. in % of car height
0.0	0.1510	34.0	0.0782	20.1
10.0	0.1153	30.9	0.0616	18.1
20.0	0.0743	25.8	0.0296	12.0
30.0	0.0396	17.7	-0.0022	-1.2
40.0	-0.0023	-1.5	-0.0361	-32.0

Table XLIII

PROTOTYPE MODEL--MODIFIED RUDDERS

BODY NO.2	CABIN NO.9
Angle of attack	0.5 Degrees
Elevator angle	0.0 Degrees

YAW ZERO DEGREES

Rudder angle in degrees	Drag coef. C_D
0.0	0.166
10.0	0.202
20.0	0.352
30.0	0.544
40.0	0.735
Floating	0.166
$C_n=0$	0.180

YAW TEN DEGREES

Rudder angle in degrees	Drag coef. C_D
0.0	0.249
10.0	0.210
20.0	0.265
30.0	0.418
40.0	0.570
Floating	0.210
$C_n=0$	0.210

YAW TWENTY DEGREES

Rudder angle in degrees	Drag coef. C_D
0.0	0.566
10.0	0.466
20.0	0.416
30.0	0.497
40.0	0.595
Floating	0.416
$C_n=0$	0.445

YAW THIRTY DEGREES

Rudder angle in degrees	Drag coef. C_D
0.0	1.000
10.0	0.845
20.0	0.727
30.0	0.710
40.0	0.789
Floating	0.710
$C_n=0$	0.720

YAW FORTY DEGREES

Rudder angle in degrees	Drag coef. C_D
0.0	1.412
10.0	1.205
20.0	1.030
30.0	0.920
40.0	0.940
Floating	0.937
$C_n=0$	0.970

YAW FIFTY DEGREES

Rudder angle in degrees	Drag coef. C_D
0.0	1.710
10.0	1.496
20.0	1.288
30.0	1.143
40.0	1.083
Floating	-----
$C_n=0$	1.140

APPENDIX II

Reduction of Data

APPENDIX II

REDUCTION OF EXPERIMENTAL DATA

Lift and drag coefficients were calculated from the conventional formulas

$$C_L = \frac{L}{q\ S} \qquad \text{and} \qquad C_D = \frac{D}{q\ A}$$

In these equations (S) refers to the total area of the model as seen in the plan view, and (A) refers to the projected frontal area of the model. In the tables these values were given in square inches. They were of course changed to proper units before substituting in the above formulas.

Pitching

Referring to Figures 9, 11, 12, 13, 14, 49, and to Reference 3.

The aerodynamic moments for the Prototype Model taken about the point of contact of the wheel with the ground are obtained from the following equations:

$$M = \text{P.M.F.}\left[11.8 - 1.523\cos(\theta \pm \gamma)\right] - (\text{L}-\text{P.M.F.})\left[3.54 + 1.523\cos(\theta \pm \gamma)\right] + D\left[1.523\sin(\theta \pm \gamma) + 0.75\right] \qquad (1)$$

This equation gives the moment in inch grams about the specified axis. The equation is used in connection with the original wind tunnel data, and the measured <u>air</u> forces are considered as plus when acting in the direction indicated (Fig. 49). The symbol (γ) refers to the angle of pitch and may be either plus or minus. The aerodynamic angle of attack is 0.5^o greater than this angle due to the upward

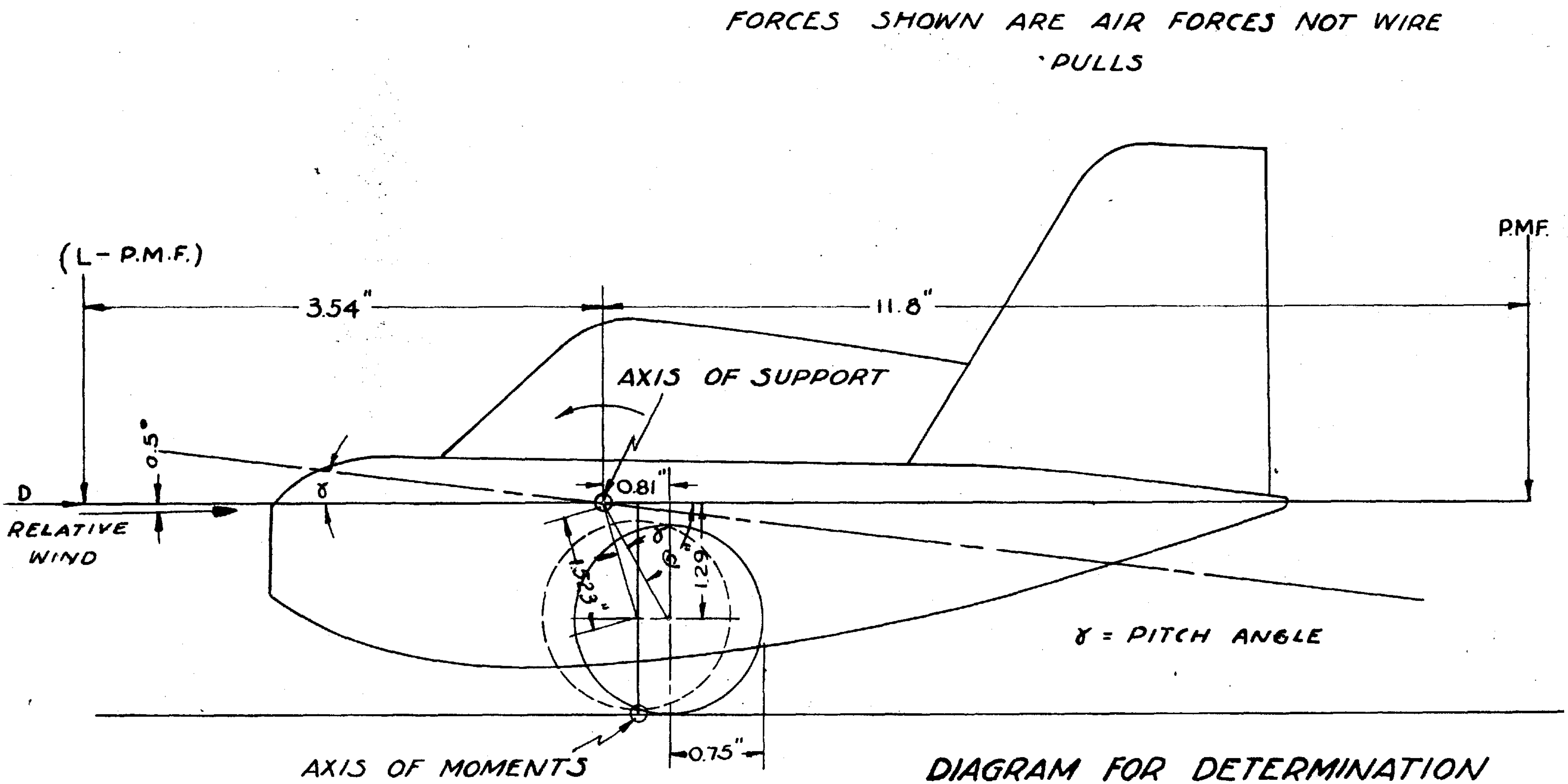

DIAGRAM FOR DETERMINATION OF PITCHING MOMENTS

NO SCALE

FIG. 49

inclination of the air stream.

For the Tail Boom Model this equation in the same units becomes:

$$M = P.M.F.\left[11.80-1.287\cos(\beta\pm\gamma)\right] - (L-P.M.F.)\left[3.54 + 1.287\cos(\beta\pm\gamma)\right] + D\left[1.287\cos(\beta\pm\gamma)+0.75\right] \qquad (2)$$

In all cases substitution was made of net values (measured force minus balance tare minus aerodynamic tare) and the correct sign as indicated by the previous notation was used. The moment obtained from the use of equations (1) or (2) was changed to the coefficient form by means of the standard formula:

$$C_M = \frac{M}{q\,S\,\ell}$$

where (S) is the plan area of the model and (ℓ) is its length. Correction was, of course, made in the units before applying this equation.

Yawing

The yawing moments and the yawing moment coefficients were calculated for the Prototype Models from the following equation: (See Figs. 9, 11, 12, 13, 14, 50, and Reference 3)

$$N = Y.M.F.(11.8-d) - (C+R)(3.54+d) - DE \qquad (3)$$

$$D = 0.81\cos\theta \qquad\qquad E = 0.81\sin\theta$$

This equation gives the moment in inch grams about a vertical axis passing through the center of the wheel axle. The arrows (Fig. 50) indicate positive directions for the <u>air</u> forces acting on the model.

The equation for the Tail Boom Model is the same as

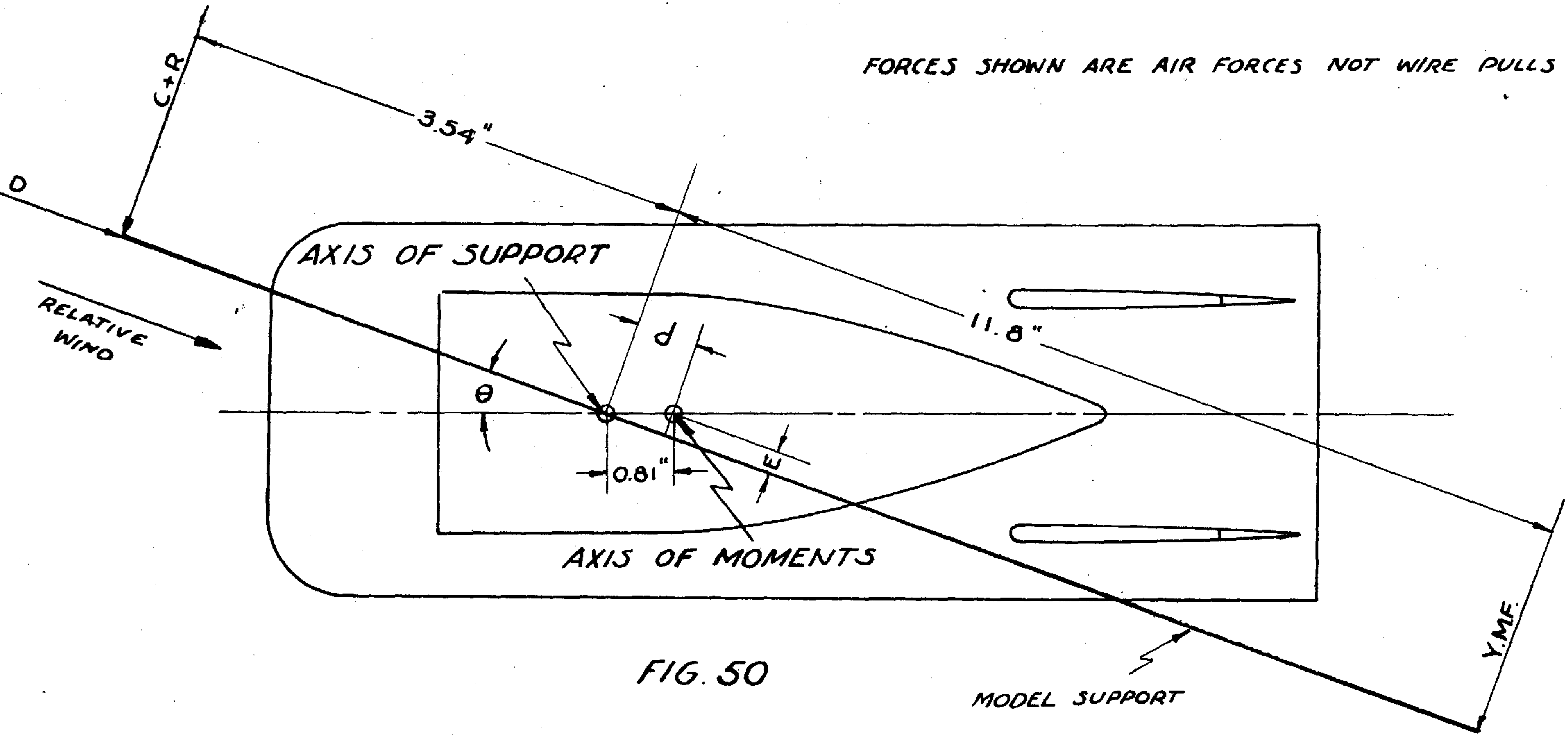

FIG. 50

DIAGRAM FOR DETERMINATION
OF YAWING MOMENTS
NO SCALE

equation (3) except for different values of (d) and (E). For these values see Fig. 12.

The yawing moment coefficient (C_N) was obtained from equation (3) by the use of the standard formula:

$$C_N = \frac{N}{q\,S\,\ell}$$

where (ℓ) is the overall length of the model and (S) is the total area as seen in the plan view. Before applying this equation (N) was corrected for the proper units.

Rolling Moments

The rolling moments and rolling moment coefficients were obtained only for the Prototype Model. Fig. 51 shows this model in position in the model support. The rolling moment in inch grams is:

$$R = \left(2.04 - \frac{5.12 \times R.M.F.}{C.W.F.}\right) \times C.W.F. \qquad (4)$$

In the use of this formula, proper regard was given to the signs of the various terms. The C.W.F. is equal to the force marked (C) plus the Y.M.F. plus the R.M.F. and is so tabulated in the original data.

In order to obtain the rolling moment coefficient (C_R) the standard equation:

$$C_R = \frac{R}{q\,S\,\ell}$$

was used. In this equation (S) is the plan area of the model and (ℓ) is its length. In the use of this equation the proper correction was applied to (R) so that the units would be constant with (ℓ) and (S).

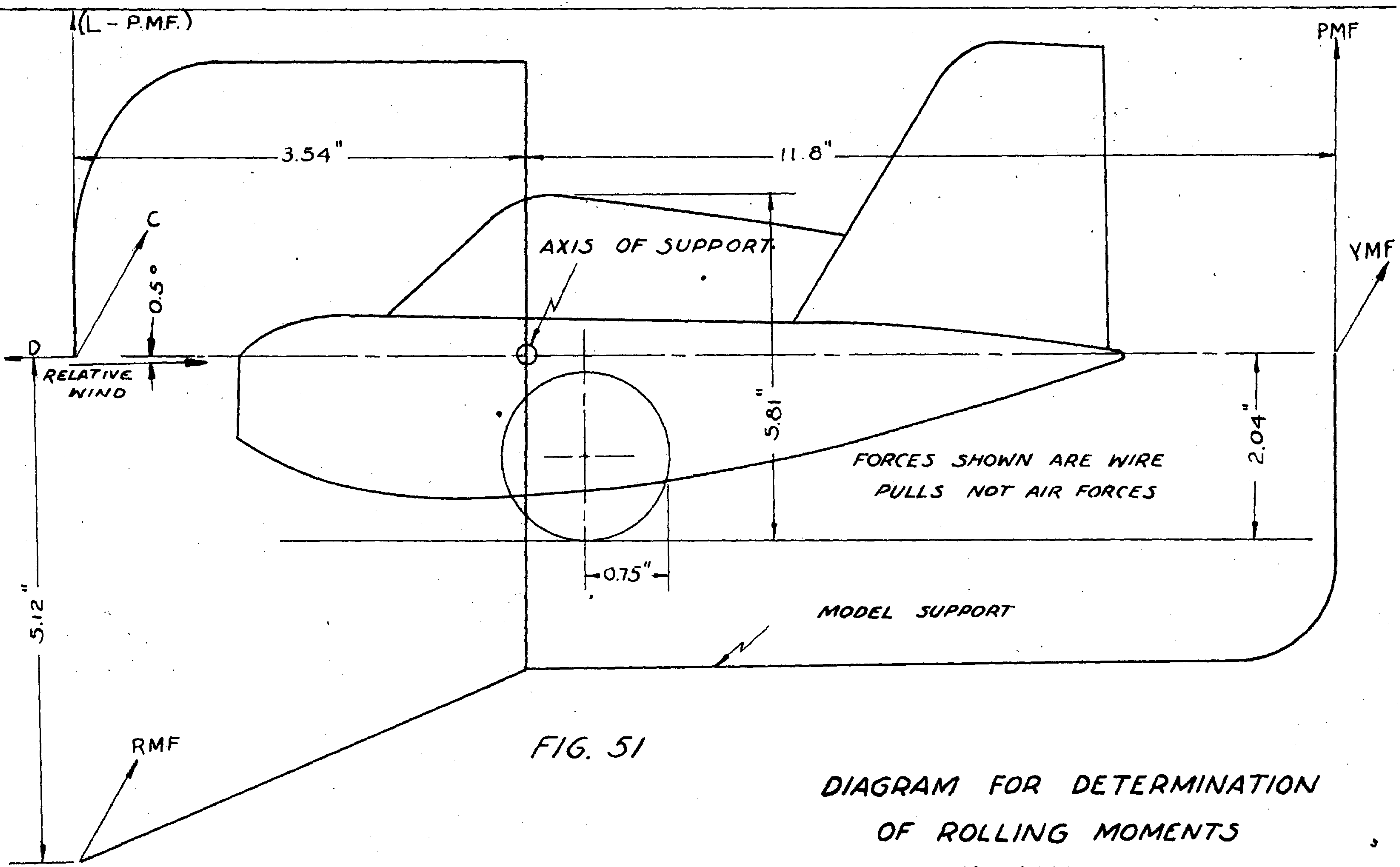

FIG. 51

DIAGRAM FOR DETERMINATION OF ROLLING MOMENTS
NO SCALE

In the original data all forces were tabulated as air forces acting on the model, and not as wire pulls acting on the model. The convention used in regard to signs is explained on page 36 of this report. In all the formulas referred to in the appendix the value of (q) is the same (ie., 75.8 mm. of Hg.)

The method of reducing the data obtained from the coasting tests is given on page 32 of this report. The calculations in regard to fuel economy are of such a simple and obvious nature that no detailed reference is made to them here.

APPENDIX III

REFERENCES

-----

(1) Is Fifty Miles Per Gallon Possible With Correct Streamlining? - W. E. Lay - S. A. E. Journal - April and May 1933.

(2) The Development of a Rear Engine Streamlined Car - Sir Dennestown Burney - S. A. E. Journal - March 1932

(3) Student Technical Reports Nos. 4-7 Inclusive 1932 - Daniel Guggenheim School of Aeronautics, Georgia School of Technology, Atlanta, Georgia.

(4) Report on Tractive Resistance - Iowa State Experiment Station.

(5) Report on Skidding Characteristics - Iowa State Experiment Station.

(6) Air Forces Moments and Damping on Model of Fleet Airship Shenandoah - N.A.C.A. Report No. 215 - A. F. Zahm, R. H. Smith, and F. A. Lowden.

(7) Ideal Transmission Performance Set As Criterion for Development - E. S. Hall - S. A. E. Journal - April 1934.

(8) Other References:

Wind Tunnel Tests and Body Designs - Julis Andrade - S. A. E. Journal - July 1931.

Streamlining Applied to the Automobile - Othmar K. Marti - S. A. E. Journal - November 1931.

The Tear Drop Car - Walter T. Fishleigh - S. A. E. Journal November 1931.

Some Questions About High Speed Driving - J. E. Hale - S. A. E. Journal - November 1931.

Wind Resistance vs. Car Performance - Louis Schwitzer - S.A.E. Journal - June 1931.

Brake Design Control Factors - B. B. Bachman - S.A.E. Journal September 1933.

Side Winds Abate Performance Gains Hoped For From Streamlining.- S.A.E. Journal - November 1933.

Economy of Streamlining in Automobiles - S.A.E. Journal - March 1932.

APPENDIX IV

ACKNOWLEDGEMENTS

The research which forms the basis of this report would not have been possible were it not for the contributions in time, labor and material made by personal friends of the author.

The author is deeply grateful to Professor Montgomery Knight, who cooperated fully with him during the construction and testing of the car and who gave much valuable advice and helpful criticism during the testing of the models and the compilation of the data.

Thanks must also be extended to the following friends who furnished free storage space for the full size machine both during and after the construction period:

C. G. Milling

W. J. Ward

R. A. Crites

E. E. White

Mrs. Ernest Pope

Wendell Jones

The following individuals worked long hours without pay, or, in one or two cases, with very inadequate pay, helping the author design, construct and/or test either the full scale machine or the models:

Robert E. Shackleford

H. E. Hoben

L. I. Turner, Jr.

H. W. Hoyt

Forrest Bloodworth

A. Y. Pope

Frank Goins

H. R. Stogner

B. K. Craig

J. L. Witherstine

P. E. Mullowney

M. Whitlock

William Brandau

A. A. de Almar

J. B. Dent

A. L. Ervin

W. L. O'Ferrall

W. T. Weymouth

S. D. Terrell

R. A. Hall

J. N. Gentry

Mackay D. Solengerger

M. W. Neil

The following individuals donated valuable material to the author or aided him in obtaining material below cost:

H. R. Stogner

W. T. Weymouth

H. G. Lesley

Bob Turner

C. G. Milling

The following individuals allowed the free use of their

tools and equipment during the construction of the full size machine:

C. G. Milling

R. A. Crites

H. R. Stogner

W. J. Ward

Mackay D. Solenberger

Wendell Jones

E. E. White

M. W. Neil

Joe Groom

The following C. W. A. workers rendered invaluable service in the preparation of this report:

M. W. Pirkle

J. M. Gentry

J. A. Anderson

Dave Centor

A. J. York

Thanks is also due to many members of the staff of the Daniel Guggenheim School of Aeronautics and the Georgia School of Technology, who cooperated with the author in every way during the progress of this investigation.

T. Edward Moodie

May 19th, 1934